Investigations into the Occurrence, Formation and Fate of *N*-Nitrosodimethylamine (NDMA) in Air and Water

by

Jinwei Zhang

A Dissertation Presented in Partial Fulfilment
of the Requirements for the Degree
Doctor of Philosophy

Approved April 2016 by the
Graduate Supervisory Committee:

Pierre Herckes, Co-Chair
Paul Westerhoff, Co-Chair
Matthew Fraser
Everett Shock

ARIZONA STATE UNIVERSITY

May 2016

ABSTRACT

N-Nitrosodimethylamine (NDMA), a probable human carcinogen, has been found in clouds and fogs at concentration up to 500 ng/L and in drinking water as disinfection by-product. NDMA exposure to the general public is not well understood because of knowledge gaps in terms of occurrence, formation and fate both in air and water. The goal of this dissertation was to contribute to closing these knowledge gaps on potential human NDMA exposure through contributions to atmospheric measurements and fate as well as aqueous formation processes.

Novel, sensitive methods of measuring NDMA in air were developed based on Solid Phase Extraction (SPE) and Solid Phase Microextraction (SPME) coupled to Gas Chromatography-Mass Spectrometry (GC-MS). The two measuring techniques were evaluated in laboratory experiments. SPE-GC-MS was applicable in ambient air sampling and NDMA in ambient air was found in the 0.1-13.0 ng/m^3 range.

NDMA photolysis, the main degradation atmospheric pathway, was studied in the atmospheric aqueous phase. Water soluble organic carbon (WSOC) was found to have more impact than inorganic species on NDMA photolysis by competing with NDMA for photons and therefore could substantially increase the NDMA lifetime in the atmosphere. The optical properties of atmospheric WSOC were investigated in aerosol, fog and cloud samples and showed WSOC from atmospheric aerosols has a higher mass absorption efficiency (MAE) than organic matter in fog and cloud water, resulting from a different composition, especially in regards of volatile species, that are not very absorbing but abundant in fogs and clouds.

NDMA formation kinetics during chloramination were studied in aqueous samples including wastewater, surface water and ground water, at two monochloramine concentrations. A simple second order NDMA formation model was developed using

measured NDMA and monochloramine concentrations at select reaction times. The model fitted the NDMA formation well (R^2 >0.88) in all water matrices. The proposed model was then optimized and applied to fit the data of NDMA formation from natural organic matter (NOM) and model precursors in previously studies. By determining the rate constants, the model was able to describe the effect of water conditions such as DOC and pH on NDMA formation.

ACKNOWLEDGMENTS

First and foremost, I would like to thank my advisors, Dr Pierre Herckes and Dr Paul Westerhoff, for their support and guidance on my science projects as well as life. Without their help I would not have been able to accomplish and achieve my goals. I really appreciate their encouragement, criticism and inspiration. I would also like to acknowledge my supervisory committee members, Dr Matthew Fraser and Dr Everett Shock as well as Dr Hilairy Hartnett and Dr Timothy Steimle for all of their advice and assistance with my dissertation projects.

I would like to acknowledge all of my labmates and friends in Herckes and Westerhoff Groups at ASU: David Hanigan, Youliang Wang, Jershon Eagar, Aurelie Marcotte, Sarah Frey, Denise Napolitono, Christy Rose, Taka Nosaka, Samantha Donovan, Jun Wang and Fariya Sharif. I would like to thank all of the Arizona State University School of Molecular Science staff for their hard work and help. I would like to thank all my other friends in Arizona and other states in United States

At last, I want to say thank you to my parents and sister, who have provided much support, encouragement and understanding. I want to thank my wonderful wife, Chengyu, for her support and love in the past ten years.

TABLE OF CONTENTS

Page

LIST OF TABLES viii

LIST OF FIGURES ix

CHAPTER

1 INTRODUCTION AND BACKGROUND 1

1.1 *N*-Nitrosodimethylamine (NDMA) Occurrence 1

1.2 NDMA in Atmosphere 3

1.3 NDMA in Drinking Water 6

1.4 Rationale and Objectives 13

2 NDMA MEASUREMENT IN AIR 16

2.1 Introduction 16

2.2 Materials and Methods 19

2.2.1 Chemicals and Materials 19

2.2.2 NDMA Gas Sampling Test 19

2.2.3 Positive and Negative Artifact Formation Test 20

2.2.4 Ambient Air Sampling 21

2.2.5 Extraction and Analysis of NDMA 21

2.3 Results and Discussion 23

2.3.1 Evaluation of SPME as Sampling Medium 23

2.3.2 SPE Sampling Tests 25

2.3.3 Positive Artifact Formation Test 28

2.3.4 Negative Artifact Formation Test 29

2.3.5 Ambient SPE Results 30

CHAPTER Page

2.4 Conclusions....31

3 OPTICAL PROPERTIES OF WATER SOLUBLE ORGANIC CARBON (WSOC) IN ATMOPHERIS AEROSOLS AND FOG/CLOUD WATERS 33

3.1 Introduction....33

3.2 Experimental and Analytical Methods....36

3.2.1 Sample Collection....36

3.2.2 Sample Preparation....36

3.2.3 Sample Analysis....37

3.2.4 Photolysis Set-up....38

3.3 Results and Discussion....39

3.3.1 WSOC Effect on NDMA Photolysis....39

3.3.2 Wavelength Dependence of Light Absorption....41

3.3.3 WSOC in Aerosol and Fog/Cloud....44

3.3.4 MAE of WSOC....45

3.3.5 Influence of Relative Humidity (RH) of MAE....48

3.4 Conclusions....49

4 *N*-NITROSAMINE FORMATION KINETICS IN WASTEWATER EFFLUENTS AND SURFACE WATERS....51

4.1 Introduction....51

4.2 Experimental and Analytical Methods....53

4.2.1 Source Waters....53

4.2.2 Reagents....54

4.2.3 Chloramination Experiments....54

4.2.4 NDMA Analysis....55

CHAPTER Page

4.2.5 Other Analyses....56
4.3 Results and Discussion....56
4.3.1 NDMA Formation Kinetics in Wastewaters....56
4.3.2 NDMA Formation Kinetics Surface Waters....59
4.3.3 Model Fitting of NDMA Kinetics....62
4.3.4 Monochloramine Exposure....67
4.4 Conclusions....70
4.5 Acknowledgements....71
5 MODELING NDMA FORMATION KINETICS DURING CHLORAMINATION OF MODEL COUMPOUNDS AND SURFACE WATERS IMPACTED BY WASTEWATER DISCHARGES....72
5.1 Introduction....72
5.2 Model Description....76
5.2.1 NDMA Formation Model....76
5.2.2 Monochloramine Degradation....79
5.3 Results and Discussion....80
5.3.1 Modeling of NDMA Formation in NOM....80
5.3.2 Modeling of NDMA Formation from Model Compounds....82
5.3.3 Modeling of NDMA Formation of Pharmaceutical Compounds in the Presence of NOM....87
5.4 Summary and Conclusions....91
5.5 Acknowledgements....91

CHAPTER Page

6 INVESTIGATIONS ON IMPROVING THE NDMA FORMATION KINETICS MODEL....92

6.1 Introduction....92

6.2 Experimental and Analytical Methods....96

6.3 Results and Discussion....97

6.3.1 Role of Dichloramine in NDMA Formation....97

6.3.1.1 Enhancement of Dichloramine....97

6.3.1.2 Suppression of Dichloramine....98

6.3.2 Influence of Dissolved Oxygen....100

6.3.3 Effect of Buffer System....101

6.4 Conclusions....104

7 SUMMARY AND OUTLOOK....106

7.1 Summary....106

7.2 Suggestions of Future Research....109

REFERENCES....111

APPENDIX

A CHAPTER 3 SAMPLE INFORMATION....125

B SUPPORTING INFORMATION FOR CHAPTER 4....129

LIST OF TABLES

Table Page

2.1 SPE Collection Efficiency Tests 26

2.2 Sampling Parameters in This Work Compared to Thermalsob/N Sorbent Method 28

2.3 Measurement of NDMA in Gas Phase 31

3.1 Half-lives of NDMA in DI Water and WSOC at Different WSOC Concentrations 40

4.1 Water Quality, Treatment and NDMA Formed in Source Waters 65

5.1 Chloramine Decomposition Kinetics and Associated Rate Constants (Ozekin et al., 1996) 78

5.2 Optimized NDMA Formation Rate Constant and Monochloramine Decomposition Rate Constants in NOM under Various Reaction Conditions. (Data from Chen and Valentine, 2006). R^2 is Correlation Coefficient between Model and Observation. Notes: Experiments were Conducted at pH 7 with Variable Cl/N Ratios (and Ammonia Concentrations): [a] 0.7 (0.07 mM NH_3); [b] 0.3 (0.17 mM NH_3); [c] 0.10 (0.5 mM NH_3) 81

5.3 Optimized Rate Constant k_{app} for Model Compounds under Various Reaction Conditions. (NDMA data from Selbes, 2014) 87

5.4 Optimized Rate Constant k_{app} for Model Compounds in Different Water Matrices with Varied TOC. (NDMA Data from Shen and Andrews, 2011b) 89

LIST OF FIGURES

Figure Page

1.1 Structure of NDMA 1

1.2 UV-Vis Absorbance of Nitrosamines in Water and Solar Simulator Spectra (Plumlee and Reinhard, 2007) 5

1.3 NDMA Formation Pathway of DMA and (a) Monochloramine (Choi and Valentine, 2002; Mitch and Sedlak, 2002a) and (b) Dichloramine (Schreiber and Mtich, 2006b).....10

1.4 NDMA Formation Pathway of Amine Precursors and Chloramines (Selbes, et al., 2013) 11

2.1 Set-up of SPE and SPME Sampling Test 20

2.2 GC-MS Responses of NDMA Absorbed on SPME Fibers at Different Sampling Times. a: CAR/PDMS Fiber Coating b: PDMS/DVB Fiber Coating 24

3.1 Image of Irradiation Setup with the Water Chiller, Irradiation Flask, Lamp, Filters, and Power Source 39

3.2 UV-Vis Absorbance of WSOC with 1 mg/L Nitrate and 1.4 mgC/L Dissolved Organic Carbon (a), 1 mg/L Nitrate (b) and the Dissolved Organic Components (a-b).....41

3.3 AAE for WSOC from Aerosol and Fog/Cloud Samples 42

3.4 Correlation of Absorbance at 365 nm vs. WSOC for Aerosol Extracts and Fog/Cloud Samples 45

3.5 MAE Values of WSOC and Fog/Cloud Samples 46

Figure Page

3.6 Temporal Variations of WSOC MAE and RH in Aerosol Extracts from Bakersfield, CA.....49

4.1 (A) Monochloramine (NH_2Cl) Decay Kinetics in WW1 for Two Initial Monochloramine Doses. (B) NDMA Formation Observed (symbols) and Fitted by Equation 2&3 (lines). Error Bars Represent One Standard Deviation (n = 3) for Select Time Points. (pH = 8.2, Temperature = 23 ± 1 °C).....58

4.2 NDMA Formation Observed (symbols) and Fitted by Equation 2&3 (line) in SW at Two Initial Monochloramine Doses. Error Bars Represent One Standard Deviation (n = 3) for Select Time Points. (pH = 8.0, 23 ± 1 °C) 60

4.3 NDMA Formation Observed (symbols) and Fitted by Equations 2&3 (line) in GW at Two Initial Monochloramine Doses. (pH = 8.0, 23 ± 1 °C) 61

4.4 Linear Correlation between Model Predictions and Observations of NDMA Concentrations in all Waters. Data from all Reaction Time Periods are Included 66

4.5 Plots of P/P_0 versus Monochloramine Exposure for Water Samples (a) WW1, (b) WW4, (c) GW1, (d) SW1. L = Lower, H = Higher, Represent Samples with Lower or Higher NH_2Cl Concentrations 69

5.1 NDMA Formation Pathways as Proposed in the Literature: (1) Choi and Valentine, 2002; Mitch and Sedlak, 2002a. (2) Schreiber and Mitch, 2006b. (3) Selbes et al. 2013. 75

5.2 Model Prediction of NDMA Formation and Monochloramine Decay at Various pH in Surface Water. (Symbols: Observation Data, Lines: Model Predictions. Data from Chen and Valentine, 2006).....81

Figure Page

5.3 Model Prediction of NDMA Formation and Monochloramine Decay at Various Ammonia Concentrations (Cl/N ratio) in Surface Water. (Symbols: Observation Data, Lines: Model Predictions, pH=7. Data from Chen and Valentine, 2006).....82

5.4 NDMA Formation from Model Precursor Compound Data (Symbols), Model Fitting (Lines) in FP Tests (NH_2Cl 1.4mM, pH=7.5), SDS Conditions (NH_2Cl 0.04mM, pH=7.5) and SDS Conditions with Excess Ammonia. (NDMA Data from Selbes, 2014).....86

5.5 NDMA Formation from Pharmaceutical Compounds under SDS Condition (MQ Water, NH_2Cl=0.035mM, pH=7), Data (Symbols) and Model Fitting (Lines). (NDMA Data from Shen and Andrews, 2011b).....88

5.6 NDMA Formation of Amine Precursors in River Water (SDS, pH=7, TOC=6mg/L) and Modeling of NDMA Formation without Lag-time, Data (Symbols) and Model Fitting (Lines) (NDMA Data from Shen and Andrews, 2011b).....90

6.1 Theoretical Breakpoint Curve (USEPA, 1999).....93

6.2 Distribution Diagram for Chloramines with pH (Palin, 1950; USEPA, 1999).....93

6.3 NDMA Formation Kinetics of Wastewater Effluents with and without Excess NH_4^+ in Chloramine Stock Solution.....98

6.4 $NHCl_2/NH_2Cl$ Ratio with and without Excess NH_4^+ in Nano Pure Water at pH=7.....99

Figure Page

6.5 NDMA Formation Observed at Varying Dissolved O_2 Concentrations (Symbols) and Fitted by Equations 4-1&4-2 (Lines) in WW5 at Same Initial Monochloramine Dose (20 mgCl_2/L). Error Bars Represent One Standard Deviation (n=3) for Select Time Points. (pH = 8.0, 23 ± 1°C).....100

6.6 Monochloramine (NH_2Cl) Decay Kinetics at Two Dissolved O_2 Levels 101

6.7 (a) NDMA Formation from Model Precursors (pH=8); (b) NDMA Formation in Buffered (pH=8) Wastewater and Surface Water; (c) NDMA Formation in Buffered Wastewater with Buffer Concentration from 0.1 mM to 100 mM 103

CHAPTER 1

INTRODUCTION AND BACKGROUND

1.1 *N*-Nitrosodimethylamine Occurrence

*N-N*itrosodimethylamine (NDMA) is a compound with nitroso- (NO-) group bonded to the nitrogen (N) atom in dimethylamine (Figure 1.1).

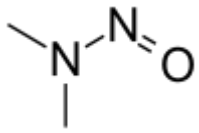

Figure 1.1: Structure of NDMA

It is a member of the N-nitrosamine family which comprises potential carcinogenic compounds. NDMA was of particular research focus in the nitrosamine family, since it is the most widely detected nitrosamine in water with high toxicity (Krasner et al., 2013). NDMA has been detected in all environmental compartments including air, soil and water (ATSDR, 1999). It was initially recognized as decomposition by-product of hydrazine-based compounds used in the rocket fuel industry (Brubaker et al., 1985; Lunn et al., 1991; Lunn and Sansone 1994). It can also be formed in many industrial processes such as those occurring in amine, tanneries, rubber, pesticide and other amine related chemical plants (Fajen et al. 1979; Spiegelhalder and Preussmann, 1981, 1983; Stefan and Bolton, 2002). NDMA is also found in a variety of foodstuffs such as cured meat (e.g. sausage, bacon), fish products, dairy and cheese products, and alcoholic beverages (Tricker and Preussmann, 1991). It originates from reactions of nitrosating agents (e.g. nitrite, nitrogen oxide) and amines contained in the food products. NDMA was also identified in indoor environments with active tobacco smoking (Brunnemann and Hoffmann, 1978; Ruhl et al., 1980). Additionally NDMA can be formed naturally as a result of chemical and biological

processes (Ayanaba and Alexander, 1974; WHO, 2002a). In recent years NDMA has been found in drinking water as a disinfection byproduct from water chlorination or chloramination. (Mitch et al., 2003; Krasner et al., 2013).

There is evidence of nitrosamine carcinogenicity in experimental animals, especially NDMA (IARC 1987; Afonso Perera 2006). Although there is no direct evidence that exposures causes cancer in humans, exposure to N-nitroso compounds from food, environment and in-vivo formation in human body have been associated with higher risk of cancer (Fajen et al. 1979; Bartsch and Spiegelhalder 1996; Mirvish 1995; Straif et al, 2000; WHO, 2002b). NDMA can enter the human body by ingestion, inhalation and through dermal exposure. Ingestion occurs when people eat and drink food and water that contains NDMA. Inhalation exposure is mainly related to polluted air and particulate matter in the atmosphere. Dermal exposure could happen when skin gets in contact with rubber-made things, detergent or water that contains NDMA. However, it was calculated that daily dermal exposure during shower from water is only 0.04% of ingestion of same water (OEHHA, 2006). While NDMA may be avoided in foodstuffs by choosing not to eat certain foods, it is not possible to avoid air inhalation and drinking water.

With increasing evidence of nitrosamines' toxicity, USEPA may soon set regulatory determinations of NDMA and other nitrosamines in water and air. Currently USEPA has included nitrosamines in the Unregulated Contaminant Monitoring Rule 2 (UCMR 2) (USEPA, 2005) and the Contaminant Candidate List 3 (CCL3) (USEPA, 2009). For NDMA in the air, the USEPA has calculated a residential air screening level of 0.07 ng/m3 (exposure of 24 h/day in 26 years) and an industrial air screening level of 0.88 ng/m3 (exposure of 1h/day in 25 years) at a target cancer risk (TR) of one in one million (10^{-6}) (USEPA, 2015). USEPA's Integrated Risk Information System

(IRIS) database indicates that a drinking water concentration of 0.7 ng/L is associated with 10^{-6} lifetime cancer risk. Local government has taken actions to regulate NDMA in drinking water. For example, California's Office of Environmental Health Hazard Assessment (OEHHA) set a public health goal at 3 ng/L for NDMA and California's Department of Public Health (CDPH) has set 10 ng/L notification for nitrosamines including NDMA in drinking water

1.2 NDMA in Atmosphere

Since the 1970s, NDMA has been reported in the air in industrial and urban locations. Most of the high NDMA concentrations measured were found to be associated with industrial processes. The highest gas phase NDMA concentrations (130 $\mu g/m^3$) ever reported were found in indoor work places in the rubber industry (Spiegelhalder and Preussmann, 1981). Fine et al. (1976) reported 36 $\mu g/m^3$ near the Food Manufacturing Corporation (FMC) facility, where NDMA was used as intermediate to manufacture unsymmetrical dimethyl hydrazine (UDMH). NDMA was also detected in polluted ambient air in concentrations up to 0.8 $\mu g/m^3$ near a dimethylamine (DMA) manufacturer (Fine et al., 1976). Occurrence of NDMA in high concentrations in indoor environment always relates to environmental tobacco smoke (ETS). Previous studies have reported NDMA concentrations up to 2-37 ng/m^3 in a closed office with smokers (Stehlik et al., 1982; Mahanama and Daisey, 1996). All the NDMA concentrations reported before were orders of magnitude higher than the USEPA suggested screening level of NDMA, mostly because they were measured in highly polluted /industrial areas or indoor environments. Due to its low vapor pressure (2.7mm Hg at 20 °C) NDMA, is more likely to exist in gas phase than to absorb to particulate matter (Baisautova, 2008). However, nitrosamines, including NDMA, have also been detected in particulate matter. Total nitrosamines concentrations were

measured at 5.2 ng/m^3 in urban airborne PM2.5 samples in U.K (Farren et al., 2015). Nitrosamines up to 161.4 ng/m^3 in $PM_{2.5}$ and 53.90 ng/m^3 in $PM_{2.5\text{-}10}$ were monitored during winter time in Zongulda, Turkey (Akyüz and Ata, 2013).

Airborne NDMA can be from direct emission through industrial processes or generated through atmospheric processes. NDMA can be produced by nitrosation of alkylamines. In the dark, nitrosating agents such as nitrous acid (HONO) formed from reaction of nitrous oxides (e.g. NO_x) and water vapor react with gas phase alkylamines such as DMA to form NDMA (Hanst et al., 1977).

$$NO + NO_2 + H_2O \rightarrow 2HONO \qquad \text{Equation 1-1}$$

$$(CH_3)_2NH + HONO \rightarrow (CH_3)_2NNO + H_2O \qquad \text{Equation 1-2}$$

However, later studies found that nitrosamines degrade rapidly in sunlight by direct photolysis or by reacting with atmospheric oxidants such as ozone or OH radical (Tuazon et al., 1984). The UV-Vis absorption spectrum of NDMA shows two absorption bands at ~230nm and ~330 nm relating to $\pi \rightarrow \pi^*$ and $n \rightarrow \pi^*$ transitions, respectively (Figure 1.2) (Plumlee and Reinhard, 2007). Absorption at 230 nm is not in the range of natural sunlight in the atmosphere, but NDMA absorption around 330nm overlaps with sunlight and is responsible for the direct photolysis of NDMA. In the gas phase, NDMA gets photolyzed quickly with a half-life of 5min (Tuazon et al., 1984). NDMA in pure deionized water undergoes a similarly fast photolysis with half-lives of 3-18 min depending on irradiation intensity (Stefan and Bolton, 2002; Plumlee and Reinhard, 2007; Hutchings et al., 2010; Chen et al., 2010). The short half-lives of NDMA in air and water suggest that it is not persistent in the environment.

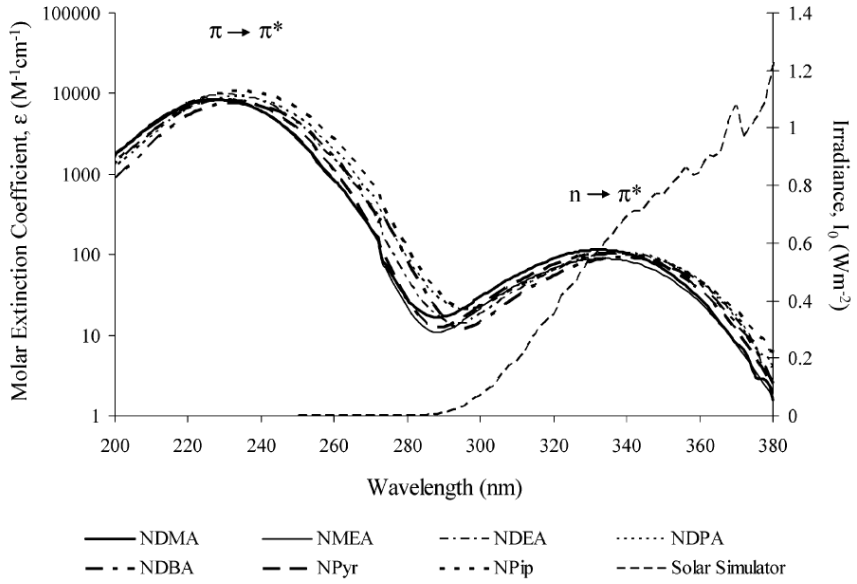

Figure 1.2: UV-Vis absorbance of nitrosamines in water and solar simulator spectra (Plumlee and Reinhard, 2007)

Recently NDMA was detected at high concentrations (up to 497 ng/L) in atmospheric droplets (clouds and fogs) (Herckes et al., 2007; Hutchings et al., 2010). In the Hutchings et al. (2010) study, it was suggested from model calculations that the NDMA in droplets was not from the in-cloud nitrosating reaction between DMA and nitrite due to the low formation yields (~1%). The source of NDMA in clouds and fogs is probably from gas phase formation of NDMA and partitioning of gas phase NDMA into aqueous phase because of the high water solubility of NDMA. In lab experiments the NDMA photolysis rate was significantly reduced in the presence of organic carbon (DOC = 2.0 mgC/L) and nitrite (1 mg/L). The lack of NDMA photolysis was attributed to light-shielding by nitrite as it competes with NDMA for sunlight photons near 330 nm (Stefan and Bolton, 2002). The WSOC may also affect photolysis of NDMA since previous research showed there is a reduction of NDMA photolysis with increasing DOC in surface water matrices (Stefan and Bolton, 2002; Plumlee and Reinhard, 2007; Chen et al., 2010). Due to such possible light-shielding effect in droplets, the high

concentrations of NDMA in fogs may result from NDMA formation in gas phase, accumulation in the droplets in the dark and persistence with little photolysis in droplets during 'day' time.

Most recently NDMA and other nitrosamines have been of growing concern with development of amine-based CO_2 capture technologies (Sorensen et al., 2015). NDMA, N-nitrosodiethanolamine (NDELA) and N-nitrosomorpholine (NMOR) at concentrations ranging between 5 and 47 ng/m^3 were detected in an amine-based CO_2 capture pilot plant in Maasvlakte, Netherlands (da Silva et al., 2013). In post combustion CO_2 capture (PCCC) plants, amines are used as solvents to capture and store CO_2 to decrease the CO_2 emissions. Nitrosamines can be formed as amine degradation products though reactions with NO_x in the flue gas (Masuda et al., 2000; Reynolds et al., 2012). The amines in emission gas could also react with nitrosating agents (e.g. NO_x) present in atmosphere from various combustion sources to form nitrosamines. Such reactions will generally follow mechanisms similar to the pathway in Equations 1-1&1-2. The NDMA formed in the air would probably partition into cloud droplets and end up in soil or surface water by precipitation if not photolyzed.

1.3 NDMA in Drinking Water

NDMA was found in drinking water wells near a rocket engine testing facility using unsymmetrical dimethylhydrazine (UDMH)-based rocket fuel in Sacramento County, CA in 1998 (Mitch et al., 2003). In 2002, two drinking water production wells impacted by aquifer recharge wastewater suspended operations due to the presence of NDMA (DHS, 2002).

NDMA can be formed during drinking water treatment by several processes including ozonaton, chlorination, catalytic formation and chloramination (Krasner et al., 2013). Ozonation of DMA has been reported to only form NDMA at low yields

(<0.02%) at acidic or basic pH (Andrzejewski et al., 2008; Yang et al., 2009). Ozonation of certain industrial amine precursors containing hydrazine (e.g. UDMH) or sulfamide functional groups, forms NDMA with more than 50% yield, resulting in more than 10 ng/L NDMA formation in drinking water (Schmidt and Bruch, 2008; Von Gunten et al., 2010). However, research on ozonation suggested its importance on NDMA formation in drinking water is restricted to source waters with certain precursors.

Chlorination of nitrite in the presence of NDMA precursors can also lead to NDMA formation. Choi and Valentine (2003) reported such formation starting with the formation a dinitrogen tetraoxide (N_2O_4) intermediate from nitrite acidification. The intermediate then forms NO* which will nitrosate the amine precursor (e.g. DMA). The pathway is of little importance in drinking water due to the low formation yields and low concentrations of nitrite in drinking water (Shah et al., 2012). However, NDMA formed by nitrosation may be enhanced four-fold during breakpoint chlorination if breakpoint chlorination is conducted to achieve a significant free chlorine residual in the presence of nitrite (Schreiber and Mitch, 2007).

Activated carbon can catalyze the formation of NDMA from secondary amines. Reactive nitrogen species formed on surface of activated carbon react with a secondary amine like DMA and form NDMA at low yields (<0.3%) (Padhye et al., 2011). With the low concentrations of DMA in drinking water, the pathway is considered unlikely to be important (Mitch and Sedlak, 2004; Krasner et al., 2013).

Compared to chlorination or ozonation, most studies have found that NDMA formation is mainly associated with chloramination (Choi and Valentine, 2002; Mitch and Sedlak, 2002a; Krasner et al., 2013). In drinking water treatment chloramines, instead of chlorine, are used as disinfectant to limit the formation of trihalomethanes (THM)

during chlorination (Mitch et al., 2003). Chloramines have been used increasingly in drinking water systems and the population using drinking water containing chloramines has increased from 17% in 2007 to 22% in 2010 in United States (Li, 2011). NDMA detections in high concentrations in treated drinking water (67 ng/L) and in higher concentrations in distribution systems (up to 180 ng/L) are associated with chloramination (Charrois et al., 2004). Russel et al (2012) reported 35% of samples from water systems using chloramine and only 3% of samples from those using chlorine presented detectable levels of NDMA. All samples that had NDMA concentrations higher than 50 ng/L, were from systems with the highest fraction of chloramine use (Russel et al., 2012). Plants using chloramine with longer hydraulic contact times in plant and distribution system (e.g., 12–18 hr) tend to form more NDMA in the water system than plants using chloramine for shorter (e.g., 0.5–2 hr) contact times (Krasner et al., 2012).

The precursors of NDMA are from three main sources: wastewater treatment effluent, natural organic matter (NOM) and in-plant treatment chemicals. Wastewater has been identified as the most important precursor source producing 300-1300 ng/L NDMA in chloramination (Mitch and Sedlak, 2004). NOM can be precursor for NDMA when nitrogen in organic matter reacts with chloramines. Water treatment chemicals also showed the potential for NDMA formation. For example, coagulation polymers such as polyamine or polyDADMAC, used in drinking water treatment to facilitate coagulation before filtration, degrade and release NDMA precursors in chlorination, leading to higher NDMA formation potential (FP) (Najm and Trussell, 2001; Kohut and Andrews, 2003; Bolto, 2005; Park et al., 2009).

Amines containing DMA functional group are expected as the precursors of NDMA in chloramination (Kemper et al., 2010). Extensive studies have reported

NDMA formation from various amine precursors by chloramination. Nitrosamines formed from primary amines decay quickly and are not stable (Ridd, 1961). DMA, the secondary amine precursor of NDMA, has been studied a lot as the model precursor of NDMA (Mitch and Sedlak, 2002a; Choi and Valentine, 2003; Andrzejewski et al., 2008) due to its occurrence in natural waters. Mitch and Sedlak (2002a) and Choi and Valentine (2002) proposed a NDMA formation pathway where unprotonated DMA undergoes a nucleophilic substitution reaction with monochloramine. The formed UDMH intermediate is then oxidized by monochloramine to form NDMA (Figure 1.3a). It was later found that NDMA formation yield in chloramination of UDMH is at least two orders of magnitude lower than that in chloramination of DMA; and the formation rate was also much slower in chloramination of UDMH (Schreiber and Mitch, 2006b). Besides monochloramine, the importance of dichloramine and dissolved oxygen was then discovered. It was observed that dichloramine which forms via monochloramine disproportionation coexists with monochloramine and significantly enhances NDMA formation even at trace levels comparted to monochloramine. A new reaction pathway involving dichloramine and dissolved oxygen was then proposed (Figure 1.3b).

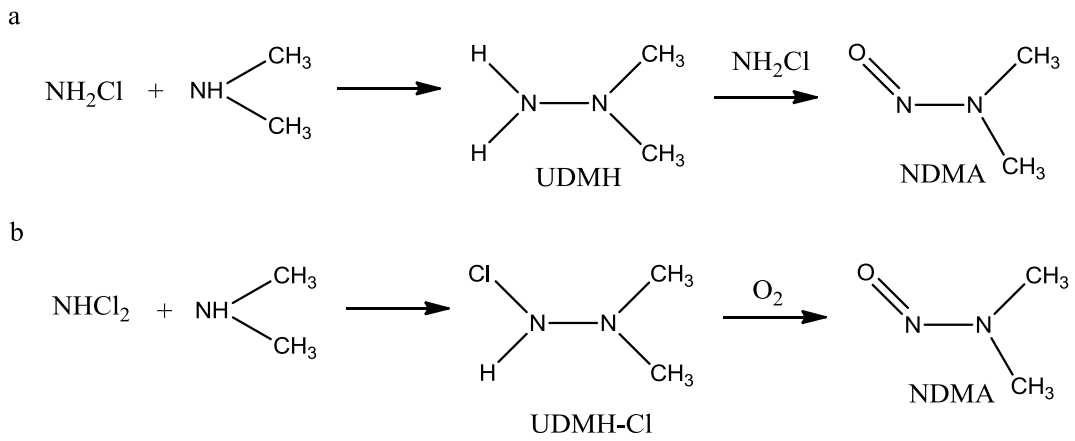

Figure 1.3: NDMA formation pathway of DMA and (a) monochloramine (Choi and Valentine, 2002; Mitch and Sedlak, 2002a) and (b) dichloramine (Schreiber and Mitch, 2006b)

In this pathway dichloramine reacts to form NDMA via the formation of a Cl-UDMH intermediate and the intermediate is then oxidized by dissolved oxygen in water to produce NDMA (Figure 1.3b). Some tertiary amines, such as trimethylamine (TMA), can also act as a significant NDMA precursor in chloramination (Mitch and Schreiber, 2008). In the presence of chlorine or chloramine, TMA can decay quantitatively to release DMA that forms NDMA in chloramination via the reaction in Figure 1.3b. However, with the low NDMA yield and low alkylamine (DMA or TMA) concentrations, NDMA formed via this pathway is insufficient to explain any substantial NDMA formation.

A lot of research has focused on identifying NDMA precursors, especially pharmaceuticals and personal care products, in wastewater. Some other tertiary amines with NDMA yields higher than DMA were found. For example, ranitidine, the active component in Zantac, a medication to decrease stomach acid production, forms NDMA at yields between 60-90% (Le Roux, 2011; Shen and Andrews, 2011a, b). In a more recent study, another pharmaceutical precursor, methadone, was also identified as an important NDMA precursor in wastewater or surface water (Hanigan et al., 2015).

NDMA yields from methadone ranged from 23%-70% depending on chloramine dose. In one wastewater sample, up to ~60% of NDMA formation was likely from methadone. These high formation yields indicate that such tertiary amines do not form NDMA through formation of a DMA intermediate, suggesting a completely different reaction pathway. Selbes et al (2013) studied NDMA formation from 21 selected amines (10 aliphatic and 11 aromatic) and they suggested that the NDMA formation mechanism starts with a nucleophilic attack of the DMA functional group on the nitrogen in chloramines (Figure 1.4). Through this pathway amines with electron withdrawing groups next to DMA functional groups react preferentially with monochloramine while amines with electron donating groups react preferentially with dichloramine. The NDMA formation yields are associated with the structure of the leaving group in the amine precursors. Most amine precursors could react with both dichloramine and monochloramine but at different yields or rates. Therefore, the formation of NDMA is likely a combination of reactions between both chloramine species and amine precursors at varying yields and rates.

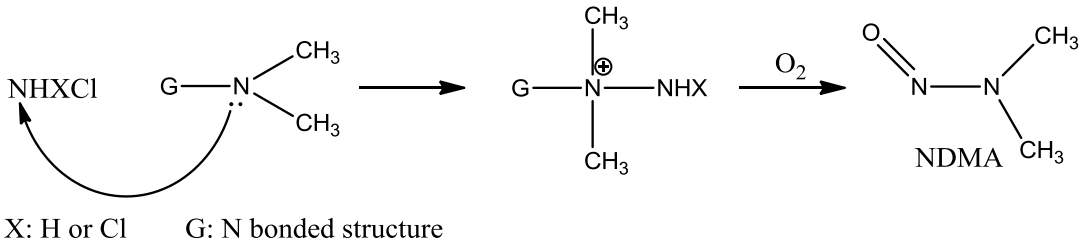

Figure 1.4: NDMA formation pathway of amine precursors and chloramines (Selbes, et al., 2013).

NDMA formation during chloramination could be affected by lots of factors besides the precursor amines structure and stability. Chloramine speciation may be the most important factor. Reactions between chlorine and ammonia form chloramines. The speciation of chloramines depends on pH, chlorine to ammonia ratio. In general,

monochloramine formation is dominant at pH higher than 8 with 5:1 or less Cl_2:N mass ratio. Chloramine chemistry is detailed in Chapter 6. In general, dichloramine would start to form as pH decrease and Cl_2:N increase. The pH also has an impact on the amine precursor. For example, the maximum NDMA formation from precursors such as DMA or ranitidine were observed between 7 and 8 (Mitch and Sedlak, 2002b; Kim and Clevenger, 2007; Shen and Andrews, 2013a). It was suggested that at pH lower than 7 there are less non-protonated amines to undergo the nucleophilic substitution on chloramines; and at higher pH, there is lower dichloramine formation resulting in lower NDMA production. However, due to the fact that NDMA formation is not limited to only one chloramine species, the pH effect on NDMA would vary with precursors and their reactivity to chloramines. Chloramine dose and contact times are important factors. Experiments have shown higher NDMA concentrations with higher chloramine doses (Sacher et al., 2008) or longer contact times in drinking water distribution systems (Russell et al., 2012).

NDMA formation kinetics of some amine precursors have been investigated. Schreiber and Mitch (2006) suggested the rate of NDMA formation from DMA and dichloramines are associated with DMA, dichloramine and dissolved oxygen concentrations. Le Roux et al. (2012) reported the ranitidine decomposition in chloramination follows a first order kinetics and a second-order reaction kinetics was assumed for NDMA formation from ranitidine and monochloramine. However, the NDMA formation was not found related to decomposition of ranitidine. Shen and Andrews (2011b) applied the concept of dose-response curves to model NDMA formation kinetics. The developed model fitted NDMA formation from four pharmaceuticals (e.g. ranitidine) in surface water very well, but it did not provide information of the formation mechanisms. Although wastewater effluents are thought

as the major source of NDMA precursors, no kinetics research has ever been conducted in wastewater due to the complexity of precursor types and various NDMA formation mechanisms.

1.4 Rationale and Objectives

NDMA toxicity, occurrence and formation have been widely studied over several decades now, in food, air and water. Despite all this work, NDMA exposure of the general public is still not well understood because of knowledge gaps in terms of occurrence, formation and fate, both in air and water. This work aims to contribute to closing these knowledge gaps on NDMA exposure through contributions to atmospheric measurements and fate as well as aqueous formation processes, by using experimental as well as modeling approaches.

With the re-emerging concern of potential NDMA exposure in air, as a result of carbon sequestration efforts, novel, sensitive but cheap methods of measuring gas phase NDMA concentrations are required. Analytical methods based on Solid Phase Extraction (SPE) and Solid Phase Microextraction (SPME) coupled with Gas Chromatography-Mass Spectrometry (GC-MS) were developed and evaluated in Chapter 2 of this thesis. Typical analytical methods in previous studies were not able to measure NDMA in ambient air at ng/m^3 concentration or were expensive and logistically challenging to perform. We have therefore developed SPE and SPME based methods successfully used in determining NDMA in other matrices such as drinking water or foodstuffs to the determination of NDMA in air. The SPE method was then applied in field sampling and NDMA were measured in ambient air. The new methods will provide us with more easy and economical ways to measure NDMA at in gas phase and help to investigate NDMA formation, transportation and health risk in the atmosphere.

The fate of atmospheric NDMA is strongly linked to its photolysis, which is the main atmospheric sink of the compound together with cloud processing. The fate of NDMA in fogs and clouds remains not well understood because of the potential "screening effect" resulting from the competition of photons from other cloud constituents like ions and organic matter. Any such screening effect will delay atmospheric photodegradation, potentially enhancing lifetimes by orders of magnitude. In Chapter 3 NDMA photolysis experiments were conducted in the presence of inorganic ions and dissolved organic carbon in atmosphere relevant concentrations. The results show substantial reduction in photolysis rates, largely due to organic compounds. An extensive characterization of the water soluble organic carbon was then performed to show that the optical properties like mass absorption coefficient (MAE) and absorption angstrom exponents (AAE) change by atmospheric sample type (aerosol, fog, cloud) and by location or particle size. The results suggest that the absorptivity of water soluble organic matters in aerosol more than that in atmospheric aqueous phases (fog, cloud) and is dependent on sources of aerosol particles.

Besides the air we were also interested in the aqueous formation during water treatment, in particular chloramination. Until now very little research has been performed on NDMA formation kinetics in complex water sources. In Chapter 4 NDMA formation kinetics during chloramination were explored in surface and wastewater effluents. Two doses of chloramines were used to simulate FP conditions and simulated distribution system (SDS) conditions. A second order reaction model of NDMA formation from monochloramine and precursors was developed based on kinetics data of NDMA formation and monochloramine decomposition during chloramination. The model fits NDMA formation well ($R^2 > 0.88$) in all source waters; and rate constants were in a narrow range (0.01–0.09 $M^{-1}s^{-1}$) for different waters.

In Chapter 5 the NDMA formation kinetics model developed in Chapter 4 was applied to NDMA formation data from the literature including different water sources and model compounds. The kinetic model parameters were optimized and the resulting model performances are discussed. The model fitted NDMA formation from model compounds and surface water under a variety of reaction conditions. The rate constants were able to describe how water conditions such as DOC and pH affect the NDMA formation kinetics.

The developed model in Chapter 4&5 needs to be further developed. It only takes monochloramine into account as the oxidant while dichloramine have shown influence on the NDMA formation kinetics. In Chapter 6 some more experiments were designed and conducted to further develop the kinetic model of NDMA formation. Parameters such as dissolved oxygen, chloramine speciation and buffer solution were included in this part.

Finally Chapter 7 summarizes the findings of this work and provides an suggestions for future follow up work.

CHAPTER 2

N-NITROSODIMETHYLAMINE (NDMA) MEASUREMENT IN AIR

2.1 Introduction

N-Nitrosodimethylamine (NDMA) is classified by the U.S. Environmental Protection Agency (EPA) as a probable human carcinogen (U.S.EPA, 2002). NDMA has been of great concern since it was discovered at up to 130 μg/m^3 and 36 μg/m^3in industrial and ambient air respectively in the 1970s (Fine et al., 1976a, b; Walker et al., 1978). These concentrations of NDMA were monitored primarily in industrial areas (such as rubber, leather and rocket fuel production) and around sources of nitrosamine precursors. NDMA and tobacco-specific nitrosamines were then detected in indoor environments with active tobacco smoking (Brunnemann et al., 1977; Stehlik et al., 1982; Mahanama and Daisey, 1996). At that time substantial research on occurrence in air and resulting human exposure was performed.

In recent years NDMA in ambient has received renewed interest for several reasons. First, recent studies have detected NDMA in concentrations up to 500 ng/L in fogs and clouds (Herckes et al., 2007; Hutchings et al., 2010), due to the high water solubility of nitrosamines and hence a concentration of these species in atmospheric droplets. Although NDMA is very easily photolyzed in the gas phase (Tuazon et al., 1984), it can be formed in nighttime air as the result of the atmospheric reaction of dimethylamine with nitrogen oxides (Hanst et al., 1977) and the subsequent partitioning into the cloud droplets appears to contribute most of the NDMA in fogs and clouds (Hutchings et al., 2010). In addition, model calculations have shown that NDMA may remain in air for more than 4 hours even past sunrise. This led to an emerging concern for the development of carbon sequestration and storage. In fact, in the process of amine-based CO_2 sequestration, where in post-combustion, the amines from the

absorber and NO_x from the flue gas are jointly emitted, have high potential to from nitrosamines in air (Strazisar et al., 2003; Nielsen et al., 2012). NDMA was also reported in particulate matter $PM_{2.5}$ and PM_{10} at ng/m3 level (Akyüz and Ata, 2013; Farren et al., 2015). U.S.EPA has calculated a residential air screening level of 0.07 ng/m^3 (exposure of 24 h/day in 25 years) and an industrial air screening level of 0.88 ng/m^3 (exposure of 1h/day in 25 years) at target cancer risk of 10^{-6} (U.S.EPA 2015). Hence, monitoring NDMA in air is crucial with the reemerging concern about NDMA in the air.

Techniques of sampling or monitoring NDMA as well as other nitrosamines in air have been developed over the past few decades. Among them are wet sampling techniques using cold traps and wet traps such as KOH (Spiegelhalder and Preussmann, 1983; Mahanama and Daisey, 1996) ; however, these labor intensive wet trap techniques had sample recovery problems (Mahanama and Daisey, 1996) and the preparation of aqueous traps was challenging in field settings. Then sampling cartridges containing various dry sorbents (e.g. silica gel) were developed to collect NDMA from the gas phase (Rounbehler et al., 1980; Spiegelhalder and Preussmann, 1983). Still some limitations persisted such as the need for a nitrosation inhibitor to prevent nitrosamine formation during sampling or the possibility of sample breakthrough. Thermosorb/N, designed and developed specifically for Nitrosamine sampling, was found to be the only sorbent free of artifact formation (Rounbehler et al., 1980). Thermosorb/N cartridges with Gas Chromatography-Thermal Energy Analyzer (GC-TEA) or Gas Chromatography–Mass Spectrometry (GC-MS) have been applied in standard nitrosamines monitoring methods such as those by the Occupational Safety & Health Administration (OSHA) or the National Institute for Occupational Safety and Health (NIOSH) with a detection limit at µg/m^3 levels (OSHA, 1981; NIOSH, 1994).

In the recent studies the detection limit of nitrosamine was reported less than 0.1ng/m^3 by using thermosorb/N and GC-TEA (Tønnesen et al., 2011). The low detection limit was achieved using a specifically constructed multi-line sampling device and very large volume (>100 m^3) air sample which is substantially larger than the validated sample volume of thermosorb/N as sorbent, causing unknown sample breakthrough. It was still not practical for NDMA or nitrosamine measurement in ambient air at low concentration.

Besides the offline measuring techniques, real time or online methods measuring nitrosamine in air directly by using instruments such as GC-MS (Agilent, 2012), Proton-Transfer-Reaction Time-of-Flight Mass Spectrometry (PTR-ToF-MS) (Karl et al., 2013) and selected ion flow tube mass spectrometry (SIFT-MS) (Langford et al., 2015)were also developed. Lacking extraction and concentration prior to injection, these methods are quite limited because of their high detection limits, typically at ~µg/m^3 level.

In recent years however, NDMA also became an emerging contaminant in drinking water due to its formation as disinfection byproducts during chloramination. Numerous methods were developed to monitor NDMA and other nitrosamines in aqueous samples. Solid phase extraction (SPE) coupled with GC-MS was one of the most widely used method determining NDMA in wastewater and drinking water (Munch and Bassett, 2004; Hanigan et al., 2012; Selbes et al., 2013). Solid phase microextraction (SPME) with GC-MS or GC-TEA were also employed for measuring nitrosamines in aqueous and food matrices (Andrade et al., 2005; Grebel et al., 2006; Pérez et al., 2008; Hung et al., 2010).

In the present work we are evaluating the use of commercial SPME or SPE cartridges for atmopheric monitoring of NDMA. Laboratory experiments were

performed to evaluate the use of SPE cartridges and SPME fibers in the measurement of gas phase NDMA. Positive and negative artifact formation was investigated for the more sensitive SPE method and the optimized method was applied to determine NDMA and other nitrosamines in ambient samples.

2.2 Materials and Methods

2.2.1. Chemicals and Materials

NDMA (solution in methanol, 5000 mg/L), EPA 8270 nitrosamine mix (solution in methanol, 2000 μg/L) and dimethylamine (DMA) (solution in methanol, 2.0 M) were purchased from Sigma-Aldrich (St. Louis, MO). N-nitrosodimethylamine-d6 (NDMA-d6) (1 g/L in methylene chloride (DCM)) was purchased from Cambridge Isotopes (Andover, MA). All the above stock solutions were then diluted to desired concentrations using DCM (Optima Grade, Fisher Scientific, Waltham, MA). All standards were stored in a freezer prior to use. Aqueous NDMA solutions were prepared by dissolving NDMA into >18 MΩ cm deionized water (Milli-Q, Millipore) to desired concentrations. Anhydrous sodium sulfate was purchased from Sigma-Aldrich (St. Louis, MO). Nitric oxide gas (>99.5%) was purchased from Praxair (Bethlehem, PA) and diluted to desired concentrations with lab air at 22 ± 1°C.

2.2.2. NDMA Gas Sampling Test

To test the NDMA sampling approaches, a simple laboratory-made setup was used as detailed in Figure 2-1. Continuous airflow containing gas phase NDMA was generated by pumping air through an aqueous NDMA solution of known concentration in a 250 mL gas washing bottle. In the SPE sampling tests, a continuous gas flow went through two successive coconut charcoal SPE cartridges (2 g/6 mL, Supelco, Bellefonte, PA). The second cartridge was used to test for possible breakthrough. During the entire

sampling, SPE cartridges were wrapped with Aluminum foil to prevent photolysis of collected NDMA.

A similar set-up was used for SPME testing. The air containing NDMA passed through an SPME gas sampling bulb (Sigma-Aldrich, St. Louis, MO) at a constant flowrate as shown in Figure 2.1. A manual SPME holder was employed in extraction and desorption of all the samples. Two different fibers, an 85 μm carboxen/ polydimethylsiloxane (CAR/PDMS) and a 65 μm polydimethylsiloxane/divinylbenzene (PDMS/DVB) were evaluated. All SPE and SPME tests were carried out at 22 ± 1 °C in the laboratory.

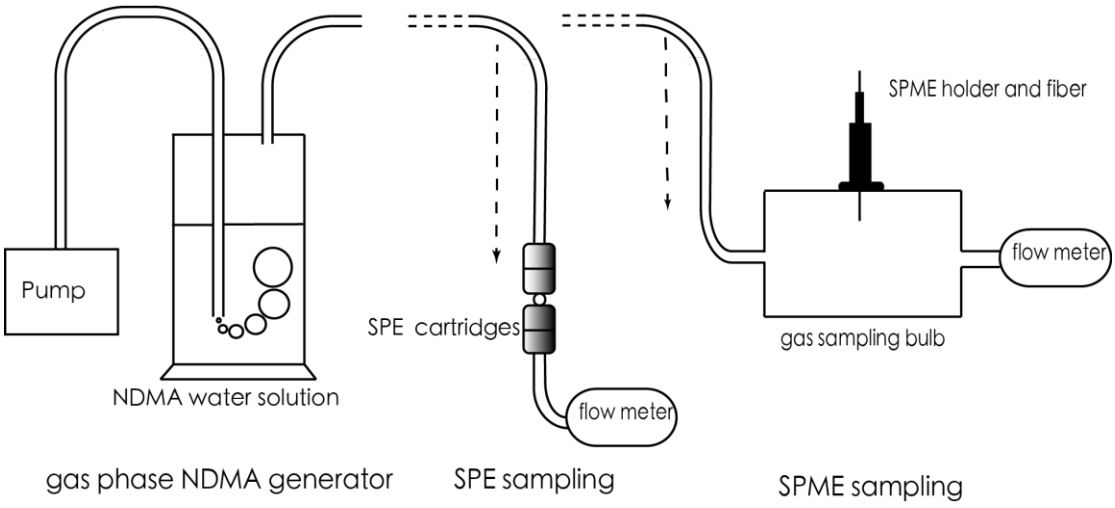

Figure 2.1: Set-up of SPE and SPME sampling test

2.2.3 Positive and Negative Artifact Formation Tests

One potential artifact during NDMA collection onto SPE cartridges is NDMA formation through reactions between dimethylamine (DMA) already sorbed onto the cartridge and nitric oxides (NO_x). To test the potential impact of this artifact, SPE cartridges were loaded with DMA passing a DMA solution over the cartridge followed by drying the cartridge with nitrogen gas for 30 minutes. Then laboratory air mixed with NO_x at concentrations ranging from 0 to 30 ppb was passed through the pretreated

SPE cartridges. For each sample, NO_x containing air was passed through cartridges for 0.5-8 h at 3.7 L/min. Control experiments without preload DMA and /or NO_x were operated under similar experimental conditions.

A negative artifact could occur if NDMA sorbed to the SPE cartridges degrades during sampling, e.g. is oxidized or photolyzed. This negative artifact was evaluated by passing ambient dry air with high oxidant concentrations through SPE cartridges which were preloaded with NDMA. Sampling times ranged from 5 minutes to 1 hour. All these negative artifact tests were performed on the roof of Life Science Building in Arizona State University Tempe campus and in sunny afternoons between 2 PM and 4 PM in summer when oxidants such as ozone and OH radical were at their highest concentrations and no detectable gas phase NDMA were found.

2.2.4 Ambient Air Sampling

Ambient air samples were collected at the Tempe campus of Arizona State University, in Western Norway and in Bakersfield, California. The weather during sampling was clear with no rain or fogs. Air samples were acquired using a laboratory-built gas sampler consisting of an air pump that was operated at 5- 8 L/min drawing ambient air through a coconut charcoal SPE cartridge. The flowrates were monitored at the beginning and the end of the sampling period. The cartridges were wrapped in aluminum foil during the collection and then kept frozen after collection until analysis.

2.2.5. Extraction and Analysis of NDMA

Prior to extraction, all SPE cartridges were spiked with 100 μL NDMA-d6 at 1ppm as internal standard. Nitrosamines and NDMA-d6 were then eluted from SPE cartridges with 30 mL of DCM. After extraction, the DCM extracts were treated with anhydrous sodium sulfate to remove water residual and then concentrated under stream

of Ultra High Purity (UHP) nitrogen gas to 250 μL. The final extracts were stored in amber vials in freezer prior to GC/MS analysis.

The sample extracts were analyzed using an Agilent 6890N/5973 inert GC/MS operated in positive chemical ionization mode with ammonia as the reagent gas (Charrois et al., 2004). In brief, the chromatographic column used was an Agilent DB-1701P (30 m × 0.250 mm × 0.25 μm)(Santa Clara, CA) and followed a pulsed splitless injection (initial pulse 15 psi for 45 s and then 10 psi) set at 250°C with a reduced diameter SPME inlet linear (Sigma Aldrich, St. Louis, MO). The helium carrier gas was initially pulsed at 1.9 mL/min for 45 s and then reduced to 1.3 mL/min for the rest of the run. The oven temperature was initially 40°C for 3 min followed by an increase to 80 at 4°C /min, and a final temperature increase to 120 at 20°C/min when NDMA were tested. The column interface temperature was set at 200°C. The mass selective detector was set to analyze for mass-to-charge 92 (NDMA + NH_4^+) and 98 (NDMA-d6 + NH_4^+). The GCMS was calibrated with a series of authentic standards and quantification was performed against the NDMA-d6 internal standard.

In SPME tests, each fiber was conditioned in the GC inlet at 250°C to remove any contaminants for 5 minutes and cooled down to room temperature prior to sampling. SPME fibers were exposed in a gas sampling bulb where laboratory air containing NDMA passed through. After a defined amount of exposure the fiber was retracted into the needle and immediately injected into the heated injection port at 250°C for 5 minutes using the same GC-MS method described above. Blank air samples were also tested to determine the possible contamination from the laboratory air.

2.3 Results and Discussion

2.3.1. Evaluation of SPME as Sampling Medium

Two SPME fibers, an 85 μm CAR/PDMS fiber and a 65 μm PDMS/DVB fiber, were examined for gas phase NDMA measurements. A variety of SPME fibers were developed and applied to measure N-nitosamines in water and food matrices in previous studies (Andrade et al., 2005; Grebel et al., 2006). These two fibers were selected because they were more widely used with more N-nitrosamines extraction compared to other fiber coatings such as polyacrylate (PA) and carbowax/divinylbenzene (CW/DVB).

Sorption of NDMA on a SPME fiber is an equilibrium process, the fiber equilibration times were tested from 30 minutes to 9 hours for both SPME fiber coatings at different NDMA concentrations. Figure 2.2a and 2.2b show the effect of time on the NDMA recoveries on two SPME fibers respectively. For the CAR/PDMS fiber, the response area of NDMA kept increasing with time even after 9 hours (Figure 2.2a) suggesting that equilibrium was not yet reached. Previous studies reported shorter equilibrium time (4 h) of NDMA extraction in headspace of water by CAR/PDMS fiber at 65 °C, possibly due to the change of absorptivity at different temperatures. In contrast, equilibrium was reached within 30 minutes at tested concentrations for PDMS/DVB fiber (Figure 2.2b). Previous studies measuring NDMA in beer reported 200h as equilibrium time for the same SPME fiber. It is possibly because of the competition or interference of other more volatile compounds from beer.

NDMA gas phase concentrations were calculated from aqueous concentrations and Henry's constant derived from our measurements. For the same NDMA concentration in air (9 $\mu g/m^3$) for all extraction time periods the NDMA signals and

hence adsorbed NDMA in the CAR/PDMS fiber were more than one order of magnitude higher than that in the PDMS/DVB fiber. It agreed with previous findings that CAR/PDMS fiber outperformed the PDMS/DVB fiber in terms of NDMA recovery (Grebel et al., 2006; Ventanas and Ruiz, 2006). CAR and DVB are both porous solids which enhance the sorption. Pore size distribution is different. CAR had a higher proportion of micropores (<20 Å) than the DVB (Lestremau et al., 2001), making it more efficient to extract low molecular weight polar compounds such as NDMA.

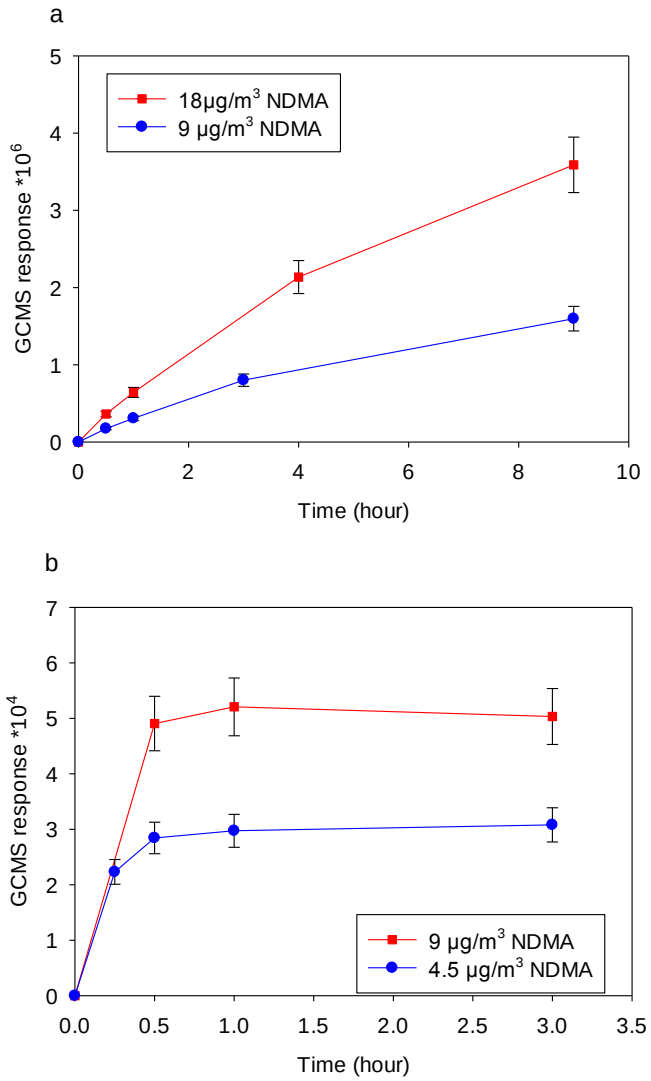

Figure 2.2: GC-MS responses of NDMA absorbed on SPME fibers at different sampling times, a: CAR/PDMS fiber coating, b: PDMS/DVB fiber coating

Linear regression analysis of adsorbed NDMA at three concentration levels was performed for both SPME fiber coatings by plotting the calibration curves of obtained mass spectrum response area versus the gas phase concentration of NDMA. Extraction time of 30 minutes was chosen for both SPME fibers. Though the CAR/PDMS had longer equilibrium time, it still could be used in NDMA analysis by using non-equilibrium extraction at a selected extraction time (Grebel et al., 2006). The correlation coefficients were 0.97 and 0.81 for PDMS/DVB and CAR/PDMS fibers respectively, showing better performance of PDMS/DVB in quantitative analysis than the CAR/PDMS. The poorer linearity of CAR/PDMS could be due to the low reproducibility caused by CAR coating (Popp and Paschke, 1997) and non-equilibrium regime. The influence of the air flowrate was also tested by varying the sampling flow through the gas sampling bulb from 0.1 L/min to 1L/min (PDMS/DVB fiber) in 30mins sampling intervals. The amounts of NDMA detected were very stable with a low standard deviation (4.9%, n = 4).

The achieved detection limits, which was calculated as concentrations which signal-to-noise (S/N) ratio equals 3, were 8 ng/m^3 and 0.5 ng/m^3 for PDMS/DVB fiber and CAR/PDMS fiber, respectively. The detection limit was not sensitive enough to detected NDMA at levels lower than 1 ng/m^3. However the SPME sampling method might be suitable in NDMA measurements in industrial environments where NDMA concentrations far above 10 ng/m^3 were reported.

2.3.2. SPE sampling tests

In a first stage, the sampling efficiency of commercial SPE cartridges was tested. No NDMA was detected in the third cartridge when three cartridges were used in series, even at high gas phase NDMA concentrations (16 µg/m^3) and/or high flowrates (6 L/min). Two consecutive cartridges were used in tests to quantify breakthrough and

physical losses by re-volatilization of sorbed material. The collection efficiency was defined as the amount of NDMA collected in the first cartridge divided by the amount of NDMA in both cartridges. The collection efficiency and breakthrough were evaluated in two ways. First is to pump the air containing NDMA through the cartridges. Flowrate ranged from 0.3 L/min to 5.8 L/min. The NDMA concentration were changed from 16 μg/m_3 to 3 ng/m^3. Laboratory air only was also tested with NDMA concentration of 0.8 ng/m^3. As shown in Table 2-1, the SPE cartridge had collection efficiencies higher than 90% in most tests. NDMA concentrations and flowrates showed no effect on the collection efficiency. Second is pumping the air through the two cartridges after spiking 100 ng NDMA on the upstream cartridges. The cartridges were dried with laboratory air for 30 minutes at 5.8L/min. After 30 minutes drying, the downstream cartridge was connected to collect the breakthrough or the physical losses from the first cartridge. No detectable NDMA was found in the second cartridges after the cartridges were dried.

Table 2.1. SPE collection efficiency tests

Flowrate L/min	NDMA Conc. ng/m3	Collection Efficiency
0.3-1.3	1800-16000	93-99
2	159	92
3.7	18-130	82-93
5.8	3-6	95
5.8[1]	0.8	98
5.8[2]		100

[1]. Lab air only
[2]. NDMA preloaded

Based on our experiment, the Henry's law constant of NDMA, determined using the calculated gas and aqueous phases concentrations of NDMA was $5.3 \pm 0.4 \times 10^{-7}$

atm×m^3/mol at 22°C. With huge variance of flowrates (0.1-6 L/min) and NDMA concentrations (3-16000 ng/m^3) the calculated Henry's law constant only change with a small variance (< 10%). Previous studies reported several different Henry's law constant at different temperatures (Mirvish et al., 1976; Haruta et al., 2011). At 22°C, Henry's law constant determined in our experiments was twice of the reported Henry's constant (2.63×10^{-7} atm×m^3/mol at 20°C) which was estimated by using vapor pressure and water solubility data (Mirvish et al., 1976). The difference was not substantial considering the fact that the tests in this work were in a dynamic aqueous-gas system and were at a higher temperature. The Henry's law constant in our dynamic experiment conditions can be used to determine NDMA gas phase concentrations when NDMA water phase concentrations are known. For NDMA, the sensitivity of the analytical detection method, which was estimated as 3 times of the background noise, was 0.04 pg/injection. For an air sample of 0.1 m^3 (~30 min at 3L/min), the detection limit of the overall method was 0.06ng/m^3. With larger sampling volumes e.g. 2 m^3 obtained by extending sampling time or increasing flowrate the detection limit can be as low as 0.003 ng/m^3. With such a low detection limit, small sample volume and simple set-up sampling instrument, the SPE sampling method with the following GCMS analysis presented in this work is more applicable than all previous methods in NDMA measurement in ambient air.

Table 2.2: Sampling parameters in this work compared to Thermosorb/N sorbent method.

	SPME GCMS		SPE (activated carbon) GCMS	Thermosorb/N UHPLC[1]
	CAR/PDMS	PDMS/DVB		
Sample time (h)	>0.5	0.5	0.5-8	167
Sample Volume (m^3)	-	-	0.1-2	20
Detection limit (ng/m^3)	~1	8	0.003	0.01
Sample breakthrough	-	-	<10%	unknown
Flowrate (L/min)	-	0.1-1	0.3-6	2

1. Nielsen et al., 2012

2.3.3 Positive Artifact Formation Test

The sources of atmospheric NDMA are not only direct emissions of NDMA by industrial processes but also nitrosation of atmospheric amines (Hanst et al., 1977). These nitrosating reactions could possibly occur on the surface of the collection cartridges during sampling if sorbed amines react with a nitrosating reagent (i.e. NO_x), leading to a positive artifact formation. The latter was a concern as it was reported that commercial activated carbon could catalyze the formation of reactive nitrogen specious (e.g. NO) from oxygen and nitrogen in the reactive sites on the activated carbon surfaces (Padhye et al., 2011). Therefore the possible formation of NDMA from the reactions between Dimethylamine (DMA) and such NO_x during the sampling process was explored. One nanomole DMA in DCM solution was spiked onto the cartridges, simulating maximum DMA in 0.1 m^3 ambient air (Ge et al., 2011). Pure NO was diluted in lab air to 30 ppb_v which was similar to the upper limit of NO_x concentrations in ambient conditions. After pumping the NO_x/air mixture through the cartridges, the cartridges were extracted following the SPE procedures.

No NDMA was detected on the DMA preloaded cartridges. Only at substantially higher DMA (1μM) loadings, NDMA was detected. The overall NDMA

formation yield (NDMA formed/DMA spiked) was 0.15% when lab air with no NO_x passed the cartridges. The formation yield increases to 0.24% in the presence of air containing 30 ppb_v NO_x. Previous studies reported the similar NDMA formation yields 0.05% -0.29% in air-dried activated carbon particles from preloaded DMA (Padhye et al., 2011). In actual ambient air (~pmol/m^3) the DMA concentrations are orders of magnitudes lower than those in our experiments (nmol/m^3) (Ge et al., 2011). While NDMA can and will form by nitrosation of amines on the cartridge during sampling, the resulting artifact is negligible compared to typical ambient concentrations. This is even more true as the DMA collected in real air samples would be much less than we used in lab test due to the fact that sampling was a continuous process but total amount of DMA was loaded in SPE cartridges in the beginning.

2.3.4 Negative Artifact Formation Test

Negative artifact formation by losses of sorbed NDMA could also be possible during sampling. While physical losses and hence breakthrough, were discussed above (section 2.3.2), chemical loss mechanisms are also possible. In particular direct photolysis of NDMA is possible and is the major loss mechanism for NDMA in the gas phase (Hutchings et al., 2010). However during SPE sampling, photolysis could be easily prevented by wrapping cartridges in aluminum foil.

Other than photolysis, atmospheric reactions between NDMA and oxidants such as ozone or hydroxyl radicals could possibly lead to NDMA sampling losses (Tuazon et al., 1984). Therefore, the possible oxidation of NDMA was investigated by loading NDMA on a cartridge and passing ambient air through the cartridge. No significant loss of the preloaded 2 ng NDMA was observed after 2 hours of sampling at 6 L/min. This is not unexpected as reported gas phase reaction rates of NDMA reaction with O_3 and OH· (< 1.0×10^{-20} and 3.0×10^{-12} cm^3/molecule/s) and the upper

limits of O_3 and OH· concentration (2×10^{12} cm^{-3} and 1×10^{6} cm^{-3}) the half-life of NDMA was more than 3 months and 2.5 days in presence of O_3 and OH· respectively. Therefor the effect of such oxidation processes on NDMA sampling appears negligible.

2.3.5 Ambient SPE Results

With a lower detection limit, the SPE sampling method was applied to determine NDMA in ambient air samples. NDMA concentrations observed at different sites are summarized in Table 2.3. All NDMA concentrations in our observations were orders of magnitude lower than in previous studies in 1970s & 1980s (40-36,000 ng/m^3) which mostly focused on the heavily polluted industrial indoor environments and urban areas clearly impacted by or adjacent to such industries (Fine et al., 1976b; Spiegelhalder and Preussmann, 1983). However, NDMA concentrations measured at all sampling sites are higher than the 0.07 ng/m^3 residential air screening concentration at 10^{-6} lifetime cancer risk level by EPA.

In Tempe (AZ) NDMA was detected in relatively low concentrations, ranging from 0.4-0.7 ng/m^3. There are no nitrosamine or amine related industries in the vicinity. The low humidity in Tempe can be another reason for low concentrations of NDMA since NDMA formation in air from nitrosation is preferable during nighttime when the air is humid (Hanst et al., 1977). Air samples from Norway showed a similar but lower concentration of NDMA in air (0.1-0.3 ng/m^3). In other studies measuring NDMA at similar locations no NDMA or nitrosamine was found (Nielsen et al., 2012). However, NDMA found in this work agreed with the expected NDMA concentration range (0.02-0.1 ng/m^3) based on DMA concentrations monitored (0- 31 ng/m^3) and potential NDMA formation yield (~ 0.3%) in other studies.

The highest NDMA concentrations (5.9 -13.0 ng/m^3) in our studies were found in Bakersfield, CA. There are several possible explanations. Bakersfield is located in the Central Valley in California where NOx and humidity are relatively high and there is higher probability of amine precursors because of the presence of large feedlots.

Table 2.3: Measurement of NDMA in gas phase

Location	NDMA (ng/m^3)	Ref	Scenario
Tempe, AZ (2011-2012)	0.4-0.7	This work	ambient outdoor
Bakersfield, CA (2013)	5.9-13.0	This work	ambient outdoor
Mongstad,Norway (2012-2013)	0.1-0.3	This work	area around the Mongstad refinery
Fresno, CA (2010)	8.4	(Hutchings et al., 2010)	ambient outdoor
Mongstad, Norway (2011)	ND	(Nielsen et al., 2012)	area around the Mongstad refinery
Linz, Austria (1987)	10-40	(Spiegelhalder and Preussmann, 1986)	ambient outdoor
Los Angeles, CA (1978)	30-1000	(Gordon , 2012)	Industrial sites
Baltimore, MD (1976)	400-32000	(Fine et al., 1976b)	Industrial sites

It is noteworthy that in the air samples from Bakersfield, CA, other nitrosamines including nitrosodibutylamine (NDBA) and nitrosodiethylamine (NDEA) were also detected. Both NDBA and NDEA had similar concentrations to NDMA in all air samples from Bakersfield. However their concentrations must be considered estimates since laboratory tests, such as collection efficiency or artifact formation has not been conducted.

2.4 Conclusions

In this work, SPME and SPE techniques with following GCMS analysis were evaluated as sampling method measuring gas phase NDMA in ambient air. SPME-GCMS method was tested using PDMS/DVB and CAR/PDMS fibers. SPME sampling is not a favorable method to determine NDMA air concentrations due to the high

detection limits (> 1 ng/m^3). However, SPME method had its own advantages over other methods. It is solvent free, environmentally friendly and labor efficient. SPME technique could still be used to monitor high NDMA concentration especially for high NDMA concentration in indoor environment. The developed SPE-GCMS method is shown to be favorable for the analysis of NDMA in air in many aspects. The simple set-up and small sample volume needed in this method make it easy and economical for outside ambient sampling. The high collection efficiency and small positive/negative potential artifacts make it applicable in various sampling conditions. The detection limit for NDMA with this method was less than 0.003 ng/m^3, lower than the EPA risk level (0.07 ng/m^3) and previous methods.

By using SPE-GCMS method, NDMA was found in all ambient samples in a rather small range (0.1-13.0 ng/m^3) among different locations. Presence of other nitrosamines was also detected. Further evaluation will be needed on SPE or SPME sampling performances of other nitrosamines.

CHAPTER 3

OPTICAL PROPERTIES OF WATER SOLUBLE ORGANIC CARBON (WSOC) IN ATMOSPHERIC AEROSOLS AND FOG/CLOUD WATERS

3.1 Introduction

In recent years, there has been a growing concern about nitrosamine compounds, especially nitrosodimethylamine (NDMA), due to their carcinogenicity. They have been widely found not only in drinking water (Mitch et al., 2003) but also in the atmospheric waters like fogs and clouds (Herckes et al., 2007). A recent study discussed the enrichment of nitrosamines in fogs and clouds and emphasized on the fact that while nitrosamine photolyze readily, they will concentrate in fog and cloud droplets especially at night time (Hutchings et al., 2010) and might persist into the daytime. Post combustion CO_2 capture (PCCC) plants are currently using amines (e.g. monoethanolamine, piperazine) as solvent to capture and store CO_2, leading to emission of amines and their degradation products (Rochelle, 2009; da Silva et al., 2013a; da Silva and Booth, 2013). Nitrosamines are of concern for PCCC because they can form from their corresponding amines and NO_x which are in flue gas or in ambient air (Veltman et al., 2010; Reynolds et al., 2012; da Silva et al., 2013b). Several nitrosamines including NDMA, N-nitrosodiethanolamine (NDELA) and N-nitrosomorpholine (NMOR) have been observed at concentrations ranging from 5 to 47 ng/m^3 in emission from a PCCC pilot plant (da Silva et al., 2013b).

It was reported that the main source of NDMA in fogs and clouds is not in cloud nitrosation of amines to NDMA (Hutchings et al., 2010). With a low Henry's constant (2.63×10^{-7} atm m^3/mol) (Mitch et al., 2003), NDMA formed in the gas phase will partition into the atmospheric aqueous phase and accumulate. However, it does not

explain by itself NDMA's occurrence in clouds and fogs at high concentrations since NDMA has been reported to be highly photoreactive in aqueous solution with half-lives ranging from 3-18 min depending on experimental conditions (e.g. irradiation intensity) (Stefan and Bolton, 2002; Plumlee and Reinhard, 2007; Hutchings et al., 2010). The organic matter in a wastewater matrix was found to have limited impact on NDMA photolysis by decreasing photolysis rate by 20%-70% (Chen et al., 2010). Still no studies exist on NDMA photolysis in atmospherically relevant matrices (fog, clouds) or the organic matter in the atmosphere could have stronger impact on NDMA photolysis than waste water organic matter and substantially change NDMA lifetime in the atmosphere.

Atmospheric aerosols are an important part in radiative forcing of climate. Among atmospheric aerosols, carbonaceous aerosol are a significant fraction and carbonaceous material can be divided into elemental or black carbon (EC or BC) and organic carbon (OC). It was thought that EC mainly absorb light whereas OC scatters radiation in the atmosphere (Hallquist et al., 2009). Several recent studies found organic species also absorb solar radiation effectively (Andreae and Gelencser, 2006), and organic species can contribute up to 50% of the light absorption (Kirchstetter et al., 2004), especially in the UV-vis range. Up to 70 % of atmospheric OC is water soluble organic carbon (WSOC) (Jeffrezo et al., 2005; Feng et al., 2006; Park and Cho, 2011). Light-absorbing aerosol organic carbon is often referred to as brown carbon (BrC) and mostly soluble as part of the WSOC. WSOC is important because it influences the ability of aerosols to act as cloud condensation nuclei (CCN) and the dissolution of WSOC into clouds and fogs affects cloud chemistry. Since the absorption of WSOC is significant in the UV-vis range (hence "brown" carbon), WSOC is expected to impact the photochemistry of light-sensitive compounds such as NDMA, which are easily

photolyzed in atmosphere but in clouds will compete with the organic matter for photons.

The sources of atmospheric WSOC include primary emissions including biomass burning or fuel combustion and secondary formation from gas and particle phase precursors (Sullivan et al., 2006; Miyazaki et al., 2006; Weber et al., 2007; Yan et al., 2009). Many studies have investigated the light absorbing or optical properties of WSOC or BrC in atmospheric aerosols. The wavelength-dependent absorption is usually characterized as proportional to $\lambda^{-Å}$. The absorption angstrom exponents (AAE), Å, exhibits distinct variations between BC and OC and in WSOC from different sources, locations and seasons (Kirchstetter et al., 2004; Cheng et al., 2011; Du et al., 2014; Kirillova et al., 2014; Kim et al., 2016). The mass absorption efficiency (MAE) of WSOC is another optical property that varies by location, season and origin (Hecobian et al., 2010; Cheng et al., 2011; Zhang et al., 2011). However, limited information is available on the influence of WSOC on cloud photochemistry.

The present work investigates the effect of WSOC and inorganic ions on NDMA photolysis in the atmospheric aqueous phase. The optical properties of WSOC were then investigated in atmospheric aerosol, fog and cloud droplets from different locations and from a variety of sources including urban, rural, biomass burning and vehicle emission. Two representative optical parameters, AAE and MAE, were compared between aerosol and fog/cloud sample as well as among aerosol from different sources, providing information on how the optical properties and hence the effects of WSOC on the cloud photochemistry might vary.

3.2 Experimental and Analytical Methods

3.2.1 Sample Collection

Particulate matter samples for spectral characterization were obtained from a number of field studies in the US, Mexico and Canada for ambient aerosol samples and from controlled burn experiments for biomass burning source samples. Details are provided in Appendix A.

Cloud samples were obtained from field studies in Arizona (Hutchings et al., 2009) and Whistler, Canada (Lee et al., 2012). Fog samples were obtained from studies in Fresno, CA and Davis, CA (Ehrenhauser et al., 2012) as well as from rural Pennsylvania (Straub et al., 2012)

Ambient aerosol samples ($PM_{2.5}$) for the photochemical experiments were collected in Fresno (CA) during an earlier study (Ehrenhauser et al., 2012) and on the Tempe campus of Arizona State University (ASU). More detailed site descriptions are provided in Appendix A.

3.2.2 Sample Preparation

The water soluble organic carbon (WSOC) fraction was determined as follows. One section of a quartz fiber for each aerosol sample ($PM_{2.5}$ and $PM_{>2.5}$) was extracted under ultrasonication with 15mL deionized (DI) water (>18MΩ cm) for 30 minutes. All water extracts of aerosol samples as well as fog and cloud water samples were filtered through a 0.22 µm pre-fired QFF filter (Whatman, UK) using syringe filtration in a stainless steele filterholder. Filtered aliquots were stored in a refrigerator in the dark at 4 ºC until analysis.

NDMA solutions in prepared by diluting NDMA in 150 mL DI water and in 150 mL water soluble extracts from two aerosol samples collected in Fresno (CA) and Tempe (AZ). Nitrate and nitrite were added into aliquots to simulate the occurrence of

NO_3^- and NO_2^- at environmentally relevant concentrations. NaOH or H_2SO_4 were used to adjust the pH to desired value.

3.2.3 Sample Analysis

Nitrate and nitrite were determined by ion chromatography (Dionex IC20) using a Dionex AG12A guard column, an AS12A separation column, and suppressed conductivity detection. The pH value in different water matrices was determined by pH meter (Denver Instruments) after calibration against pH 4 and 7 buffer solutions.

All photolysis tests were performed using 500 ppt NDMA solutions in batch experiments. Each experiment used 150 mL of solution which were extracted using a method similar to EPA method 521 and analyzed using gas chromatography- mass spectrometry (GC/MS) after the experiment. NDMA extraction and analysis details can be found elsewhere (Hanigan et al., 2012; Zhang et al., 2016).

DOC concentrations in samples were determined using a total organic carbon (TOC) analyzer (Shimadzu TOC-5050A) which was calibrated against potassium hydrogen phthalate standards. The light absorption spectra of WSOC extracts or fog and cloud samples were recorded over a wavelength range from 200 to 700 nm with Shimadzu Multispec-1501 UV-Vis spectrometer. The absorption spectra were characterized using the absorption angstrom exponents (AAE) and the mass absorption efficiency (MAE). The AAE was obtained by Equation 3-1:

$$A_\lambda = K \cdot \lambda^{-\mathrm{AAE}} \qquad \text{Equation 3-1}$$

Where A_λ is the absorbance at wavelength λ, K is a constant. AAE values were calculated based on the linear regression fit of A_λ between 300 and 600 nm on log-log plots.

The MAE is the absorption efficiency normalized to the organic carbon concentration. In some fields it is also referred to as the specific absorbance (SUVA)

in UV range in surface water (Chen and Westerhoff, 2010). Mass absorption efficiency (MAE) at 365 nm was used to characterize the light absorptivity of OC in different water extracts or fog/cloud samples. It was calculated using the following Equation 3-2, similar to other studies (e.g. Du et al., 2014):

$$MAE_{365} = \frac{A_{365}}{WSOC\ concentration} \qquad \text{Equation 3-2}$$

3.2.4 Photolysis Set-up

All irradiation experiments are carried out within a solar simulator set up (Figure 3.1) consisting of a Spectra-Physics (Stratford, CT) 200-500W power supply, a 300W ozone free Xe lamp, a water filter, an air mass 1.5 global (AM 1.5G) filter, a manual shutter, a recirculating water chiller, and a 200mL jacketed flask. The jacketed flask can be sealed with an O-ring and a Teflon lid which has a Suprasil quartz window with an opening diameter of 3.2 cm. This solar simulator utilizes the AM1.5G filter to simulate solar irradiation at a 48.2^{o} solar zenith angle which corresponds to the solar irradiation in the 48 contiguous states of the United States. The combination of the 300W ozone-free Xe lamp, the water filter, and the AM1.5G filter produces typically an actinic flux of 1.07×10^{16} photons $cm^{-2}s^{-1}$ for this solar simulator. The actinic flux has been determined using 2-nitrobenzaldehyde as a chemical actinometer following the procedures of Allen et al (2000) and the actinic flux will be re-verified regularly. This actinic flux is comparable to the actinic flux at the Earth's surface in Phoenix, Arizona at noon during winter which is 1.31×10^{16} photons $cm^{-2}s^{-1}$ (Finlayson-Pitts and Pitts, 1999).

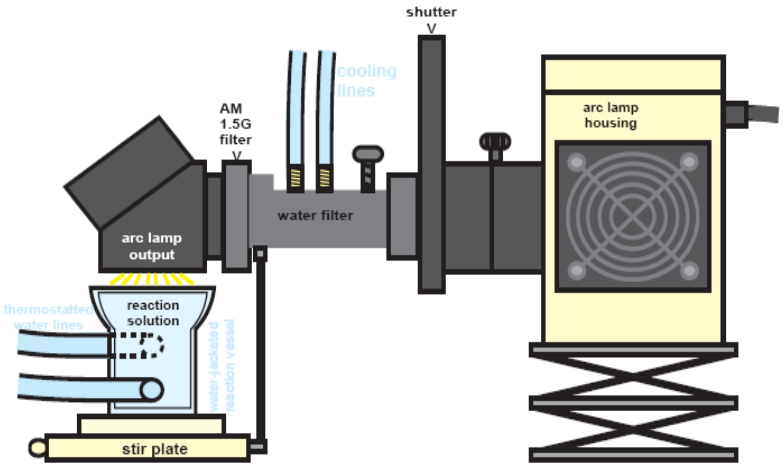

Figure 3.1: Image of irradiation setup with the water chiller, irradiation flask, lamp, filters, and power source

3.3 Results and Discussion

3.3.1 WSOC effect on NDMA photolysis

NDMA photolysis rates have been characterized in select matrices like surface water (Chen et al., 2010) in which organic matter could potentially decrease the photolysis rates of NDMA. Due to limited sample of fog and clouds, water extracts of aerosol samples were used as surrogate of atmospheric organic matter. We investigated the impact of WSOC from ambient aerosol samples described in section 3.2.2. WSOC showed dramatic effects on the photolysis rates. Even at moderate WSOC concentrations of 7-9 mgC/L, well within the range of many cloud and fog observations (Herckes et al., 2013), the photolysis rates are decreased by a factor of 2-3 resulting in double to triple lifetimes (Table 3.1). At the higher end of the WSOC concentrations, the photolysis was completely suppressed in our tests.

Table 3.1: Half-lives of NDMA in various matrices and at different WSOC concentrations

WSOC	DOC (mgC/L)	Half-life t1/2 (min)
Nanopure Water	0	14.2
Tempe, AZ	9.3	37.3
	16.0	66.6
	23.4	--[1]
Fresno, CA	7.5	39.9
	20.4	117

1. No degradation was observed in 120 min.

Possible interferences including pH and inorganic ions (NO_3^-, NO_2^-) were also investigated. No effect of pH was observed during 2 h photolysis in NDMA solution at pH from 1.2 to 6.8 which covers a wide range of cloud and fog pH observations (Herckes et al., 2013). These observations are contrary to previous studies which saw a pH effect on NDMA photolysis (Plumlee and Reinhard, 2007).

Nitrite and nitrate are common components of fogs and clouds. It was suggested that both species could affect NDMA photolysis since they have similar absorbance around 300nm as NDMA which mainly absorbs at 330nm (e.g. Plumlee and Reinhard, 2007; Hutchings et al., 2010). Our results show that at high end of environmentally relevant concentrations (2000 µeq/L and 100 µeq/L for nitrate and nitrite respectively) these inorganic species could result in an increased atmospheric lifetime of NDMA (relative to its aqueous phase photolysis) of 30~50%. However in a more typical concentration range for nitrate and nitrite, as in clean to moderately polluted clouds and fogs, the effect would only be in the 10-20% range. Therefore WSOC likely has the strongest impact on NDMA photochemistry in atmospheric aqueous phase.

3.3.2 Wavelength Dependence of Light Absorption

The absorption spectra of aerosol extracts and fog/cloud filtered samples were measured between 200nm and 700nm. Figure 3.2 shows the UV-Vis spectra of aerosol extracts which have 1 mg/L nitrate and nitrate standards at 1 mg/L. Nitrate has strong absorbance at wavelength < 250 nm and contributes up to 50% of the total absorbance at 200 nm in WSOC. However, absorbance of nitrate is negligible at wavelengths > 250 nm in the presence of WSOC. The majority of the absorbance was from the organic components in WSOC.

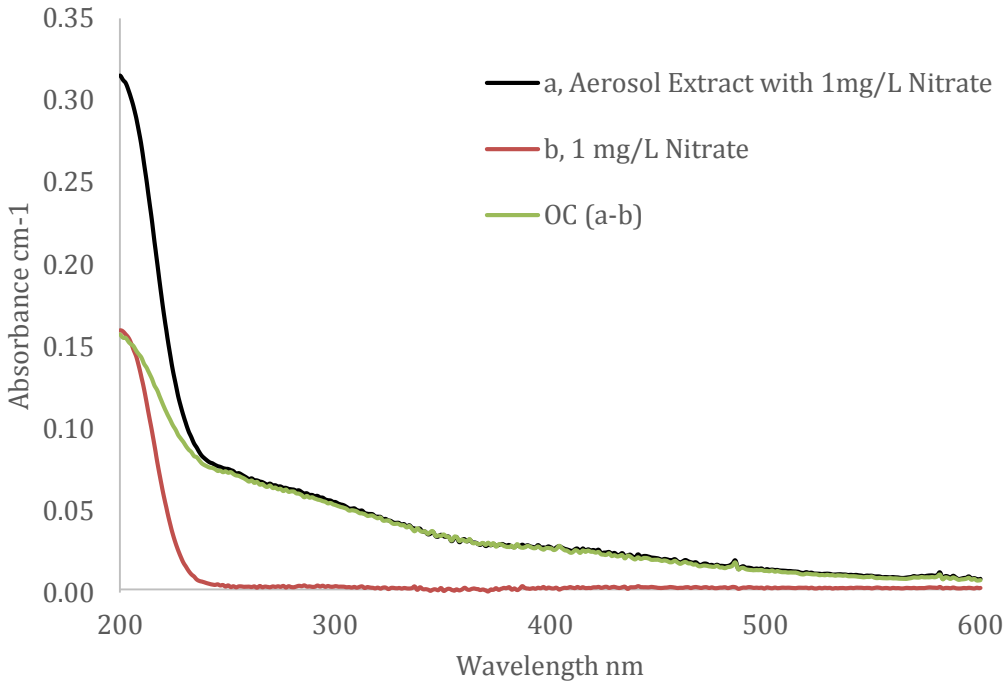

Figure 3.2: UV-Vis absorbance of WSOC with 1 mg/L nitrate and 1.4 mgC/L dissolved organic carbon (a), 1 mg/L nitrate (b) and the dissolved organic components (a-b).

The wavelength dependence of light absorption was investigated using the AAE calculated between 300 nm to 600 nm. In most samples, signals below 300 nm had interference of inorganic species and therefore were not included. The AAE of aerosol, fog and cloud samples were shown in Figure 3.3.

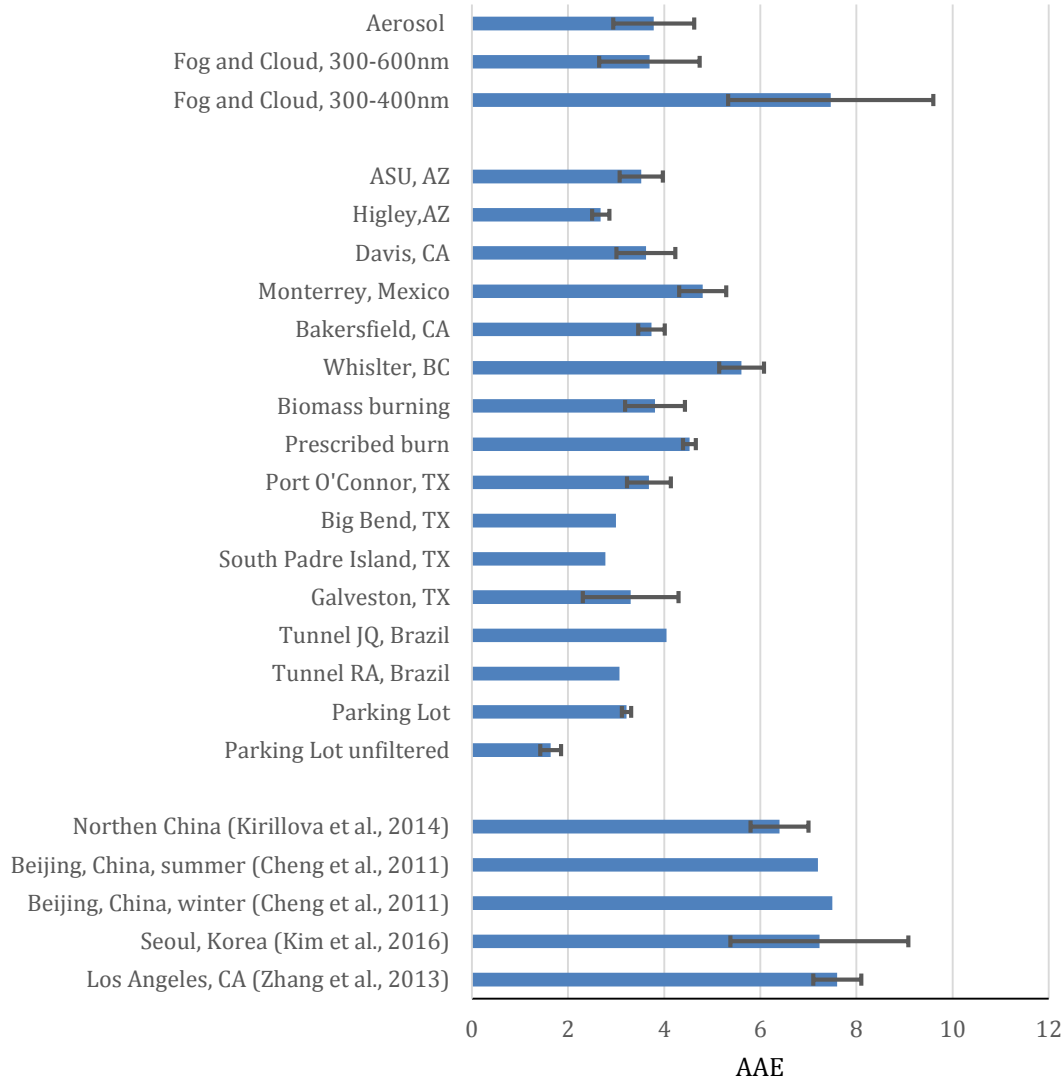

Figure 3.3: AAE for WSOC from aerosol and fog/cloud samples

The AAE of unfiltered and filtered aerosol water extracts from the emission impacted aerosols were compared (Parking Lot & Parking Lot unfiltered in Figure 3-3). AAE in unfiltered extracts (1.64 ± 0.22) were substantially lower than filtered extracts (3.57 ± 0.44). It was reported the AAE for BC is close to 1, while AAE of organic matter is larger than 1 (Bond, 2001; Kirchstetter et al., 2004). The soot in unfiltered extracts might have lowered the AAE of the light-absorbing organic matter. In addition, absorption in unfiltered extract does not follow the Equation 3-1 well with lower log-log regression R^2 (0.81) than filtered extracts (0.99). In this work, the AAE

of all WSOC extracts varied between 2.52 and 6.45 with average of 3.78 ± 0.84. The linear fit of the log(λ) and logA(λ) showed good correlations, with $R^2 > 0.92$ except the samples from Bakersfield, CA. For the fog and cloud sample, AAE were between 2.02 and 5.12 with an average 3.69 ± 1.04. This is the first attempt ever characterizing the absorptivity of dissolved organic carbon by AAE in fog and cloud samples.

The cloud and fogs samples show a wider range of AAE compared to aerosol WSOC although there are fewer samples and lower R^2 values (0.22-0.98) were observed in some fog/cloud samples, suggesting different organic components between aerosol and fog/cloud and among fog/clouds samples from different locations as well. Additionally, it was found for fog/cloud that the AAE calculated between 300 nm and 400 nm (7.46 ± 2.13) are substantially different from above AAEs above 400 nm. The AAE suggests that chromophores absorb mainly below 400 nm in fog/cloud water. However, in aerosol extracts a similar trend of AAE was not observed.

The AAE observed in aerosol extracts were lower than what was reported using similar extraction methods in previous studies. For example, the AAE was calculated to be 7.23 ± 1.58 and 7.2-7.5 for WSOC in aerosol from Seoul and Beijing respectively (Cheng et al., 2011; Du et al., 2014; Kim et al., 2016). AAE values close to 7 were reported for water extracts collected in Los Angeles and the southeastern United States (Hecobian et al., 2010; Zhang et al., 2013). It was suggested based on AAE values in previous studies that BrC are mainly from biomass burning and SOA formed from anthropogenic precursors since biomass burning humic-like substances (HULIS) and SOA have similar AAE (~ 7) (Hoffer et al., 2006; Bones et al., 2010; Kim et al., 2016). However, in our study, the biomass burning aerosols showed a much lower AAE than (3.81 ± 0.62) than previous studies (Figure 3.3). Auto emission impacted aerosol samples, parking structure (3.21 ± 0.10), Tunnel JQ (4.05) and Tunnel RA (3.07) have

similar AAE values with other samples collected in urban (e.g. ASU or Monterrey) or rural areas (e.g. Higley or Davis).

Previous studies saw a seasonality in AAE values, in particular higher AAE values in summer compared to other seasons which was mainly attributed to the enhanced formation of SOA and strong photochemistry during summer time (Du et al., 2014; Kim et al., 2016). A similar seasonal pattern of AAE was not observed in our study in Arizona. AAE of aerosols in warmer months (Apr-Sep, 3.77 ± 0.47, n = 9) are in similar to those during the other months (Oct-Mar, 3.31 ± 0.93, n = 10). Despite the small difference of aerosol extracts AAE from varied sources such as biomass burning or vehicle emission, the narrow range of AAE values suggested that the composition of chromophores or the BrC components in aerosols might be similar.

3.3.3 WSOC in Aerosol and Fog/Cloud

In this study, absorption at 365 nm was used as an indicator of WSOC light absorptivity and screening effect of WSOC. Strong correlations were observed between A_{365} and WSOC for all aerosols extracts ($r = 0.81$, $p < 0.01$, Figure 3.4), indicating the mass normalized light absorptivity of WSOC is similar despite possibly different WSOC composition and sources.

In fog and cloud samples, A_{365} did not correlate with WSOC as well as in aerosol extracts ($r = 0.72$, $p < 0.01$, Figure 3.4), suggesting a larger variation of WSOC composition by sample location or source. In addition, in the whole range of WSOC, fog and clouds had lower absorption than WSOC extracts. This is consistent with what is known about the composition of fog and clouds organic matter in previous studies. In fog and cloud a substantial fraction (~24%) of organic matter are small molecular weight acids such as formic and acetic acids (Herckes et al., 2013). These small volatile organics (e.g. formic and acetic acids) have very low absorptivity at 365 nm. While

they are abundant in fogs and clouds, they are not commonly found in aerosol WSOC due to their high volatility. Hence we observe a kind of 'dilution' effect where a strong contribution of weakly absorbing species lowers the A_{365} of WSOC in fogs and clouds. Thus the screening effect on photolysis of NDMA in fog and clouds caused by WSOC might be lower than that in the simulated aerosols.

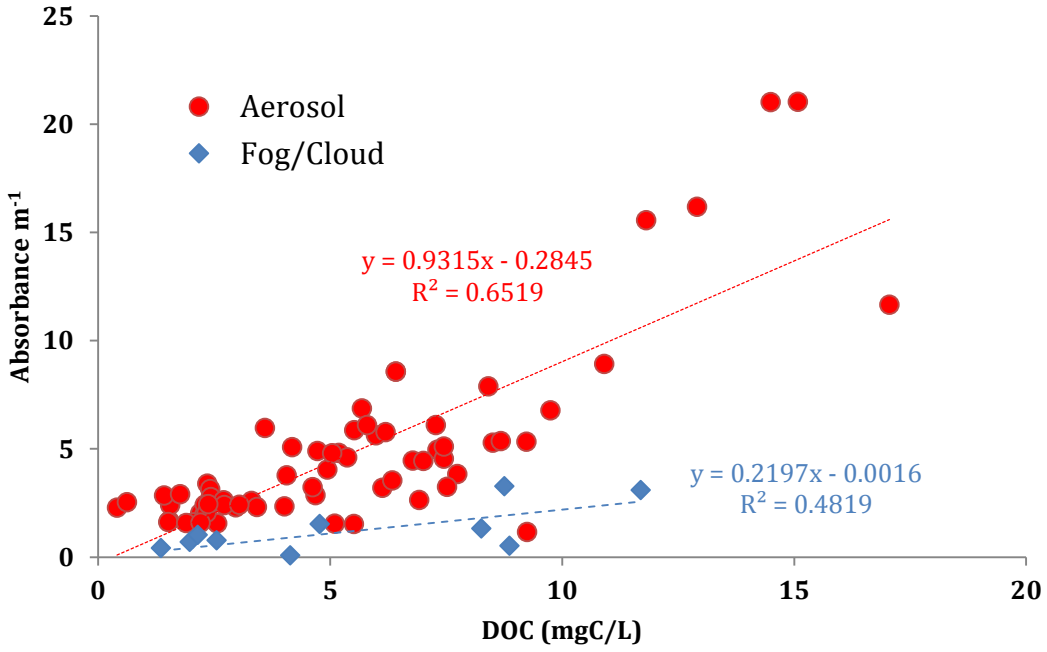

Figure 3.4: Correlation of Absorbance at 365 nm vs. WSOC for aerosol extracts and fog/cloud samples

3.3.4 MAE of WSOC

An extensive set of WSOC and fog/cloud samples was characterized optically and the MAE at 365nm was calculated by Equation 3-2. Figure 3.5 summarizes MAE values for WSOC from aerosol and fog/cloud samples collected in various environments and locations.

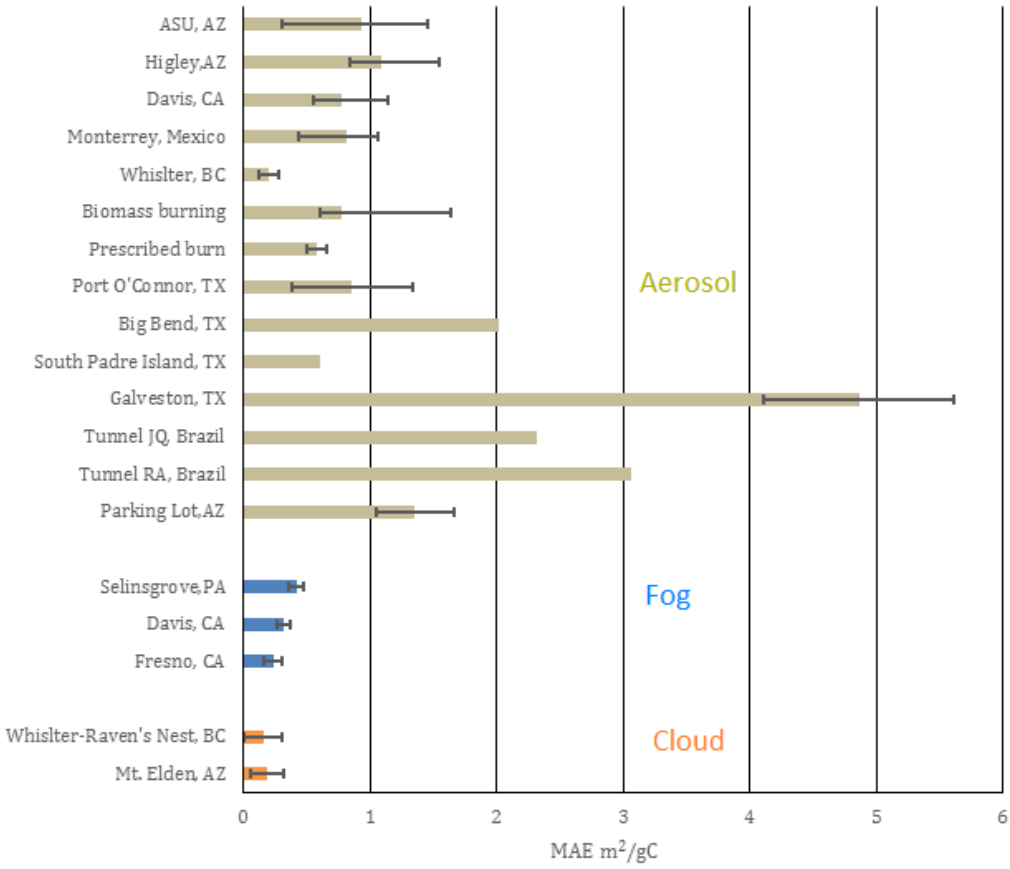

Figure 3.5: MAE values of WSOC and fog/cloud samples

WSOC from locations except Whistler, BC exhibit higher MAE than cloud/fog samples. The lower MAE in cloud/fog samples were possibly due to the presence of small volatile organics in cloud/fog as discussed in section 3.3.3. For WSOC, MAE in Whistler aerosol samples was substantially lower than all the other aerosol samples collected elsewhere. These samples were collected in a remote area on Whistler Mountain where SOA formation from biogenic VOCs is dominant and organics in those samples have smaller fraction of anthropogenic contribution than other samples. Previous studies reported a higher MAE of WSOC during summer in Los Angeles where SOA formation is dominant by anthropogenic VOCs than Atlanta where SOA are mainly from biogenic VOCs (Brown et al., 2007; Muller et al., 2008; Zhang et al., 2011). It was also confirmed by chamber experiments that SOA produced from

biogenic VOCs were less light-absorbing than that produced from anthropogenic VOCs (Nakayama et al., 2010; Zhong and Jan., 2011). This was consistent with the observed differences in MAE between fogs and clouds. The MAE values in fog samples (0.32 ± 0.10 m^2/gC) were higher than those in cloud samples (0.17 ± 0.14 m^2/gC). It may be because the fog samples were collected in lower altitude locations that were more influenced by anthropogenic compounds which have higher absorptivity. Cloud samples were all sampled at mountain sites which were more remote and which experienced a stronger impact of biogenic sources, showing lower MAE than fog samples collected in polluted urban areas.

For the other aerosol samples, MAE values also varied by sample locations and sources. WSOC in aerosol collected in Galveston showed highest MAE (4.86 ± 0.75 m^2/gC) (Figure 3.5). The high absorbing OC could come from the heavy polluted emission from many refinery and petrochemical plants in Galveston. High MAE values of WSOC were also found in samples associated with vehicle emissions. The MAE of samples collected in Tunnel JQ, Brazil and Tunnel RA, Brazil are 2.31 m^2/gC and 3.06 m^2/gC (Figure 3.5), respectively. Although there is only one sample from each location, the two tunnel samples exhibited highest MAE values amongst all samples. The Tunnel JQ sample were more associated with gasohol or ethanol fueled light duty vehicles emission while the Tunnel RA sample were more related to diesel-fueled heavy duty vehicles emission. The difference of MAE between these two samples might suggest the different absorptivity of chromophores from the two emission types. WSOC of parking lot samples have a lower MAE (1.36 ± 0.30 m^2/gC) than the tunnel samples, possibly due to the less intensive traffic activity in parking lot. However, parking lot aerosol samples still have higher MAE than urban or rural samples (e.g. ASU or Higley). The high MAE values of WSOC from mobile emission were consistent with

previous studies. For example, it was reported by Hecobian et al. (2010) that the absorptivity of WSOC was substantially higher in morning rush hour than the rest of the day, suggesting high absorptivity might be associated with primary vehicles emission. Du et al. (2014) also reported high MAE (2.89 m^2/gC) of WSOC from primary emission sources.

For urban or rural aerosol samples including ASU, Higley, Davis and Monterrey in this study, WSOC exhibited MAE values similar to that of biomass burning and prescribed burning samples. It was reported that the biomass burning is one of the major sources of the WSOC in aerosols (Hecobian et al., 2010; Cheng et al., 2011; Du et al., 2014).

A seasonal pattern of MAE values was observed in many studies in East Asia and the United States. MAE in Seoul were 1.02 and 0.28 m^2/gC for winter and summer, respectively (Kim et al., 2016). Observations in Beijing (Cheng et al., 2011; Du et al., 2014) and southeastern United States (Hecobian et al., 2010) showed similar seasonal variations. It was suggested that the higher MAE was linked to more biomass burning in winter than in summer. However, in our study no such seasonal pattern was observed in aerosol samples collected on ASU's campus. The reasons could be that there is less of a difference between SOA in the summer than in the winter month which is consistent with annual data on PM2.5 in the region.

3.3.5 Influence of Relative Humidity (RH) on MAE

Some studies suggest that haze or cloud processing cloud lead to the formation of more light absorbing carbon (Ervens et al., 2011). This hypothesis was investigated with a temporal dataset form aerosol samples collected in Bakersfield, CA during a high RH period. MAE values were calculated in 330 nm where NDMA got photolyzed. It is known that water vapor plays important role in formation organic aerosols.

Previous study reported that the ratio of WSOC between particle phase and gas phase increased with RH when RH was above ~60% (Hennigan et al., 2009). The uptake of liquid water by particles probably would enhance the partitioning of small volatile organic acids, leading to a decrease in MAE of WSOC in general. It was consistent with the absorptivity of WSOC change in Bakersfield sample. As shown in Figure 3.6, MAE changes seem to track the RH change during our sampling. The MAE values increased following the decrease of the average RH and they decreases when RH was high.

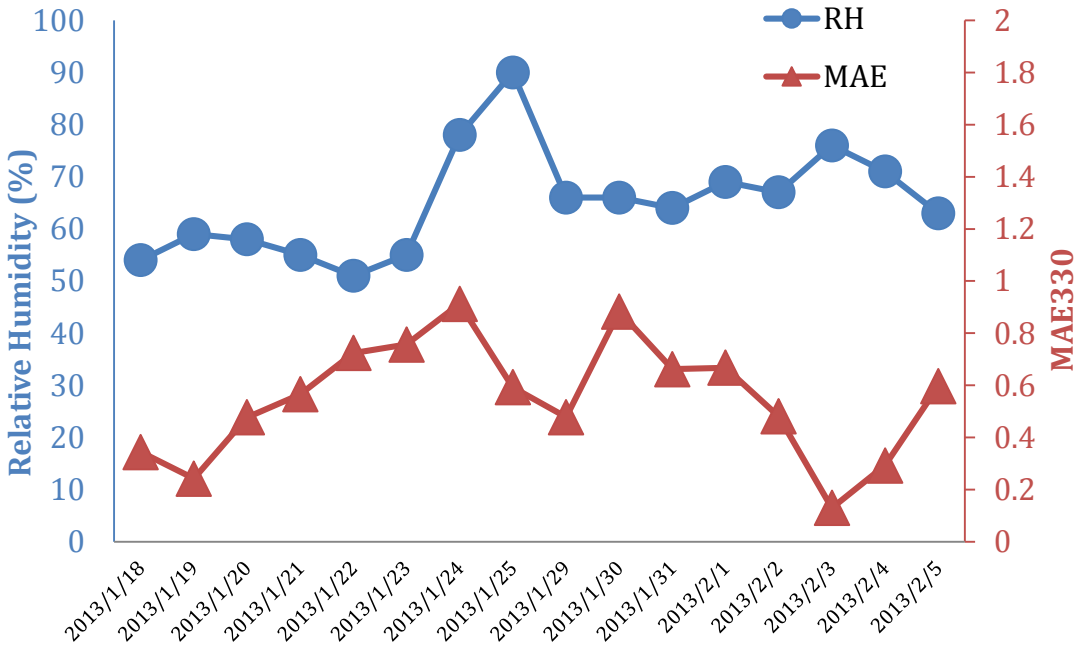

Figure 3.6: Temporal variations of WSOC MAE and RH in aerosol extracts from Bakersfield, CA

3.4 Conclusions

The screening effect of WSOC from atmospheric aerosols on NDMA photolysis and optical properties of WSOC from aerosol extracts and atmospheric aqueous phases (cloud/fog) were investigated. It was found that WSOC had more effect than inorganic species on NDMA photolysis. The organic matter screening effect observed was

substantial and even under moderate DOC concentrations for fogs and clouds, the lifetimes were increased 2 to 3 fold.

It was also found that WSOC from aerosol has a higher mass absorption efficiency than organic matter from fog and cloud waters. Combining AAE and MAE observations suggested substantially different composition in terms of chromophores between aerosol WSOC and fog/cloud samples. AAE values were similar for aerosol samples from various sources and locations, whereas MAE values were different by their sources. Anthropogenic activities such as vehicle emission were associated with high absorbing organic matters while the organic matter from biogenic sources appears to have lower absorptivity. No seasonal or temporal patterns of MAE values were found in our study. However, the MAE seem related to RH as the composition of WSOC in aerosol may change with RH.

The results of light absorptivity of WSOC in aerosol and fog/cloud samples provide more knowledge on the composition of WSOC from different samples and the formation processes of aerosol and fog/cloud and information to modeling of photolysis of light-sensitive species in atmosphere. More efforts should be made to investigate the chemical speciation of light-absorbing organic constituents in aerosol and fog/clouds for more sample sources with more samples.

CHAPTER 4

N-NITROSAMINE FORMATION KINETICS IN WASTEWATER EFFLUENTS AND SURFACE WATERS

4.1 Introduction

Occurrence studies and potential carcinogenicity of *N*-nitrosamines (NAs) in drinking water are leading the United States Environmental Protection Agency (USEPA) and some Canadian Provinces to set health standards and regulatory determinations for individual or groups of NAs. Over the past decades, NAs have emerged as a large scale concern because water utilities have increasingly relied upon chloramines for residual disinfection to meet trihalomethane (THM) and haloacetic acid (HAA) regulations (Krasner et al., 2013). Six NAs were included in Unregulated Contaminant Monitoring Rule 2 (UCMR2), and five of those were then included on the third Contaminant Candidate List (CCL3) (USPEA, 2009). *N*-nitrosodimethylamine (NDMA) was the most commonly detected NA in UCMR2 (34% of chloraminated drinking waters) with detections of four other NAs being rare (<1% of samples) and typically occurring in samples with high NDMA concentration (Russell et al., 2012). NAs, including NDMA, are classified as probable human carcinogens in water at low ng/L levels associated with a 10^{-6} lifetime cancer risk (USEPA, 2015). Based on this assessment, California's Office of Environmental Health Hazard Assessment (OEHHA) set a public health goal at 3 ng/L for NDMA (OEHHA, 2006) and California's Department of Public Health (CDPH) has set 10 ng/L notification for three nitrosamines (CDPH, 2013). Because of their potential to cause cancer, the USEPA may soon make a regulatory determination for NAs.

A recent review indicates that most studies have found that NDMA formation is more associated with chloramination than with chlorination (Krasner et al., 2013).

Systems using chloramines as the primary, rather than secondary, disinfectant have high NDMA Formation Potential (FP) (i.e., >50 ng/L) in plant effluent, indicating the potential for precursor deactivation by strong pre-oxidants such as chlorine. Since nitrosamine formation is a kinetically slow process, plants using chloramine with long hydraulic contact times in plant plus distribution system (e.g., 12–18 hr) tend to have more NDMA in the effluent than those using chloramine for short (e.g., 0.5–2 hr) contact times (Krasner et al., 2012). NDMA concentrations tend to increase throughout chloraminated distribution systems (Krasner et al., 2012a; Krasner et al., 2012b; Valentine et al., 2005; Krasner et al., 2009; Liang et al., 2011).

NA formation in drinking water requires an organic nitrogen-based precursor plus an oxidant (e.g., inorganic chloramine, ozone) (Choi and Valentine, 2002; Lee et al., 2007). Oxidation chemistry, including inorganic reactions with bromide and ammonia (Schreiber and Mitch, 2005; Le Roux et al., 2012), is important; however, little information is available regarding which organic precursors control the rate and extent of NA formation in drinking water. Mechanistic studies indicate that yields of NDMA from chloramination of most secondary and tertiary model amines are ~0–2% but can be >80% for certain tertiary amines with β-aryl functional groups (Shen and Andrews, 2011a; Selbes et al., 2013). Wastewater-impaired source waters contain NDMA precursors, suggesting the importance of anthropogenic constituents. Specific precursors have not been characterized outside of a select few (Hanigan et al., 2015) in wastewater-impaired source waters but could include either tertiary amine-based microconstituents that form NDMA at high yield or quaternary amine-based macroconstituents of consumer products that form NDMA at low yield.

Different NDMA formation pathways during chloramination are briefly illustrated in Appendix B. Despite rich literature on pathways and yields of NDMA

formation using model compounds (Mitch and Sedlak, 2004; Schreiber and Mitch, 2006a; Schreiber and Mitch, 2006b; Mitch and Schreiber, 2008; Shen and Andrews, 2011b), less information exists related to the kinetics of NDMA formation in surface and wastewaters. Many studies rely upon NDMA FP measurements which are akin to THM-FP measurements and, while useful, lack information suitable for managing DBP formation in complex hydraulic systems. Simulated distributed system (SDS) test methods for NA's have been developed, but often include a short free chlorine period (before NH_3 addition) to mimic common drinking water treatment plant (DWTP) disinfection processes. We believe a focus on NDMA formation kinetics in raw water samples will expand our understanding (i.e. profiling) of NDMA precursors.

The aim of this paper is to investigate NDMA formation kinetics in waters with lower (surface waters) and higher (treated wastewater effluents) levels of NDMA precursors. In experiments conducted with seven different waters, the decay of monochloramine and formation of NDMA were monitored. Experimental data were fit using a second-order reaction model. We observed similar magnitudes of the fitted second order apparent rate constant for NDMA formation across a range of water sources, suggesting the model represented a possible common rate limiting step that exists in most raw waters.

4.2 Experimental and Methods

4.2.1 Source Waters

Kinetic experiments were performed in seven different waters matrices, five wastewater effluents, one surface water, and one groundwater. Secondary wastewater effluents were collected at local wastewater treatment plants (WWTP) in the Metro Phoenix and Nogales regions of Arizona. The surface water was collected from central AZ surface water supplies and the groundwater was pumped from a canal in a heavily

industrial/agricultural impacted area. All water samples were filtered immediately after sampling (10 μm, CLR 1-10 Pall Corporation, Port Washington, NY) and stored in the dark at 4 °C for less than a week.

4.2.2 Reagents

All reagent water was >18.2 MΩ-cm and of laboratory grade (Milli-Q Millipore, Billerica, MA). Sodium hypochlorite (5.65−6%), sodium borate, and sodium sulfite were purchased from Fisher Scientific (Fairlawn, NJ). Ammonium chloride and anhydrous sodium sulfate were obtained from Sigma Aldrich (St. Louis, MO). Dichloromethane (DCM) and methanol were purchased from EMD Chemical (Gibbstown, NJ). NDMA was purchased through Sigma-Aldrich (St. Louis, MO). Deuterated NDMA (NDMA-d_6) was purchased from Cambridge Isotopes (Andover, MA) and diluted to 100 μg/L in Milli-Q water.

4.2.3 Chloramination Experiments

NDMA formation by chloramination of source waters was conducted in 500 mL sample aliquots using 1 L amber bottles. A borate buffer stock solution was prepared by dissolving sodium borate and boric acid in water. Aliquots were buffered at pH 8.0 - 8.2 by adding 10mM borate before chloramination. The preformed monochloramine stock solution was prepared by adding sodium hypochlorite into a borate buffered (10 mM, pH = 8.0 ± 0.1) ammonium chloride solution to produce a N:Cl_2 molar ratio of 1.2:1. For samples from each water source, experiments were conducted using two monochloramine doses, a higher dose at 15–20 mg/L and a lower dose at 5–7 mg/L to simulate FP test and SDS test conditions. After adding monochloramine, samples were allowed to react in the dark at room temperature (23 ± 1 °C). Reaction times ranged from 0 minutes to longer than 720 hours. Residual

monochloramine was measured before quenching the residual using 5 mL of 0.5 M ascorbic acid. All samples were spiked with 1 mL of 100 μg/L NDMA-d_6 and kept in the dark at 4 ºC until extraction and analysis.

4.2.4 NDMA Analysis

NDMA extraction and concentration procedures used in this work have been described previously (Hanigan et al., 2012). Briefly, activated coconut charcoal solid phase extraction (SPE) cartridges (Restek, Bellefonte, PA) were first conditioned with DCM, methanol, and HPLC grade water. Then, 500 mL water samples with isotope (NDMA-d6) were passed through SPE cartridges. After loading, the cartridges were dried using ultra high purity (UHP) nitrogen gas, and 5 mL DCM was used to elute NDMA. After being dried with anhydrous sodium sulfate powder, the extract of NDMA in DCM was concentrated under UHP nitrogen gas to 1 mL.

The extracted samples were analyzed using an Agilent 6890N/5973 inert GC/MS operated in positive chemical ionization mode with ammonia as the reagent gas (Charrois et al., 2004). In brief, the chromatographic column used was an Agilent DB-1701P (30 m × 0.250 mm × 0.25 μm) (Santa Clara, CA) and followed a pulsed splitless injection (initial pulse 15 psi for 45 s and then 10 psi) set at 250 °C with a reduced diameter SPME inlet liner (Sigma Aldrich, St. Louis, MO). The helium carrier gas was initially pulsed at 1.9 mL/min for 45 s and then reduced to 1.3 mL/min for the rest of the run. 4 μL of sample was injected into GC through the inlet, with oven temperature of 40 °C held for 3 min, increased by 4 °C /min to 80 °C and increased to 120 °C at 20 °C/min. The column interface temperature was set at 200 °C. The mass selective detector was set to analyze for mass-to-charge 92 (NDMA + NH_4^+) and 98 (NDMA-d_6 + NH_4^+). The GC/MS was calibrated using a series of NDMA standards ranging from 1 μg/L to 1 mg/L and NDMA-d_6 (100 μg/L) as internal standard.

4.2.5 Other Analyses

Free chlorine and monochloramine concentrations were measured using N,N-diethyl-p-phenylenediamine (DPD) free chlorine and Monochlor F reagents with a Hach DR5000 spectrophotometer (Hach Company, Loveland, CO). Dissolved organic carbon (DOC) was measured using a Shimadzu Total Organic Carbon (TOC)-VCSH (Shimadzu America Inc., Columbia, MD). UV absorbance was measured using a Shimadzu Multispec-150, and pH was determined with a pH meter (Model PHI410, Beckman Counter Inc., Brea, CA). Dissolved oxygen was measured by a portable meter (Thermo Scientific Inc., Waltham, MA)

4.3 Results and Discussion

4.3.1 NDMA Formation Kinetics in Wastewaters

Figure 4.1 shows NDMA formation and monochloramine decay kinetics in a secondary treated wastewater with two different monochloramine doses. The pH values remained unchanged during the reaction. Monochloramine decayed slowly over the course of the experiment (580 hours) with a monochloramine residual remaining throughout the duration of the experiments. NDMA formation reached a maximum level of ~460 ng/L (~6 nM) within 120 hours at the higher monochloramine dose and more slowly approached a lower maximum NDMA concentration ~300 ng/L (~4 nM) at the lower monochloramine dose. In addition, at higher monochloramine doses, NDMA formation increased faster and reached its maximum in less time. Thus, the concentration of monochloramine is a crucial factor of the NDMA formation kinetics via chloramination of wastewater effluents in our experiments, both thermodynamically and kinetically. Data collected for the other wastewater effluents showed a similar impact of monochloramine on the rate and yields of NDMA formation (see Appendix B Figure A1-4). The maximum NDMA formation in each experiment

will be referred to as $NDMA_{max}$, and equals the molar concentrations of NDMA precursors (P_0) in the water under the specific experimental conditions before chloramination.

Table 4.1 summarizes $NDMA_{max}$ values for each experiment. In the wastewater effluent samples, $NDMA_{max}$ ranged from 4 to 12 nM. There was no correlation found between $NDMA_{max}$ and DOC or UV_{254}, similar to statistical analyses presented elsewhere (Chen and Westerhoff, 2010; Uzun et al., 2015). In all cases, higher monochloramine doses led to 30% to >50% higher $NDMA_{max}$ values. This was unexpected because even at very long reaction times there was adequate oxidant residual present to react with NDMA precursors. Although monochloramine is the dominant chloramine species in our test (pH = 8, N:Cl_2 molar ratio 1.2:1), dichloramine, the disproportionation product from monochloramine, was still present according to the equilibrium:

$$2NH_2Cl + H^+ \leftrightarrow NHCl_2 + NH_4{}^+ \qquad \text{Equation 4-1}$$

It has been reported that dichloramine is responsible for greater NDMA formation from NDMA precursors such as DMA (Shen and Andrews, 2011b; Schreiber and Mitch, 2006b). Additionally, NDMA precursors were found to react preferably with either monochloramine or dichloramine (Selbes et al., 2013; Le Roux et al., 2011). Thus, in our experiment, even trace levels of dichloramine formed could affect the maximum NDMA formation. At higher doses of monochloramine there would be more dichloramine enhancing the NDMA formation and in contrast a low monochloramine concentration solution would contain less dichloramine, resulting in less NDMA formation.

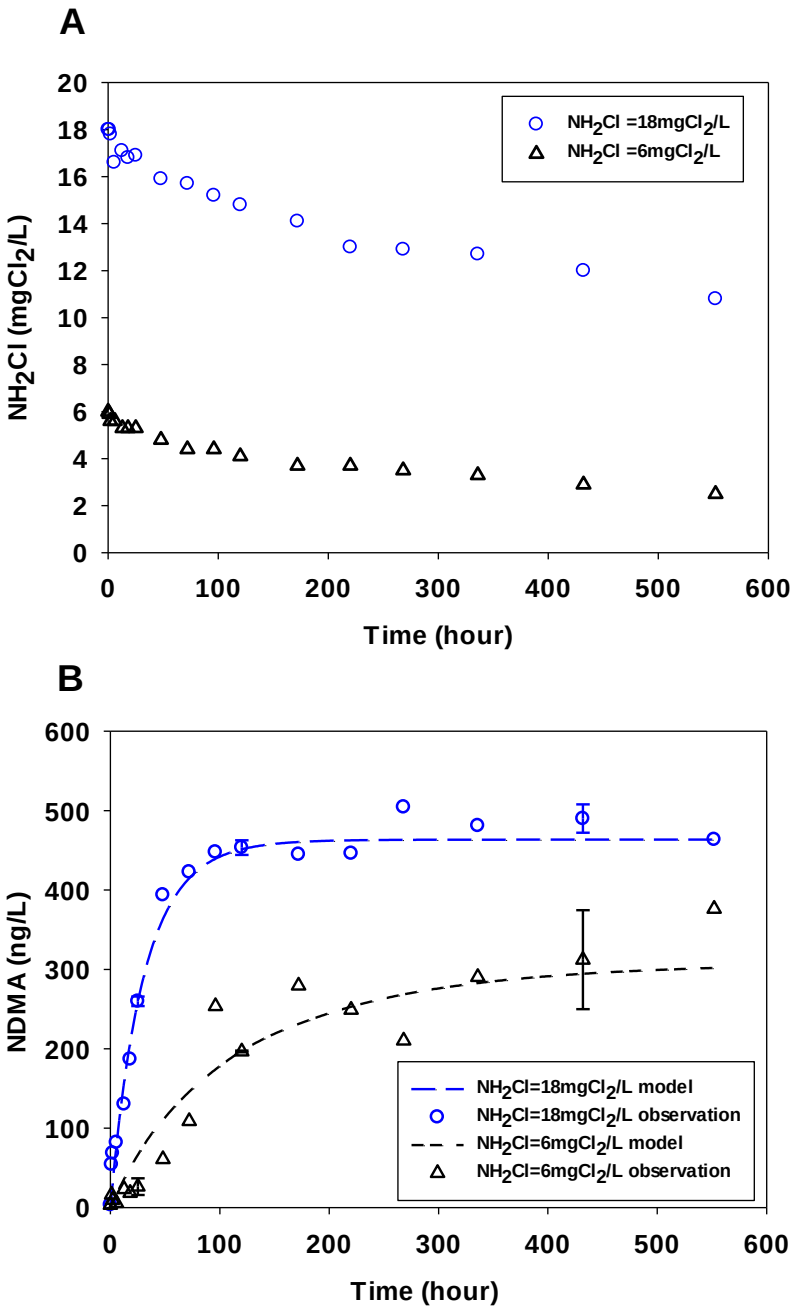

Figure 4.1: (A) Monochloramine (NH_2Cl) decay kinetics in WW1 for two initial monochloramine doses. (B) NDMA formation observed (symbols) and fitted by equation 2&3 (lines). Error bars represent one standard deviation (n = 3) for select time points. (pH = 8.2, Temperature = 23 ± 1 °C)

4.3.2 NDMA Formation Kinetics in Surface Waters.

Despite having DOC concentrations of similar order of magnitude, NDMAmax values in the surface water (3.9 mgC/L) were approximately an order of magnitude lower than in wastewater (DOC 4.6-6.2 mgC/L) (Table 1). Figure 4.2 shows that the reaction proceeded over hundreds of hours before NDMA approached a maximum concentration. NDMA formation was less and slower in surface water samples than in wastewater. Monochloramine residual slowly decayed during the experiments and was present throughout the duration of the experiments. In our test in surface water at two monochloramine doses (Figure 4.2), the quick NDMA increase within hours possibly indicated the fast reaction part of NDMA and the slow NDMA increase thereafter showed a slow and rate limiting step of NDMA formation. Similar NDMA formation kinetics tests from natural organic matter (NOM) in surface water were made by Chen and Valentine (Chen and Valentine, 2006). These authors separated NDMA precursors in NOM into two groups and postulated that the fast-reacting group reacts with monochloramine within hours while the slow-reacting group reacts with HOCl over days respectively. However, the fast-reacting group forming NDMA was not monitored in their work due to the low time resolution. Such fractionation of NDMA precursors remains controversial. The two kinetic parts (fast vs. slow) were not observed in the wastewater samples (Figure 4.1, Appendix B) in similar conditions (e.g. DOC and NH_2Cl), possibly due to the difference in amine precursors between wastewater and surface water. Similar to wastewaters, NDMA formation in surface water at high monochloramine dose was enhanced, possibly due to presence of more dichloramine.

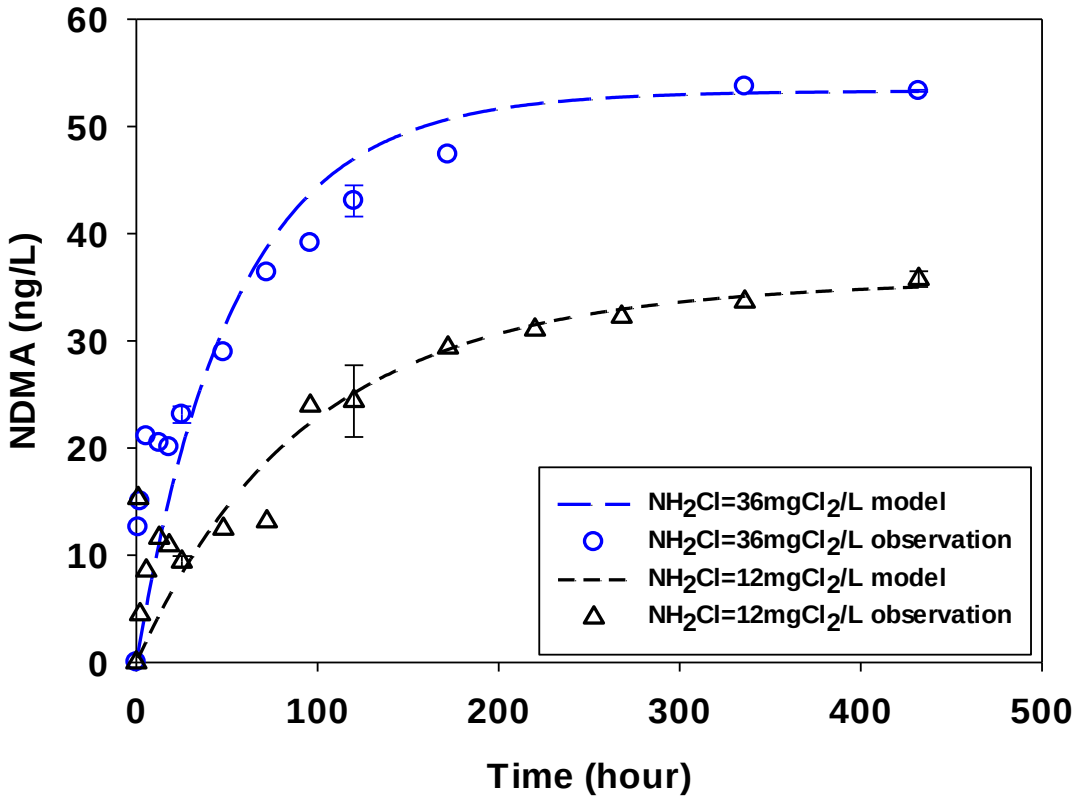

Figure 4.2: NDMA formation observed (symbols) and fitted by equation 2&3 (line) in SW at two initial monochloramine doses. Error bars represent one standard deviation (n = 3) for select time points. (pH = 8.0, 23 ± 1 °C)

The groundwater had $NDMA_{max}$ (15-20 ng/L) on the same order of magnitude with, but lower than the surface water (30-50 ng/L). It is possibly because it contained less DOC (1.78 mg/L) in groundwater. No two kinetic parts (fast vs. slow) were observed and NDMA formation reached maximum in less than 100 hours (Figure 4.3) at two monochloramine doses.

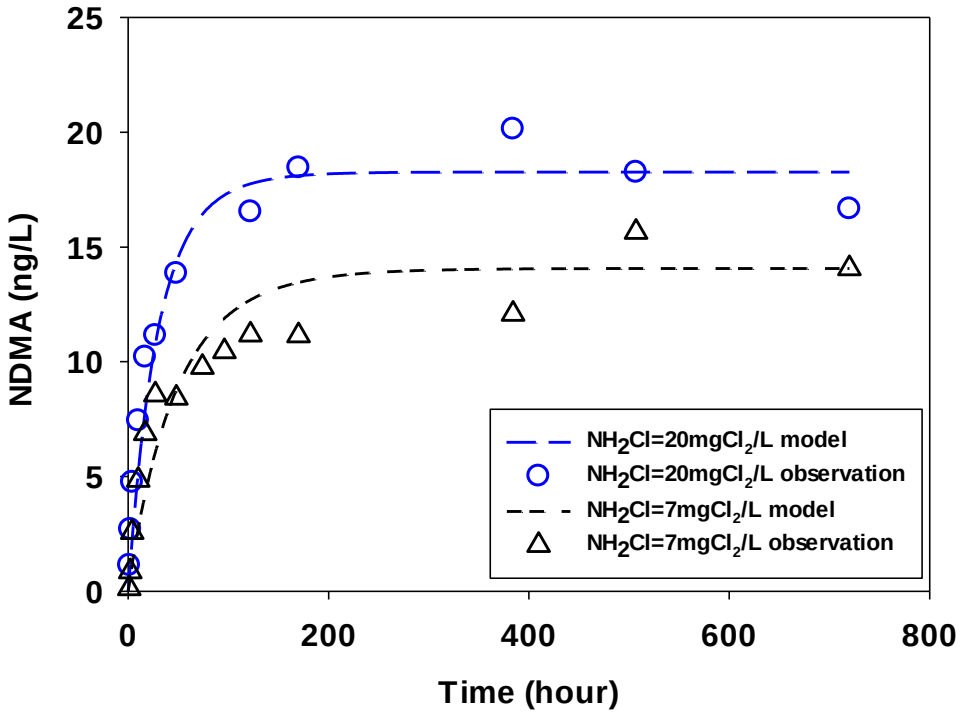

Figure 4.3: NDMA formation observed (symbols) and fitted by Equations 2&3 (line) in GW at two initial monochloramine doses. (pH = 8.0, 23 ± 1 °C)

In summary, in all water samples the overall NDMA formation at high monochloramine dose was higher than at low monochloramine dose. Wastewaters showed higher NDMA formation (200-950 ng/L) than surface waters (30-50 ng/L) and groundwater (15-20 ng/L). The reaction times for NDMA formation reaching its maximum were shorter when higher monochloramine doses were applied in wastewater and groundwater. No significant difference of such reaction times was found between the two doses of chloramine in surface water. The differences in NDMA formation potential are due to the various types and concentrations of precursors in the different source waters. Precursors such as DMA, which is more reactive with dichloramine, may explain the higher and faster NDMA formation at higher doses of monochloramine. Recent research found that pharmaceutical compounds such as methadone, which was found in wastewater effluents has high yields of NDMA and

could contribute to large fractions of total NDMA formed. It is possible that such high yield precursors are also more reactive to chloramines making the NDMA formation in wastewater relatively faster. So higher amine concentrations and higher levels of these known high yield NDMA precursors may be responsible for a higher overall NDMA formation in wastewater than in other water sources. Compared to the differences in NDMA yields in source waters, the differences in kinetics or rates were rather small. Molecular identification of NDMA precursors and NDMA formation kinetics of these precursors are needed to improve our understanding of NDMA formation in real waters.

4.3.3 Model Fitting of NDMA Kinetics.

Three main pathways for NDMA formation have been proposed and are summarized in the APPENDIX B. Initially we envisioned that different types of precursors may proceed along different mechanistic pathways to produce NDMA, involving a range of intermediates and potentially involving oxygen reactions. In tests performed in this work, fractions of NDMA precursors with different rates were not evident in surface water and were not observed in wastewater effluents. In addition, it was not practical to classify NDMA precursors (nM quantities) as either having higher or lower yields and presumably different reaction rates as they are water source specific. Based on NDMA and monochloramine concentrations observed in our kinetic experiments, NDMA formation was fit to Equation 4-2: for the reaction of NDMA precursors (P) in the presence of monochloramine (NH_2Cl):

$$\frac{d[P]}{dt} = -k_{app}[P]^m[NH_2Cl]^n \qquad \text{Equation 4-2}$$

P is the NDMA precursor concentration and k_{app} is a best fit rate constant. Here we only count the 'active' compounds that form NDMA as NDMA precursors. So we assume a 1:1 relationship between the disappearance of the precursor (P) and NDMA formation (m = 1). The rate order with respect to NH_2Cl (n) was calculated ~1 (n = 1.20 $\pm$ 0.41) by plotting log [NDMA formation rate] vs. log [NH_2Cl] in the same time period for the same water at two NH_2Cl doses. Therefore we used the second order expression (m = n = 1, Equation 2) to fit to the data. The concentration of NDMA at any time ([NDMA(t)]) is related to the maximum amount of NDMA precursors available for reaction in an experiment ($[P]_0 = [NDMA_{max}]$) as follows:

$$[\mathrm{NDMA(t)}] = [\mathrm{P}]_0 - [\mathrm{P}]_t \qquad \text{Equation 4-3}$$

where $[P]_t$ is calculated from Equation 4-2. It is noteworthy that NDMA is only one of the byproducts of reactions between organic compounds and chloramines. $[P]_0$ in Equation 4-3 refers to the precursors that would form NDMA under certain conditions (e.g. pH = 8, known NH_2Cl concentration) and was measured as $NDMA_{max}$, when NDMA stopped increasing. NH_2Cl degradation involves various reactions such as hydrolysis and reactions with inorganic or organic species (e.g. NDMA precursors). Monochloramine degradation was fit by measured NH_2Cl concentrations at selected time points with a first order model in which the decomposition rate of monochloramine was specific to experimental conditions and source waters.

Although dichloramine was thought to react with precursors forming NDMA, the model did not use dichloramine as a reactant variable. One reason is that the measurement of dichloramine is time consuming and more complicated compared to that of monochloramine (Lee et al., 2007). Additionally, under our experimental

conditions (pH = 8.0) the $NHCl_2/NH_2Cl$ ratio would be constant because the system is in equilibrium during the reaction time (Ozekin et al., 1996; Zhang et al., 2015). Thus dichloramine could be represented as ratio of monochloramine and its reaction could also be fit with our model empirically, leading to an apparent rate constant k_{app}.

Using this modeling approach, NDMA formation in treated wastewaters and in surface waters was well fit with correlation coefficients (R^2) greater than 0.9 in most tests. Optimized data fits were achieved using Kintecus (Ianni, 2002). Model fits of experimental data are shown in Figure 4.1-4.3. In wastewater effluents tests, the model overestimated the NDMA in the beginning of the test (<50 h) at low doses of monochloramine, showing a 'lag period' of NDMA formation. Such a 'lag-period' was observed in previous studies of NDMA formation from pharmaceutical compounds (e.g. ranitidine) as NDMA precursors at similar monochloramine dose (6 mg/LCl_2) in surface waters. In work conducted by Shen and Andrews, the lag and a subsequent initiation of NDMA formation from selected pharmaceuticals were successfully modeled with a dose-response curve (Shen and Andrews, 2011a). The lag and the rate constants were found correlated to TOC and SUVA values for certain pharmaceuticals. It was suggested that there was NOM-pharmaceutical binding that inhibited the initial NDMA formation (Shen and Andrews, 2011a). A similar lag-period was interpreted as indicating the possible interactions of pharmaceutical compounds with wastewater organics. A similar dose-response curve model was applied to our kinetics data. The NDMA formation was well represented with a similar correlation coefficient than in our kinetic model ($R^2 > 0.9$) (Table A2 in APPENDIX B). The wastewater effluent samples with the 'lag-period' were better fit with the dose-response curve model than our proposed model. However, the rate constant k (h^{-1}) derived from the dose-response

model showed broad variations, ranging from 0.007 h^{-1} to 0.175 h^{-1} for surface water and wastewater respectively. No correlation was found between water quality (e.g. TOC and SUVA) and model parameters (e.g. lag and rate constant k). The dose-response model also did not take into account the role of monochloramine dose, which in our kinetic experiments, impacted NDMA FP and the reaction kinetics. Finally the dose-response model is purely descriptive and does not provide insight into the underlying formation mechanisms, especially in complex water matrices.

Table 4.1 Water quality, treatment and NDMA formed in source waters

Sample ID	Source	DOC (mg/L)	UV_{254} (cm^{-1})	Upon Monochloramine Addition				
				NH_2Cl dose ($mgCl_2/L$ [μM])	pH	$NDMA_{max}$ (nM)	k_{app} ($M^{-1}s^{-1}$)	R^2
WW1	Waste-water	4.6	0.12	18 [254 μM]	8.2	6	0.04	0.99
				6 [85 μM]		4	0.04	0.95
WW2	Waste-water	6.17	0.15	20 [282 μM]	8.0	7	0.04	0.97
				7 [99 μM]		2	0.04	0.88
WW3	Waste-water	5.83	0.14	20 [282 μM]	8.0	12	0.07	0.95
				7 [99 μM]		9	0.05	0.98
WW4	Waste-water	5.32	0.17	20 [282 μM]	8.0	12	0.08	0.96
				7 [99 μM]		8	0.08	0.92
WW5	Waste-water	-	-	20 [282 μM]	8.0	8	0.08	0.97
				6 [85 μM]		5.5	0.09	0.96
SW1	Lake	3.88	0.08	36 [507 μM]	8.0	0.7	0.01	0.91
				12 [169 μM]		0.4	0.02	0.91
GW1	Ground-water	1.78	0.05	20 [282 μM]	8.0	0.2	0.04	0.91
				7 [99 μM]		0.2	0.06	0.89
SW2 †	River	3.4	-	3.5[50 μM]	8.0	0.3	0.09	0.96

† Data of NDMA formation and monochloramine were from Chen and Valentine, 2006

Table 4.1 summarizes fitted k_{app} and R^2 values for all experiments. The magnitude of k_{app} values fall within a relatively narrow range of less than one order of magnitude (0.01–0.09 $M^{-1}s^{-1}$). The goodness of fit of the model, represented by Equation 2 and 3, was evaluated by comparing observed NDMA formation data and

model prediction in Fig 4-4. The small 95% confidence intervals suggested significant correlation between model-predicted and observed NDMA formation. Data in Chen and Valentine's 2006 work on NDMA formation from NOM was also fit with our model and the k_{app} (0.09 $M^{-1}s^{-1}$) was similar to that of our wastewater and surface waters. A narrow range in k_{app} values was surprising given the very different precursors expected in varying source waters and the order of magnitude differences in $NDMA_{max}$ between sources.

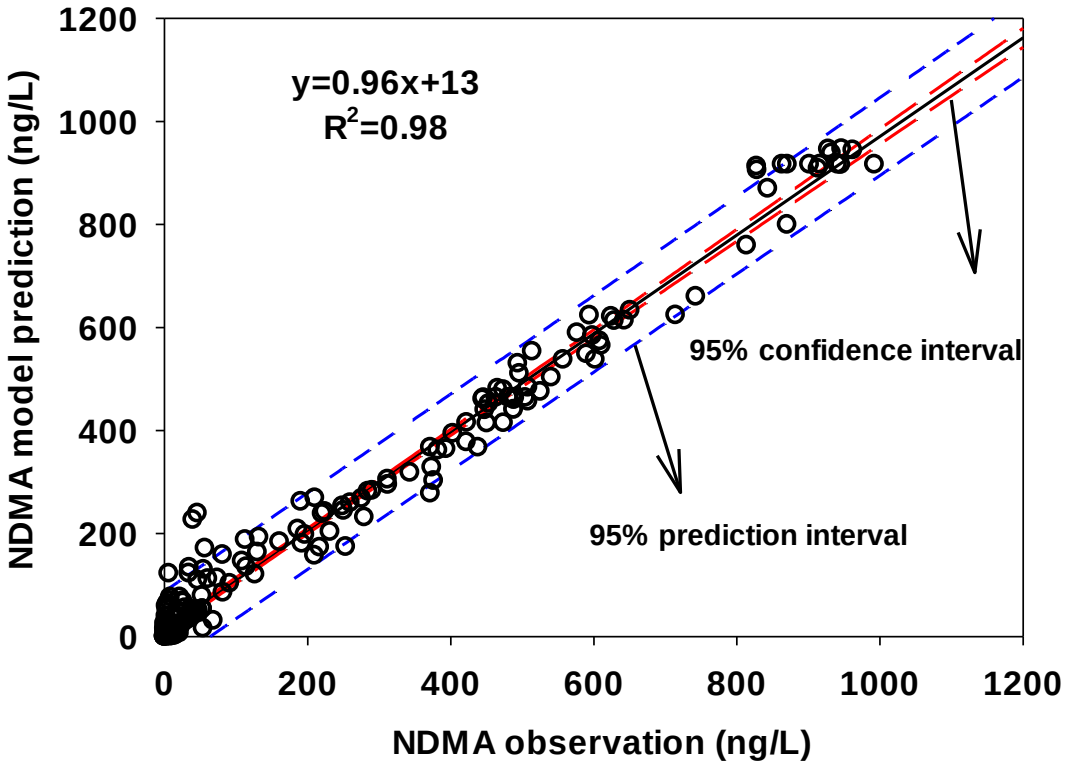

Figure 4.4: Linear correlation between model predictions and observations of NDMA concentrations in all waters. Data from all reaction time periods are included.

Most mechanistic work on NDMA formation during chloramination has been conducted with secondary amines such as DMA (Schreiber and Mitch, 2006b). It has been suggested that during chlorination some tertiary amines could decay to secondary

amines forming NDMA upon subsequent chloramination (Mitch and Schreiber, 2008). It was still unclear if such transformation reaction between amines or NDMA formation from amines was a rate limiting step. The small variance of rate constants suggests that reactions like degradation of higher order amines to secondary amine precursors, if there any were present, are rapid compared to NDMA formation. This is in agreement with the short half-life (<14 h) of trimethylamine (TMA) decomposing to DMA in presence of monochloramine and indicates that amine precursor groups, including secondary amines and tertiary amines with either low or high yields, probably have a similar rate limiting step forming NDMA in our tests.

We propose a general reaction pathway of NDMA formation from chloramination of NDMA precursors in treated wastewaters and surface waters. Precursors that include anthropogenic chemicals or natural biomolecules rapidly react with chloramines to produce intermediates. The yield of intermediates depends upon types of precursors (e.g. secondary or tertiary amines, β-aryl amines) and monochloramine dose. The intermediates then function as the precursors (P) and the subsequent conversion from intermediates (P) to NDMA undergoes a second order reaction mechanism in the presence of oxidant such as monochloramine.

4.3.4 Monochloramine Exposure.

Oxidant exposure has been used as a parameter in many oxidation reactions (e.g. ozonation) when modeled as second order reactions in waters to investigate reaction kinetics (Gunten, 2003, Ramseier et al., 2011). In this work NDMA formation was modeled as second order reaction in Equation 4-2, which can be integrated (Equation 4-4) with $\int[NH_2Cl]dt$ being the monochloramine exposure.

$$ln\frac{[P]}{[P]_0} = -k_{app}\int[NH_2Cl]dt$$ Equation 4-4

Equation 4-4 offers another way of quantifying the apparent second order rate constant k_{app}. In addition, it shows ($[P]/[P]_0$), the relative conversion of NDMA precursor, is related to the NH_2Cl exposure. Figure 5 shows the plots of $[P]/[P_0]$ against NH_2Cl exposure for water samples at low and high NH_2Cl doses. In different water samples, the reaction required different NH_2Cl exposure for the same conversion of precursors. The rate constants varied by water sources, possibly due to the varying precursor groups and their different reactivity with NH_2Cl or $NHCl_2$. From the previous discussion in this work NH_2Cl dose determines the $NDMA_{max}$ even in the same water sample, but does not affect the rate constants in wastewater and groundwater. The relative change of precursors (or increase of NDMA formation) had the same kinetics for the same water at different NH_2Cl doses (Figure 4.5a-4.5c, Figure A5-7 in Appendix B). Surface water represents an exception (Figure 4.5d). The surface water had a lower k_{app} than all other waters tested. The relative change of precursors in surface water differed with low and high dose NH_2Cl, especially when NH_2Cl exposure is less than 5×10^6 $mgCl_2 \times min/L$, possibly due to the 'fast and slow' reaction mechanism in surface water.

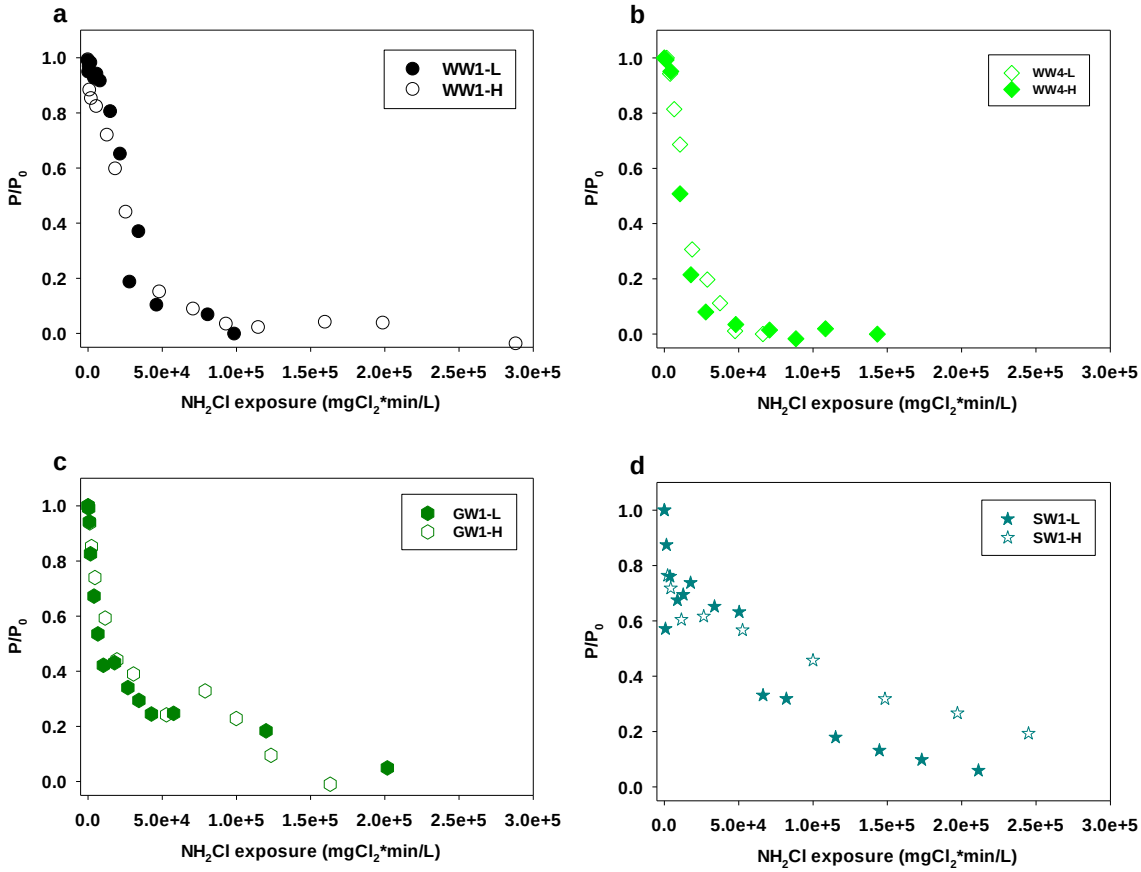

Figure 4.5: Plots of P/P_0 versus monochloramine exposure for water samples (a) WW1, (b) WW4, (c) GW1, (d) SW1. L = lower, H = higher, represent samples with lower or higher NH_2Cl concentrations.

In finished drinking water NH_2Cl concentrations (<0.06 mM) are typically lower than those used in our test (0.09-0.51 mM). From our results, NDMA formation reaction kinetics are dependent upon NH_2Cl exposure, not NH_2Cl concentrations. The rate constants could be applied to waters with lower NH_2Cl concentration and longer contact time ranges. NH_2Cl exposure and the rate constants are the key parameters for the prediction of the transformation efficiency of NDMA precursors into NDMA. With a measurement of $NDMA_{max}$ in site-specific sample and chloramine conditions, our proposed model provides a practical way to predict NDMA formation in drinking water influenced by wastewater effluents and surface waters in water plants and drinking water distribution systems.

4.5 Conclusions

NDMA formation potential and formation kinetics during chloramination were investigated in wastewater and surface water samples. Under reaction conditions in our experiments (pH = 8.0, NH_2Cl = 0.09-0.51 mM) NDMA formation increased to its maximum over hundreds of hours. NDMA maximum conversion was found to be dependent on the preformed monochloramine in the water samples.

A simple second order NDMA formation model of reactions between amine precursors and monochloramine was developed. NDMA formations were well predicted by the model with correlation coefficients higher than 0.9 in most cases. The modeled rate constants for different water samples were found surprisingly within a narrow range (0.01–0.09 $M^{-1}s^{-1}$), indicating a possible rate limiting step of NDMA formation for different amine precursor groups. With only two simple measurements (NDMA formation potential and monochloramine exposure), our model provides a practical way to predict NDMA concentrations in distribution system.

Our proposed model was validated at pH 8 and monochloramine doses between 0.09 mM to 0.51 mM with wastewater effluents and surface water samples. It would be of value to extend the work further in a larger variety of water matrices and reaction conditions such as pH, $N:Cl_2$ ratio and dissolved oxygen level, to simulate a larger variety of water treatment plants or distribution systems. Additionally, characterization or profiling of the precursors of NDMA and chloramination kinetic studies of more model precursors are needed to better understand different pools of precursors and how they could interact or contribute to NDMA formation in different water systems.

4.5 Acknowledgements

This research was supported by the Water Research Foundation (Project 4499, managed by Djanette Khiari), American Water Works Association Abel Wolman Fellowship, Water Environment Federation Canham scholarship, and the Arizona State University Fulton School of Engineering Dean's Fellowship.

CHAPTER 5

MODELING NDMA FORMATION KINETICS DURING CHLORAMINATION OF MODEL COMPOUNDS AND SURFACE WATERS IMPACTED BY WASTEWATER DISCHARGES

5.2 Introduction

Over the past decades, N-nitrosamines (NAs), which form as disinfection byproducts during chlorination, in particular chloramination, have emerged as a great concern because of an increasing use of chloramines by water utilities for residual disinfection to meet trihalomethane (THM) and haloacetic acid (HAA) regulations (Krasner et al., 2013). NAs were included in the Unregulated Contaminant Monitoring Rule 2 (UCMR2) and then listed on the third Contaminant Candidate List (CCL3) (USEPA, 2009). The USEPA classifies NAs as probable human carcinogens in drinking water at low ng/L levels associated with a 10^{-6} lifetime cancer risk. California's Office of Environmental Health Hazard Assessment (OEHHA) set a notification level of 10ng/L for NDMA (OEHHA, 2006). Because of their high carcinogenic potential, the USEPA may soon make a regulatory determination for NAs.

N-Nitrosodimethylamine (NDMA) is the most commonly investigated nitrosamine. Most studies have found that NDMA is rather associated with chloramination than with chlorination (Mitch et al., 2009; Boyd et al., 2011; Russell et al., 2012). Systems with high plant effluent NDMA (i.e., >50 ng/L) typically use chloramines as the primary rather than secondary disinfectant (Russell et al., 2012), reflecting the potential for precursor deactivation by strong pre-oxidants such as chlorine. Due to the long time-scale for nitrosamine formation, plants with long in-plant chloramine contact times (e.g., 12–18 hr) tend to have higher NDMA concentrations in

the plant effluent than those with short (e.g., 0.5–2 hr) contact times (Krasner et al., 2012). NDMA concentrations tend to increase throughout chloraminated distribution systems (Krasner et al., 2012; Valentine et al., 2005; Krasner et al., 2009; Liang et al., 2011; Krasner et al., 2012).

Primary amines can be nitrosated to yield primary NAs, however the latter are unstable and decay nearly instantaneously (Ridd, 1961). Secondary amines can be transformed to their stable NA analogues and most research focused on NDMA formation from dimethylamine (DMA) (Mitch and Sedlak, 2002; Choi and Valentine, 2002; Schreiber and Mitch, 2006a; Schreiber and Mitch, 2006b; Shah and Mitch, 2012). However, some studies indicated that the presence of DMA was not sufficient to explain the NDMA formed in surface water and wastewaters (Gerecke and Sedlak, 2003; Mitch and Sedlak, 2004). Tertiary amines may also serve as nitrosamine precursors. For example, trimethylamine (TMA) would decay instantly upon chlorination or chloramination to release DMA and then quantitatively form NDMA (Mitch and Schreiber, 2008). Mechanistic studies indicate that yields of NDMA from chloramination of most secondary and tertiary amines are very low (~0–3%) but recently a subset of tertiary amines were found to have substantially higher NDMA yields (up to 90%) compared to previously studied precursors (Le Roux et al., 2011; Shen and Andrews., 2011a; Shen and Andrews., 2011b). In particular, ranitidine, a widely found amine-based pharmaceutical, forms NDMA at yields higher than 80% (Le Roux et al., 2011; Shen and Andrews, 2011b). It was suggested that the electron donating group (furan ring) in ranitidine favors the reaction with chloramine leading to higher NDMA yields. The differences of NDMA formation yields among tertiary amines revealed the importance of tertiary amine structures (N bond leaving group) on the NDMA formation. The higher yields also suggest that tertiary amines can form

nitrosamines without proceeding through a secondary amine intermediate (Selbes et al., 2013).

Several NDMA formation mechanisms during chloramination had been proposed (Figure 5-1). Mechanistic studies using DMA as the model precursor found that unprotonated DMA undergoes nucleophilic substitution with monochloramine, yielding the unsymmetrical dimethylhydrazine (UDMH) intermediate. This UDMH is then oxidized by monochloramine to NDMA (Choi and Valentine, 2002; Mitch and Sedlak, 2002). The importance of chloramine speciation and presence of dissolved oxygen was later discovered and a second mechanism proposed ((2) in Figure 5-1). Here, dichloramine reacts to yield NDMA via the formation of the chlorinated UDMH intermediate (UDMH-Cl) and this UDMH-Cl is then oxidized by oxygen to produce NDMA (Schreiber and Mitch, 2006). Based upon competition reaction kinetics, it has been suggested that the monochloramine mechanism (1) is negligible compared to dichloramine (2) pathway. As the molar yield of NDMA from DMA is low (i.e., <5%) compared to that from other compounds (e.g., ranitidine), it was suspected that a third pathway, other than through DMA, exists. Compounds such as ranitidine may follow a different series of reactions involving nucleophilic attack of the amine group on chloramines ((3) in Figure 5.1) (Le Roux et al., 2012). Through this pathway, NDMA formed from ranitidine was more sensitive to monochloramine (Le Roux et al., 2011). Suspected NDMA precursors with electron withdrawing groups may preferentially react with monochloramine while compounds with electron donating groups react preferentially with dichloramine (Selbes et al., 2013; Liu et al., 2014). Many suspected precursors could react with both monochloramine and dichloramine. Therefore, NDMA formation is likely a combination of reactions between NDMA precursors and both chloramine species.

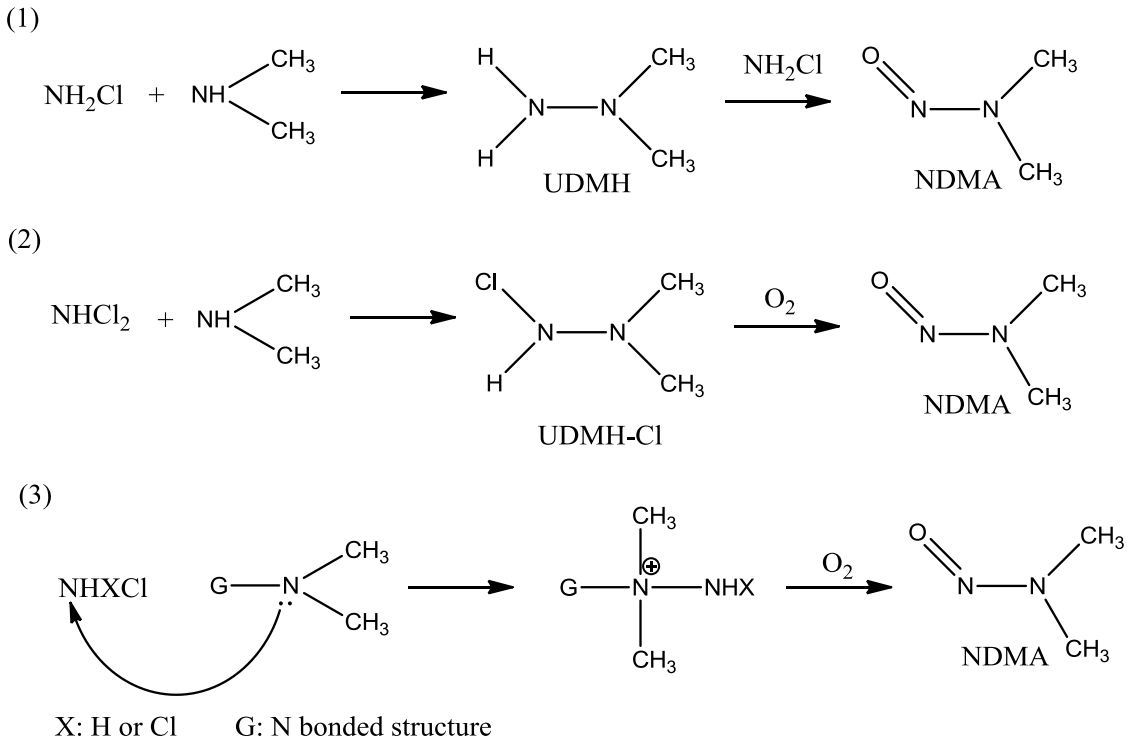

Figure 5.1: NDMA formation pathways as proposed in the literature: (1) Choi and Valentine, 2002; Mitch and Sedlak, 2002. (2) Schreiber and Mitch, 2006. (3) Selbes et al. 2013.

Despite extensive research on yields of NDMA from model compounds and in surface water or wastewater (Mitch and Sedlak, 2004; Mitch and Schreiber, 2008; Shen and Andrews, 2011b), less information exists related to NDMA formation kinetics in the latter water sources. NDMA formation from DMA has been initially modeled through UDMH and Cl-UDMH pathways ((1) and (2) in Figure 5.1) and the latter successfully predicted NDMA formation over a range of conditions (Schreiber and Mitch, 2006). A statistical model was proposed to predict NDMA formation kinetics from pharmaceutical compounds such as ranitidine in various water matrices (Shen and Andrews, 2011b). In addition, natural organic matter (NOM) was also investigated as a source of precursors in a NDMA formation model (Chen and Valentine, 2006). No attempt has been ever made to model NDMA formation in wastewater or wastewater-

impacted waters. The challenge for a model development lies in the multitude of precursors and precursor types present and hence the possibility of having various mechanisms, with distinct kinetics occurring simultaneously.

The aim of this work is to formulate and evaluate a NDMA formation kinetics model that is applicable to different water sources and model compounds. A simple second-order kinetic reaction model was developed for NDMA formation. In this model, the precursor concentration, quantified as the maximum NDMA concentration formed during chloramination under specific water conditions, and chloramine decay were used to predict transformation of precursors to NDMA. The model was parameterized using NDMA formation data from literature data on NOM and model precursor compounds (i.e. ranitidine). The optimization of the kinetic model parameters and the resulting model performance are discussed.

5.2 Model Description

5.2.1 NDMA Formation Model

As detailed in the introduction, three different pathways for NDMA formation have been proposed (Figure 6.1). The original concept of the model was that different types of precursors may proceed along different mechanistic pathways with different chloramine species and the reactions may potentially involve oxygen to produce NDMA. Such a model would classify NDMA precursors (nM quantities) as having either higher or lower yields and presumably different reaction rates with different chloramine species. In a first step, using data obtained from our research of NDMA formation in wastewater, we developed a simple second-order model for the reaction of NDMA precursors (P) in the presence of monochloramine (NH_2Cl):

$$\frac{dP}{dt} = -k_{mono}[P][NH_2Cl] - k_{di}[P]\alpha[NH_2Cl] \quad \text{Equation 5-1a}$$

$$= -(k_{mono} + k_{di}\alpha)[P][NH_2Cl] \quad \text{Equation 5-1b}$$

$$= -k_{app}[P][NH_2Cl] \quad \text{Equation 5-1c}$$

where $[NH_2Cl]$, $[NHCl_2]$ = monochloramine or dichloramine concentration at time *t*

[P] = NDMA precursor concentration at time *t*

k_{mono}, k_{di} = rate constant of NDMA formation from monochloramine or dichloramine

k_{app} = second order rate constant of NDMA formation in our model

α = ratio of dichloramine and monochloramine

Table 5.1 shows the decomposition reactions for chloramines in water (Ozekin et al., 1996). The relationship between monochloramine and dichloramine derives from reactions 3, 4 and 5. Dichloramine forms via an acid catalyzed reaction from two monochloramines, then dichloramine reacts instantaneously with monochloramine, producing nitrogen gas. In this assumption, dichloramine occurs at a low concentration and at steady state. Thus, the dichloramine concentrations can be represented as a proportion (α) of monochloramine. Equation 5.1 shows the formation kinetics of NDMA as a combination of both chloramines reactions. k_{mono} and k_{di} were the rate constants for mono- and di-chloramine reactions respectively. A new apparent rate constant k_{app} was then used in Equation 1c as the best fit second-order rate constant ($M^{-1}s^{-1}$) in terms of monochloramine and NDMA precursor. Measured monochloramine was used in the model to represent all chloramines since it is the dominant source of chloramines in neutral and basic conditions, and is easier to measure compared to dichloramine.

Table 5.1: Chloramine Decomposition Kinetics and Associated Rate Constants (Ozekin et al., 1996)

	Reaction	Rate Constant
1	$HOCl + NH_3 \rightarrow NH_2Cl + H_2O$	$k_1 = 1.0\times10^{10} M^{-1}h^{-1}$
2	$NH_2Cl + H_2O \rightarrow HOCl + NH_3$	$k_2 = 0.1 h^{-1}$
3	$HOCl + NH_2Cl \rightarrow NHCl_2 + H_2O$	$k_3 = 1.26\times10^{6} M^{-1}h^{-1}$
4	$NHCl_2 + H_2O \rightarrow HOCl + NH2Cl$	$k_4 = 2.3\times10^{-3} h^{-1}$
5	$NH_2Cl + NH_2Cl \rightarrow NHCl_2 + NH3$	k_d*
6	$NHCl_2 + NH_3 \rightarrow NH_2Cl + NH_2Cl$	$k_6 = 2.0\times10^{8} M^{-1}h^{-1}$
7	$NH_2Cl + NHCl_2 \rightarrow N_2 + 3H^+ + 3Cl^-$	$k_7 = 55.0 M^{-1}h^{-1}$
8	$NHCl_2 + H_2O \rightarrow NOH + 2HCl$	$k_8 = 6.0\times10^{5} M^{-1}h^{-1}$
9	$NOH + NHCl_2 \rightarrow N_2 + H_2O + HCl$	$k_9 = 1.0\times10^{8} M^{-1}h^{-1}$
10	$NOH + NH_2Cl \rightarrow N_2 + H_2O + HCl$	$k_{10} = 3.0\times10^{7} M^{-1}h^{-1}$
11	$NH_4^+ \rightarrow NH_3 + H^+$	$pK_a = 9.3$
12	$H_2CO_3 \rightarrow HCO_3^- + H^+$	$pK_a = 6.3$
13	$HCO_3^- \rightarrow CO_3^{2-} + H^+$	$pK_a = 10.3$

*$k_d = k_H[H^+] + k_{H2CO3}[H_2CO_3] + K_{HCO3}[HCO_3^-]$;
$k_H = 2.5\times10^{7} M^{-2}h^{-1}$
$k_{HCO3} = 800 M^{-2}h^{-1}$
$k_{H2CO3} = 40000 M^{-2}h^{-1}$

Equation 5.1c simplifies NDMA formation kinetics in different water matrices despite there being various reactions pathways of chloramines and probably multiple groups of precursor species with highly variable yields (0.017% for TMA, 90% for ranitidine) and influences of various water quality parameters on chloramine decay in water. Currently there is no method to predict NDMA formation kinetics, and most research has relied upon simulated distributed system (SDS) tests (NH_2Cl~2.5mg/L)) or formation potential (FP) tests (NH_2Cl>100mg/L). Even model compounds such as DMA showed variable NDMA yields (Le Roux et al., 2011; Mitch et al., 2009). Organic compound concentrations were thought to be associated with NDMA formation from NOM. However, there was no correlation between NDMA formation (or precursor concentration) and UV_{254} or DOC in natural waters or in wastewaters (Chen and Westerhoff, 2010). P_0 is the maximum NDMA formation which is

measurable in NDMA kinetic tests. Together with the measurement of monochloramine, the model is designed to simulate the NDMA formation processes. The concentration of NDMA at any time ([NDMA(t)]) would be related to the maximum amount of NDMA precursors available for reaction in an experiment ($[P]_0 = [NDMA_{max}]$) as follows:

$$[NDMA(t)] = [P]_0 - [P] \qquad \text{Equation 5-2}$$

where [P] NDMA precursor concentration at time t

The measured concentration of NH_2Cl or an estimated simulated monochloramine decomposition is used in the model (Chen and Valentine, 2006; Vikesland et al., 2001). NDMA formation data at different time points were fitted to the model using Kintecus (Ianni, 2002) and the rate constant, k_{app}, was optimized with the highest correlation coefficient between experimental values and model fitting.

5.2.2 Monochloramine Degradation

Monochloramine decays over time due to hydrolysis and reaction with organic and inorganic species (Table 5-1). Autodecomposition or hydrolysis forms other oxidants such as free chlorine or dichloramine, which would react with DOC. Another pathway is, in the presence of NOM, monochloramine reacting directly with organic matter. The rate of monochloramine loss in both pathways was found to be dependent on experimental conditions such as initial monochloramine concentration, DOC or pH (Durik et al., 2005). It was difficult to accurately simulate monochloramine decomposition with detailed models published in previous research because various parameters (i.e. fast and slow reactive fractions of NOM) need to be reoptimized since they are specific to reaction conditions. A simple first order degradation model with respect to monochloramine is used to simulate the decay of monochloramine in the

presence of NDMA precursors (Equation 5-3). The rate constant is specific to experiment conditions and representative for similar water qualities in general.

$$\frac{d[NH_2Cl]}{dt} = -k_{decay}[NH_2Cl] \quad \text{Equation 5-3}$$

5.3 Results and Discussion

5.3.1 Modeling of NDMA formation in NOM

Chen et al. modeled NDMA formation from reactions between NOM and monochloramine (Chen and Valentine, 2006). They suggested that NOM in surface waters could be oxidized involving two types of reactive sites of monochloramine loss. A portion of the dissolved organic carbon (DOC) could react with monochloramine rapidly within hours and the other part had a much slower reaction with free chlorine (over days). However, their model had five parameters (i.e. fast and slow reactive fractions of NOM) to be optimized which would vary between water sources. Here we fitted their experimental data with our model. The monochloramine decay was modeled as a first order reaction in Equation 5-2 and the monochloramine decay rate constants are shown in Table 5.2. The decay rate of monochloramine increased when pH was reduced from 9 to 7 since at low pH monochloramine would decay to dichloramine more easily (Reaction 5, Table 5.1).

Then the NDMA formation data was fitted with our second order model (Figure 5.2). NDMA concentration at 120 h was used as $NDMA_{max}$ (P_0) although NDMA formation had not reached its maximum at this time. The model fits NDMA formation over time well at pH 7, 8 or 9. However, at pH 6 when dichloramine is more prevalent chloramine species, the model was not able to simulate the NDMA formation because our assumption that dichloramine is proportional to monochloramine is not valid at pH

6. NDMA formation yields appear to increase with decreasing pH from 9 to 7 due to presence of more dichloramine at lower pH. The optimized rate constant k_{app} varied within a factor of three for different pH conditions, however, no obvious correlation was found between pH values and k_{app}.

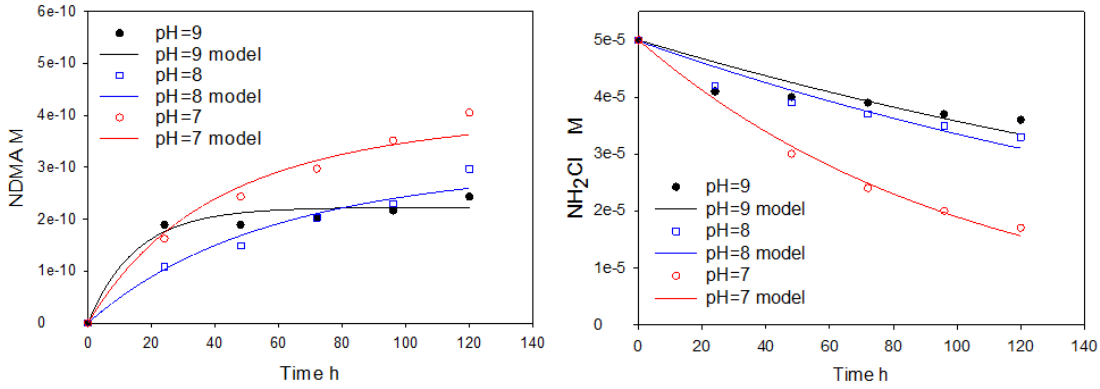

Figure 5.2: Model prediction of NDMA formation and monochloramine decay at various pH in surface water. (Symbols: observation data, lines: model predictions. Data from Chen and Valentine, 2006

Table 5.2: Optimized NDMA formation rate constant and monochloramine decomposition rate constants in NOM under various reaction conditions. (Data from Chen and Valentine, 2006). R^2 is correlation coefficient between model and observation. Notes: Experiments were conducted at pH 7 with variable Cl/N ratios (and ammonia concentrations): [a] 0.7 (0.07 mM NH_3); [b] 0.3 (0.17 mM NH_3); [c] 0.10 (0.5 mM NH_3)

pH	**k_{app} $M^{-1}s^{-1}$ (R^2)**	**k_{decay} (h^{-1})**
9	0.25 (0.96)	3.4E-03
8	0.09 (0.96)	4.0E-03
7	0.15[a] (0.95) 0.12[b] (0.95) 0.10[c] (0.84)	9.7E-03 4.1E-03 2.5E-03

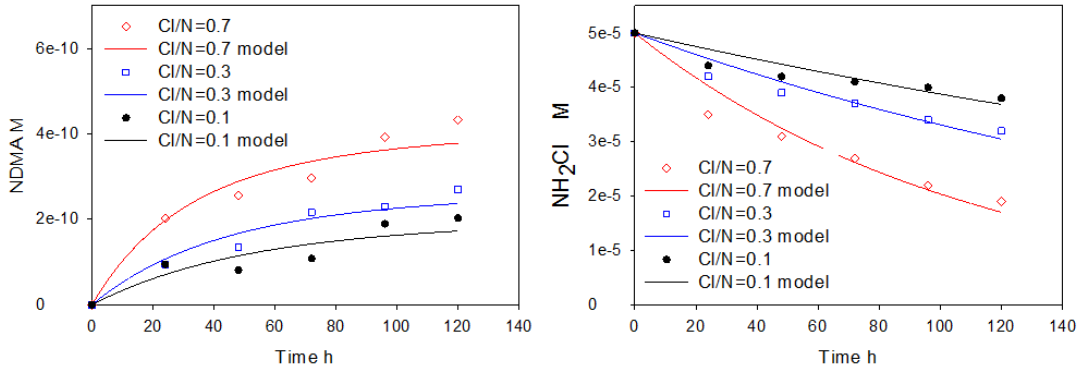

Figure 5.3: Model prediction of NDMA formation and monochloramine decay at various ammonia concentrations (Cl/N ratio) in surface water. (Symbols: observation data, lines: model predictions, pH=7. Data from Chen and Valentine, 2006)

The NDMA formation data in surface waters with various Cl/N ratios in Chen's work was also fitted with our model. Both monochloramine decay and NDMA formation were well predicted (Figure 5.3). Results showed that a decreasing Cl/N ratio reduced monochloramine decay rates, NDMA formation rates and NDMA yields. This was the result of dichloramine formation being favored at high Cl/N ratios (low ammonia concentrations) according to reaction 3 in Table 5.1.

With the monochloramine degradation measurements shown in Chen's work (Chen and Valentine, 2006), the model successfully predicted NDMA formation over time in surface waters from pH 7 to 9 and in conditions of Cl/N ratio from 0.1 to 0.7.

5.3.2 Modeling of NDMA formation from model compounds

In addition to NOM, model compounds such as DMA and ranitidine were also studied in NDMA formation kinetics experiments. Selbes reported NDMA formation from various amine precursors (Selbes, 2014). However, NDMA formation kinetics were not discussed. Here we apply our model to the NDMA kinetics data of five precursor compounds from Selbes' work (Selbes, 2014). DMA and four tertiary amines (trimethyalmine (TMA), dimethylisopropylamine (DMiPA), dimethylbenzylamine (DMBzA) and ranitidine) were selected. These five precursors were chloraminated by

Selbes in three reaction conditions: in distilled deionized water at pH 7.5, a formation potential (FP) test condition with 1.4mM monochloramine, and simulated distribution system (SDS) with 0.04mM monochloramine, and SDS condition with 100 mg/L ammonia to minimize dichloramine formation according to Reaction 3 in Table 5.1.

Monochloramine decay data was not published in Selbes' work. The monochloramine model simulation in NOM in Chen's work showed that pH has a more significant effect on monochloramine decay than DOC concentrations or Cl/N ratio. A monochloramine decay rate of 0.007 h^{-1}, between the rate constants at pH 7 (0.01 h^{-1}) and pH 8 (0.004 h^{-1}) in Chen's work, was used to predict monochloramine decomposition in the deionized water. Figure 5.4 shows NDMA formation data obtained from Selbes' work and model fitting for precursors under various conditions and the resulting rate constants are shown in the figure and listed in Table 5.3. The model successfully fitted the NDMA formation kinetics for all five chemicals in most tests. However, in SDS condition with excess ammonia, our model overestimates NDMA formation in the first half reaction time and underestimates NDMA in the second half period for ranitidine and DMBzA. It was the same with DMiPA in the SDS condition test. In previous studies it was found that ranitidine and DMBzA were more sensitive to monochloramine and DMiPA was only sensitive to dichloramine (Liu et al., 2014). In NDMA formation from tertiary amines such as ranitidine, an intermediate could form by nucleophilic substitution between ranitidine and monochloramine (Le Roux et al., 2012; Liu et al., 2014). A possible explanation could be, in conditions with high monochloramine concentrations in FP tests, this intermediate degrades quickly to form NDMA. Therefore, the presence of intermediates could 'delay' the NDMA formation and make our model overestimate NDMA formation.

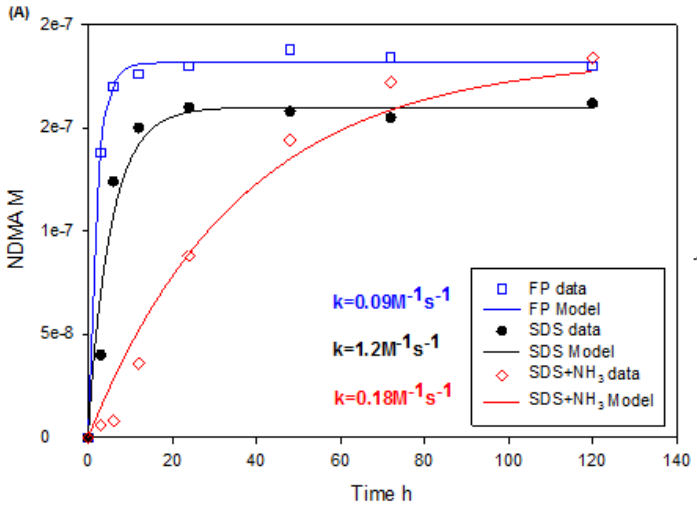

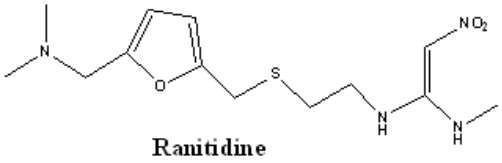

Ranitidine

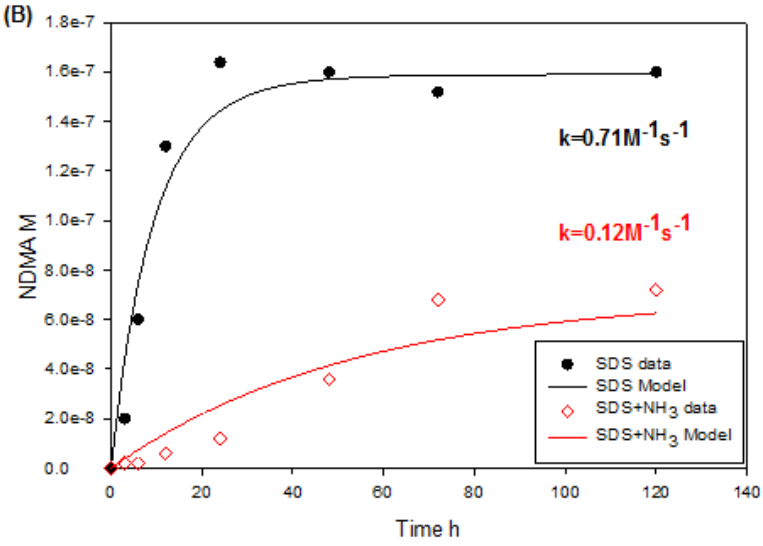

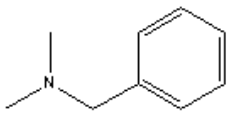

Dimethylbenzylamine (DMBzA)

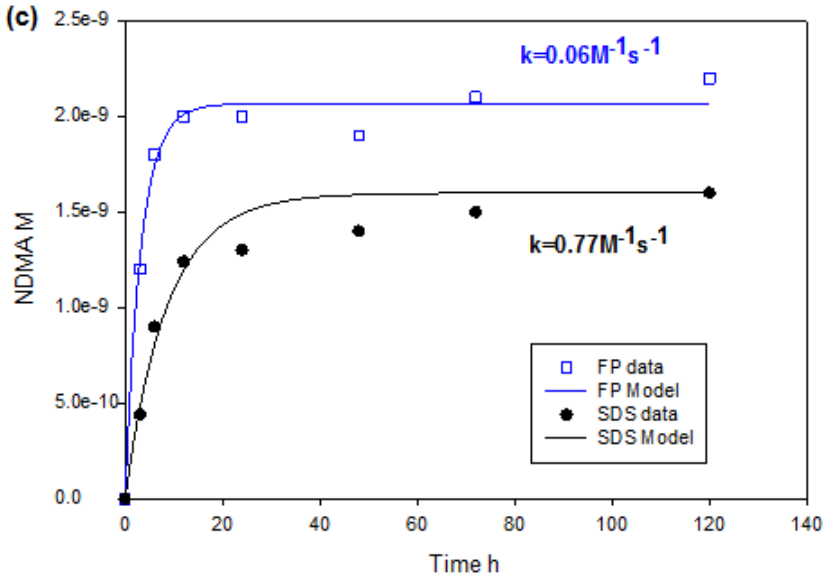

Dimethylamine
(DMA)

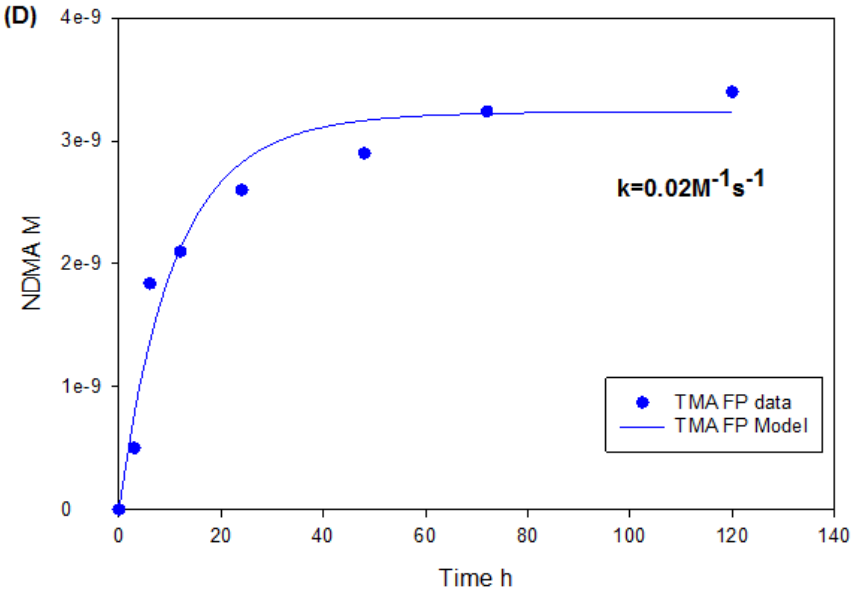

Trimethylamine
(TMA)

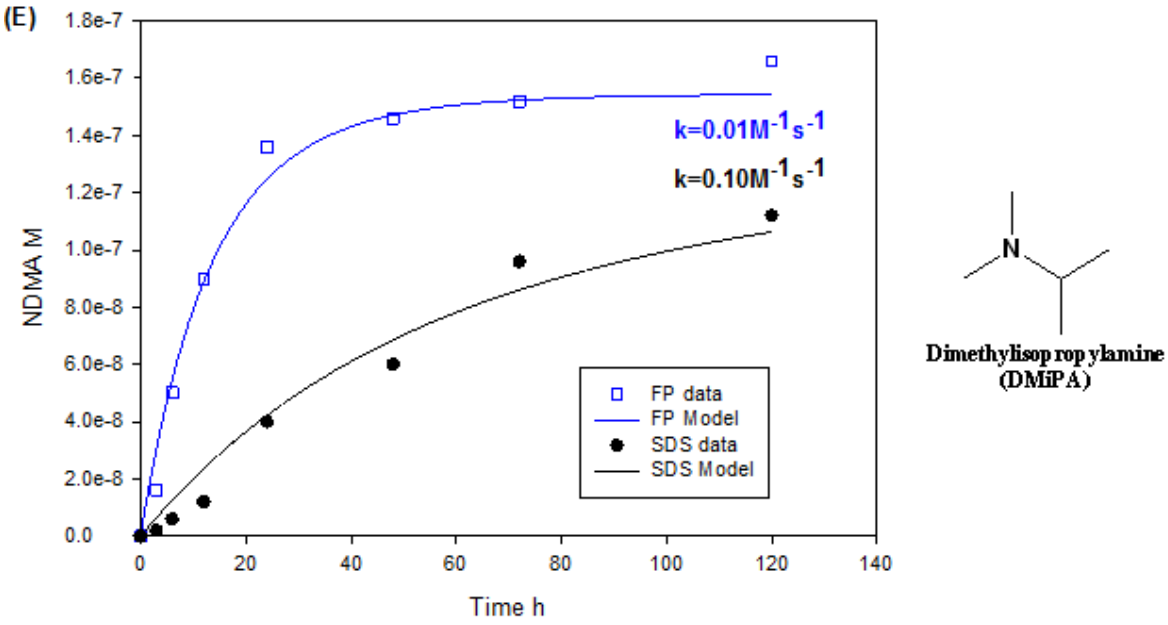

Figure 5.4: NDMA formation from model precursor compound data (Symbols), model fitting (Lines) in FP tests (NH_2Cl 1.4mM, pH=7.5), SDS conditions (NH_2Cl 0.04mM, pH=7.5) and SDS conditions with excess ammonia. (NDMA data from Selbes, 2014)

Although $k_{app} \times [NH_2Cl]$ was greater in the FP tests, indicating a faster NDMA formation in FP conditions than in SDS conditions, the optimized rate constants (k_{app}) in the FP tests were less than under SDS conditions, by an order of magnitude for model compounds. Compared to amine precursor concentrations (200 nM) in Selbes' work, the monochloramine concentrations (1.4 mM) were more than 5000 times the precursor concentrations in the FP test. Thus, in the FP test, there is a substantial excess of monochloramine present that reduced the rate constant. Rate constants k_{app} of ranitidine, DMBzA and DMA are similar and that of DMiPA is much smaller. The similar k_{app} between ranitidine and DMA was unexpected since DMA and ranitidine have very different yields (<3% and 80% respectively) and different proposed NDMA formation mechanisms. In SDS conditions with excess ammonia, optimized k_{app} for both ranitidine and DMBzA are less than those under SDS conditions, suggesting dichloramine reactions may be important. The dichloramine reaction rate constant,

which is the difference between k_{app} between two conditions, was found to be greater than the monochloramine rate constant.

Table 5.3: Optimized rate constant k_{app} for model compounds under various reaction conditions. (NDMA data from Selbes, 2014)

Compounds	NDMA Yields in FP test %	k_{app} $M^{-1}s^{-1}$ (R^2)		
		FP test	SDS	SDS+ excess ammonia
Ranitidine	~80	0.09 (0.99)	1.2 (0.92)	0.18 (0.97)
DMBzA	~80	-	0.71 (0.92)	0.12 (0.87)
DMA	1.1	0.06 (0.98)	0.77 (0.96)	-
TMA	1.7	0.02 (0.97)	-	-
DMiPA	83	0.01 (0.98)	0.1 (0.96)	-

5.3.3 Modeling of NDMA Formation of Pharmaceutical Compounds in the Presence of NOM

Our model was also applied to NDMA formation by amine precursors in the presence of NOM in natural waters. Shen et al. investigated the NDMA formation kinetics of pharmaceutical compounds in three water matrices (MQ water: TOC=0mg/L, Lake: TOC=2mg/L, River: TOC=6mg/L) under simulated distribution system condition (SDS, NH_2Cl=0.035mM or 0.07mM) (Shen and Andrews, 2011b). Four pharmaceutical compounds, sumatriptan, chlorphenamine, doxylamine and ranitidine were used in the kinetic experiments. Measured monochloramine decay concentrations over time in Shen's work were used to model monochloramine decomposition. Model fitting and optimized rate constants are shown in Figure 5.5 and Table 5.4. The model in equation 1c simulates NDMA formation from ranitidine in MQ water with a high correlation coefficient (R^2>0.93) and yields an optimized rate constant of 1.3 $M^{-1}s^{-1}$. This is similar to the rate constant (1.2 $M^{-1}s^{-1}$) in Selbes' work

under similar reaction conditions (DDW water, SDS, NH_2Cl=0.04mM) and demonstrates that our model is applicable to predict NDMA formation from ranitidine and monochloramine under similar reaction conditions.

However, for all four pharmaceutical precursors, the model overestimates the NDMA formation in the first half experiment time and underestimated NDMA in the second half. This is possibly due to the formation of an intermediate that delays the NDMA formation, as suggested previously.

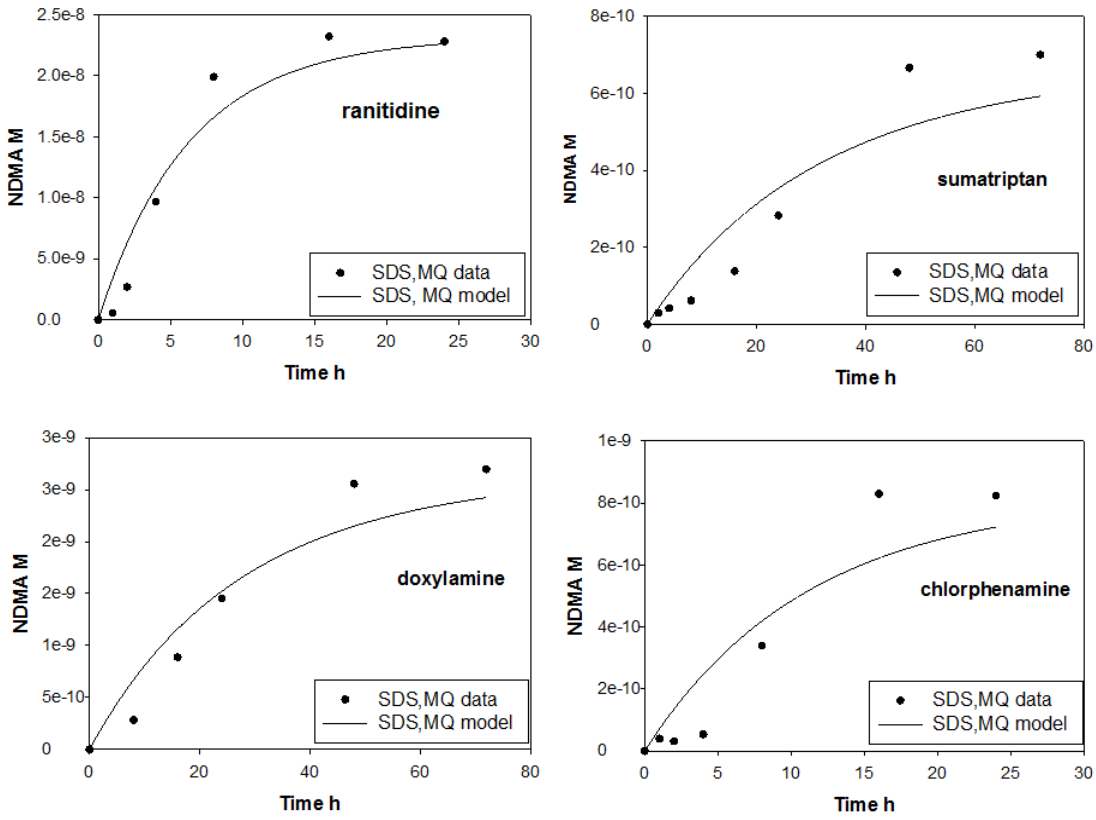

Figure 5.5: NDMA formation from pharmaceutical compounds under SDS condition (MQ water, NH_2Cl=0.035mM, pH=7), data (symbols) and model fitting (lines). (NDMA data from Shen and Andrews, 2011b).

Table 5.4: Optimized rate constant k_{app} for model compounds in different water matrices with varied TOC. (NDMA Data from Shen and Andrews, 2011b)

Compounds	NDMA Yields in SDS MQ %	k_{app} $M^{-1}s^{-1}$ (R^2)		
		SDS	2mg/L TOC	6mg/L TOC
ranitidine	~90	1.3 (0.93)	0.82	0.25
sumatriptan	~2	0.28 (0.86)	0.24	0.08
chlorphenamine	3	0.73 (0.90)	-	0.22
doxylamine	10	0.28 (0.84)	-	0.13

In Shen's work on NDMA formation from pharmaceutical compounds in natural waters, there was an initial lag-time when NDMA formation did not increase for all four pharmaceutical compounds in lake and river waters. The lag-time was longer at higher TOC concentrations. However, the lag-time could not be simulated with our proposed model. In Shen's work it was suggested that there was NOM-pharmaceutical binding that inhibited the initial NDMA formation (Shen and Andrews, 2011b). In addition, dichloramine has a lower electron density on nitrogen due to two chlorine atoms so it would be a more preferable species to interact with negatively charged NOM. Thus in the presence of NOM, dichloramine could more easily react with NOM compared to monochloramine and hence NDMA formation from dichloramine would be suppressed by NOM.

To better understand how NOM affects NDMA formation rates, our proposed model was adjusted to fit the kinetics data. As there is no NDMA formed during the lag-time, we start the model simulation at the end of the NDMA formation lag. The lag time was removed and the kinetics data was refitted with our model. The model fits the experimental data better for all four pharmaceutical compounds (Figure 5.6) and the optimized rate constants were listed in Table 5.3. The optimized second-order rate constants k_{app} were found to decrease with increasing TOC concentrations. This can be

explained by a competition between NOM and model compounds to react with mono- and/or di- chloramine. In the river water samples (TOC = 6mg/L), the optimized rate constants k_{app} for the pharmaceutical model compounds were in the range of 0.08 to 0.25 $M^{-1}s^{-1}$ (Table 4) and were comparable to the rate constants (0.02 to 0.09 $M^{-1}s^{-1}$) of NDMA formation from NOM in surface waters with similar TOC concentration (TOC =3.4 mg/L) in Chen's work we discussed previously. By using the lag model, we were able to compare the rate constant of NDMA formation at different DOC concentrations and reveal how the DOC impacted the NDMA formation kinetics.

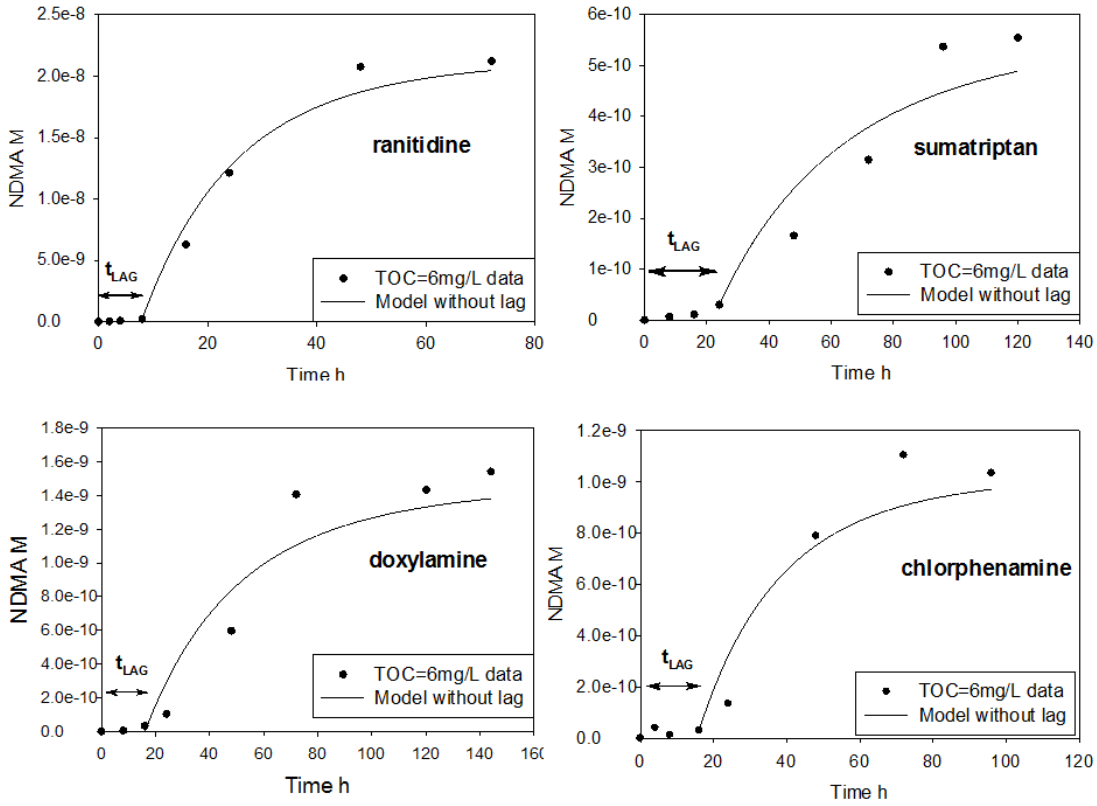

Figure 5.6: NDMA formation of amine precursors in river water (SDS, pH=7, TOC=6mg/L) and modeling of NDMA formation without lag-time, data (symbols) and model fitting (lines) (NDMA data from Shen and Andrews, 2011b)

5.4 Summary and Conclusions

A model was developed and parameterized based on NDMA formation trends observed in the literature. Results show that a second-order kinetic rate model simulates NDMA formation from NOM and model precursors over a range of reaction conditions. A narrow range of rate constants were obtained and appear to indicate a similar rate-limiting reaction step among different precursors and water sources. Though the model was not intended to reveal the relative importance of mono- or di- chloramine reactions in NDMA formation kinetics, it is applicable to describe how water conditions such as DOC and pH affect NDMA formation kinetics. In real water utilities, the model could be used to predict NDMA formation by measuring the $NDMA_{max}$ and monochloramine.

The proposed model needs to be further evaluated using a wider range of reaction conditions. For example, the importance of dissolved oxygen needs be investigated since it was found to be an important factor in NDMA formation from different amines such as DMA and ranitidine. NDMA kinetics test could be performed in other water matrices such as wastewater effluents. In addition, further detailed characterization of more precursors and their kinetics studies could help better understand NDMA formation in different water sources and a more precise model could be developed.

5.5 Acknowledgements

This research was supported by the Water Research Foundation (Project 4499, managed by Djanette Khiari), American Water Works Association Abel Wolman Fellowship, Water Environment Federation Canham Scholarship, and the Arizona State University Fulton School of Engineering Dean's Fellowship.

CHAPTER 6

INVESTIGATIONS ON IMPROVING THE NDMA FORMATION KINETICS MODEL

6.1 Introduction

In Chapter 4, I proposed a simple model on NDMA formation kinetics in varied water matrices based on a simple second order reaction model (Equation 6-1):

$$\frac{\mathrm{d[NDMA]}}{\mathrm{dt}} = k_{app}[\mathrm{Precursor}][\mathrm{NH_2Cl}] \qquad \text{Equation 6-1}$$

This model worked very well when applied to our experiments as well as to literature data with correlation coefficients more than 0.9 (Chapters 4 & 5). However this model does not take into account some of our observations as well as issues reported in the literature including the role of dichloramines in nitrosamine formation (Schreiber and Mitch, 2006b), the potential impact of dissolved oxygen (Schreiber and Mitch, 2006b; Le Roux et al., 2011) as well as an impact of the nature of the buffer in which experiments are performed.

In our experimental design and in the model monochloramine was used as the only oxidant that chloraminates the NDMA precursors to form NDMA. This assumption appears logical as the NDMA formation experiments were conducted at a pH 8 and a Cl_2:N mass ratio = 4.2.

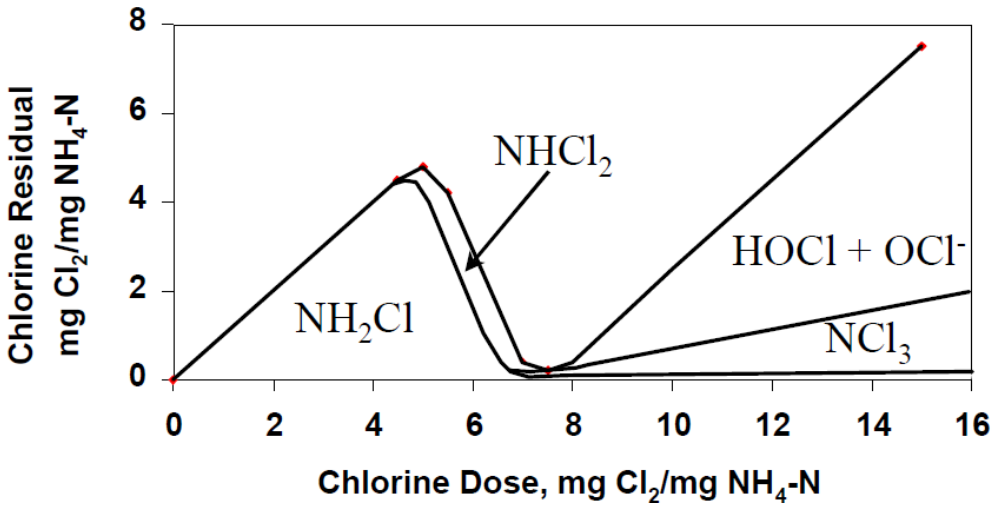

Figure 6.1: Theoretical Breakpoint Curve (USEPA, 1999)

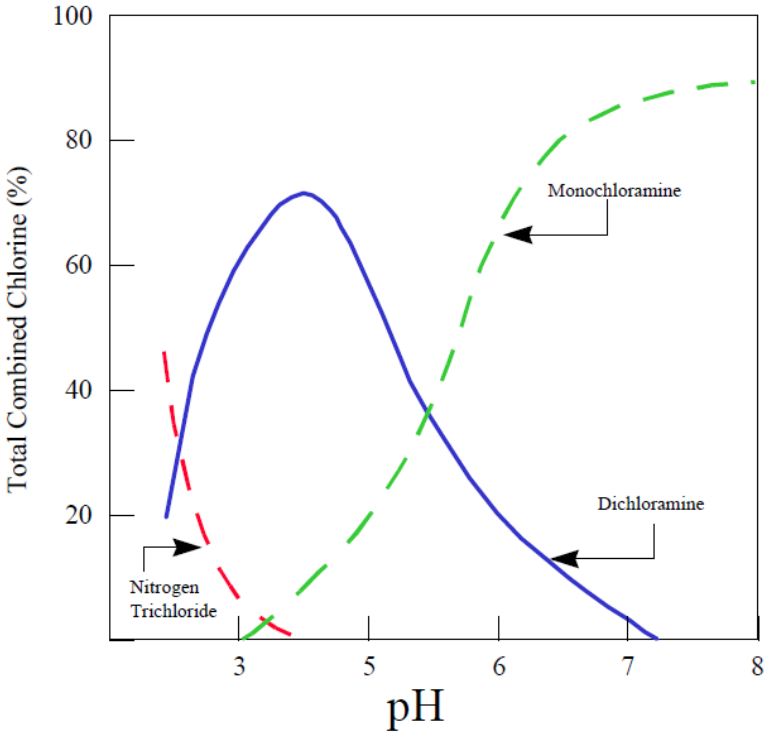

Figure 6.2: Distribution Diagram for Chloramines with pH (Palin, 1950; USEPA, 1999)

As shown in Figures 6.1 and 6.2, chloramine speciation is dependent on pH and controlled by Cl_2:N ratio. Monochloramine is the dominant chloramine species under our experimental conditions (pH = 8, Cl_2:N = 4.2) and the dichloramine formation from monochloramine is negligible.

Monochloramine is a of great advantage when aiming to develop an operational model that uses experimentally determined parameters because monochloramine concentrations can be measured accurately in our experiments, while the dichloramine quantification is challenging. In previous research chloramines were measured by two main methods. In a first approach, N,N-diethyl-p-phenylenediamine (DPD) colorimetry, is used to measure total chlorine, free chlorine and monochloramine. The dichloramine concentration then can be calculated as the difference between total chlorine- and monochloramine plus free chlorine. The detection limit of this method is 0.04 mgCl_2/L, making it not applicable to measure dichloramine at trace levels (<0.1mg/L). In a second approach monochloramine and dichloramine concentrations can be determined by measuring UV absorbance at 245nm and 295 nm and solving both equations using the respective molar extinction coefficients at 245nm and 295 nm (Schreiber and Mitch, 2005).The detection limit of the second method is ~ 0.2 mgCl_2/L. Both of these methods are hence endowed with substantial uncertainties and high detection limits.

While the model proposed in Chapter 4 considers only monochloramine, the kinetics experiments in Chapter 4, showed that dichloramine does likely affect NDMA formation even at pH 8 and a Cl_2:N ratio of 4.2. Specifically, the final NDMA conversion in samples with more monochloramine (18-20 mgCl_2/L) is higher than that with less monochloramine (6~7 mgCl_2/L). Both monochloramine doses are in large excess in all experiments. In our experiment conditions, dichloramine is thought at trace level and proportional to monochloramine. Therefore, it is probably the higher concentrations of dichloramine in samples with high monochloramine that leads to more NDMA formation. Our model using only monochloramine worked even the dichloramine is present in our experiments, probably because NDMA formation from

dichloramine can be expressed as ratio of monochloramine when dichloramine is at trace levels. However, the model can most likely not be extended to other reaction conditions when dichloramine concentrations increase with reduced pH or an increased Cl_2:N ratio. Therefore, it is necessary to investigate the NDMA formation kinetics from the reactions of both monochloramine and dichloramine (Equation 6-2) separately. It will improve the NDMA kinetics model and make it more applicable to predict NDMA formation in different reaction conditions (pH or Cl_2:N ratio).

$$\frac{\mathrm{d[NDMA]}}{\mathrm{dt}} = k_{mono}[\mathrm{Precursor}][\mathrm{NH_2Cl}] + k_{di}[\mathrm{Precursor}][\mathrm{NHCl_2}] \qquad \text{Equation 6-2}$$

A different consideration to improve the model of NDMA formation kinetics, is the potential role of dissolved oxygen in NDMA formation. In fact, it has been shown that dissolved oxygen concentrations affect the NDMA formation from model precursors such as DMA and ranitidine (Schreiber and Mitch, 2006b; Le Roux et al., 2011). However, no experimental data has been reported on complex real samples like wastewater or surface water and hence it is unknown if the amount of oxygen matters beyond idealized laboratory studies of model precursors.

Finally, most NDMA formation studies are performed under controlled pH conditions although different investigators use different reaction conditions, including the pH itself. A variety of buffer systems has been applied to maintain constant pH conditions and while the influence of pH on NDMA formation is known, no study addressed the impact of the nature of the buffer species as it is not expected to affect NDMA formation. However in the literature there are many instances of disagreement in terms of NDMA formation reported for the same amine precursors (Selbes et al., 2013) and one of the differences between studies is the nature of the buffer system.

Therefore it might be necessary to exclude the possible effect of buffer species on NDMA formation.

In this chapter I present my attempts to assess and quantify the contribution of dichloramine to NDMA formation by increasing dichloramine concentrations or eliminating dichloramine altogether. I further attempted to quantify dichloramine. Finally I investigated the effect of O_2 on the nitrosamine formation as well as potential buffer effects.

6.2 Experimental and Analytical Methods

In the experiments of NDMA formation from monochloramine and dichloramine, the preformed monochloramine stock solution (~2000 mgCl_2/L) was prepared by adding sodium hypochlorite into buffered (10 mM, Borate pH = 8.0 or Phosphate pH =7) ammonium chloride solution to produce a Cl_2:N mass ratio of 6:1. Chloramine stock solution was then spiked into DI water at ~5 mgCl_2/L. Since ammonium ion has huge interference on monochloramine concentrations measurement using Monochlor F reagents with a Hach DR5000 spectrophotometer (Hach Company, Loveland, CO). The method in our test to quantify monochloramine and dichloramine was measuring UV absorbance using the Hach DR5000 spectrophotometer at 295 nm and 245 nm and solving for their concentration from their extinction coefficients at both wavelengths.

To evaluate effect of dissolved oxygen, additional experiments were performed with varying dissolved oxygen levels in one wastewater secondary effluent (WW5 in Chapter 4). Dissolved oxygen concentrations were reduced from ~8 mg/L to below 0.1 mg/L by bubbling high purity argon gas into each sample for 5 minutes. Dissolved oxygen was measured by a portable meter (Thermo Scientific Inc., Waltham, MA). Monochloramine was added into the wastewater sample at 20 mgCl_2/L.

To evaluate the effect of buffer species on NDMA formation, three buffer solutions, borate, phosphate, and carbonate buffer solutions were made and were added into water samples and chloramine stock solutions (pH=8, 10 mM). Water samples of four amine precursors (methadone, ranitidine, *N*,*N*-Dimethyl-benzylamine (DMBzA), and *N*,*N*-Dimethylisopropylamine (DMiPA) at 25 nM were made by diluting their stock solutions into DI water. Wastewater effluent samples and surface water were sampled and treated similarly as described in Chapter 4. Monochloramine was added into precursor solutions, wastewater and surface water at 18 mgCl_2/L. Samples for NDMA formation were kept in dark at room temperature (23 ± 2 °C) for 72 hours until quenching and extraction. Quenching, extraction and NDMA analysis were the same as described in Chapter 4.

6.3 Results and Discussion

6.3.1 Role of Dichloramine in NDMA Formation

In order to assess the role of dichloramine in NDMA formation and potentially include it in the model, the dichloramine contribution needs to be isolated from the monochloramine contribution, which is challenging given the equilibrium and interconversion of the two species. Two approaches were tested, 1 enhancement of dichloramine and 2 suppression of dichloramine.

6.3.1.1 Enhancement of Dichloramine

To increase the dichloramine concentration, the Cl_2 to N_2 ratio was changed and a Cl_2:N ratio = 6:1 was chosen based on Figure 6.1. However, at pH 8 only 10% of dichloramine at maximum can be obtained. After 1 day aging, the ratio between dichloramine and monochloramine increased to ~50%, similar to previous reports (USEPA, 1999). However under these conditions the observed pH was around 2 and total chloramine decreased to <15% (2000 mgCl_2/L to 250 mgCl_2/L). Hence no

controlled experiments were possible under these conditions. We suspect that the chloramine decomposed, forming Cl_2 gas, possibly in the following reactions:

$$NH_2Cl + H_2O \rightarrow HOCl + NH_3 \quad \text{Equation 6-3}$$

$$HOCl + H^+ + Cl^- \rightarrow Cl_2 + H_2O \quad \text{Equation 6-4}$$

Experiments were conducted several times and showed similar results. The attempt of changing Cl_2:N ratio to increase dichloramine was not successful.

6.3.1.2 Suppression of Dichloramine

Rather than increasing dichloramine, another option would be to eliminate any dichloramine and hence isolate out the sole contribution of monochloramine. Therefore ammonium was first used to inhibit the formation of dichloramine in order to shift the equilibrium distribution.

$$2NH_2Cl + H^+ \leftrightarrow NHCl_2 + NH_4^+ \quad \text{Equation 6-5}$$

NH_4^+ (mass ratio NH_3: NH_2Cl = 100:4, NH_2Cl = 2000mgCl_2/L) was added in preformed chloramine stock solution. The excess NH_4^+ lowered the pH in stock solution from 8 to less than 7. Chloramine solutions with and without addition of NH_4^+ were used in wastewater effluent samples to form NDMA.

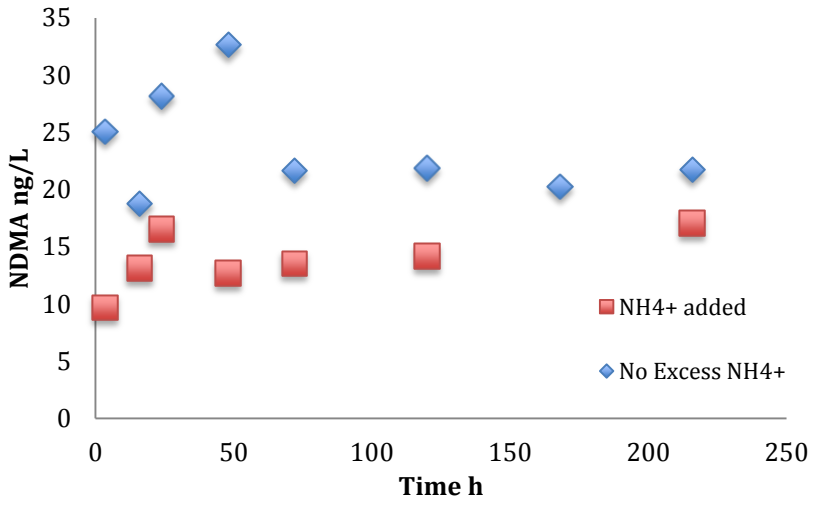

Figure 6.3: NDMA formation kinetics of wastewater effluents with and without excess NH_4^+ in chloramine stock solution

NDMA formation was lower with an excess NH_4^+ than without excess NH_4^+ (Figure 6.3). However, as the pH could not be well controlled in this method, the lower NDMA formation was possibly due to the decomposition of chloramine at the lower pH which likely decreased total chloramine concentrations, therefore adding excess NH_4^+ in stock solution was not a good way to inhibit dichloramine formation.

We then added NH_4^+ (mass ratio NH_3: NH_2Cl = 100:4) directly into buffered water solution in which pH did not change in presence of NH_4^+ during test. First at pH 8 an excess NH_4^+ was added in the water solution prior to 5 mgCl_2/L chloramine. No detectable dichloramine was found within 90 hours in both water samples with and without excess NH_4^+, probably due the high detection limit of the measurement. Then we lowered pH to 7 and dichloramine concentration was found to be 5% to 15% of monochloramine in all water samples. As shown in Figure 6.4, excess NH_4^+ does not inhibit formation of dichloramine.

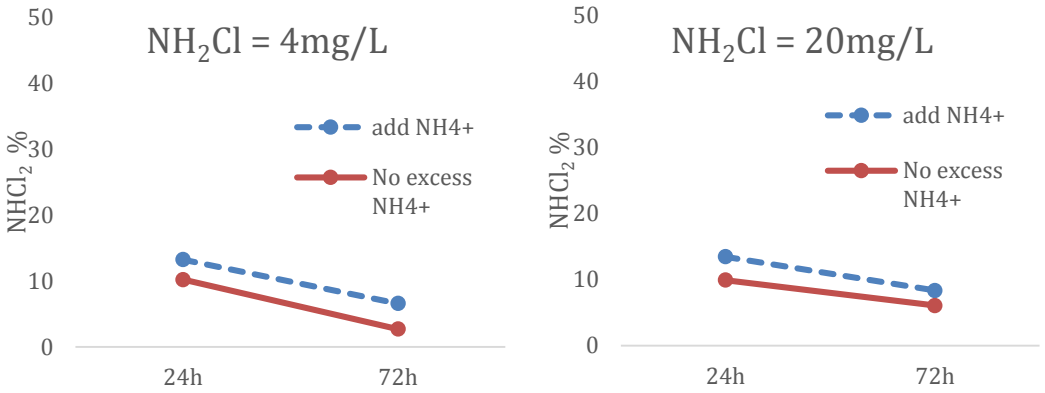

Figure 6-4: $NHCl_2/NH_2Cl$ ratio with and without excess NH_4^+ in nano pure water at pH=7.

Then ammonia (ammonium hydroxide) was used to inhibit dichloramine formation in water at pH =7. No dichloramine was detected in samples with ammonia within 24 hours. While samples without ammonia had about 15% of dichloramine. However, 10mM phosphate buffer solution we used was not strong enough to buffer

the excess ammonia. The pH of water went up to 9 after ammonia was added. In addition, after 24 hours, about 5% dichloramine was found in the water with ammonia. Ammonia could only inhibit formation of dichloramine in limited time and the pH could not be well controlled with addition of ammonia.

6.3.2 Influence of Dissolved Oxygen

The role of the dissolved oxygen on NDMA formation kinetics was studied in chloramination tests in wastewater (WW5 in Chapter 4). Figure 6-5 shows the impact of dissolved oxygen on the NDMA formation.

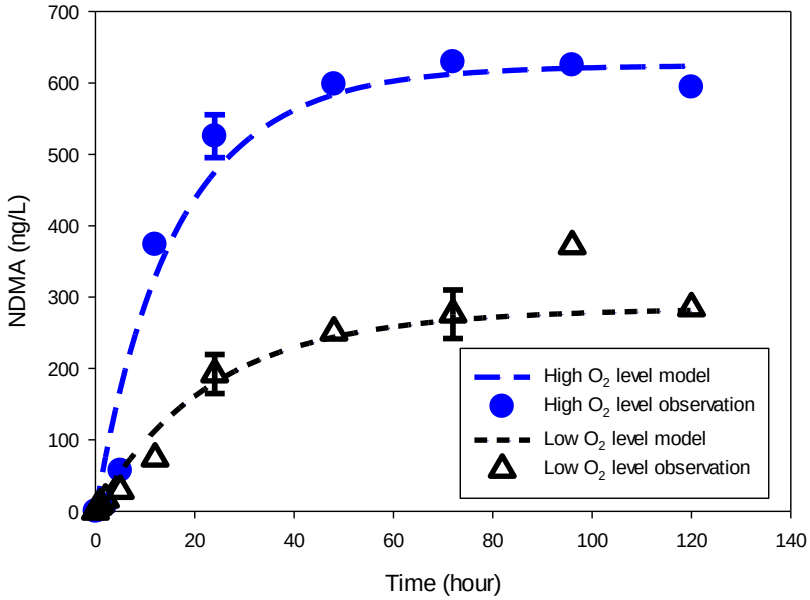

Figure 6-5: NDMA formation observed at varying dissolved O_2 concentrations (symbols) and fitted by Equations 4-1&4-2 (lines) in WW5 at same initial monochloramine dose (20 mgCl_2/L). Error bars represent one standard deviation (n=3) for select time points. (pH =8.0, 23 ± 1°C)

At two dissolved oxygen levels, the maximum NDMA formation concentrations were achieved over a similar time period (~50 hours). But similar to monochloramine, $NDMA_{max}$ (~8.4 nM) at the higher dissolved oxygen level (8.2 ± 0.1 mg O_2/L) was more than that (3.8 nM $NDMA_{max}$) formed in the presence of lower dissolved oxygen level (less than 2.3 mg O_2/L). Previous work showed a dependence

of NDMA yields on dissolved oxygen in the NDMA formation from DMA and ranitidine although their mechanisms were thought to be different (Schreiber and Mitch, 2006b; Le Roux et al., 2011). For both precursors, NDMA formation could be significantly reduced by decreasing dissolved oxygen. DMA and ranitidine are sensitive to dichloramine and monochloramine respectively, and our results could not tell if monochloramine or dichloramine was the responsible species for NDMA formed. Monochloramine degradation was observed to be much slower in the sample with low dissolved oxygen (Figure 6.6), indicating the interactions between chloramines and dissolved oxygen during chloramination.

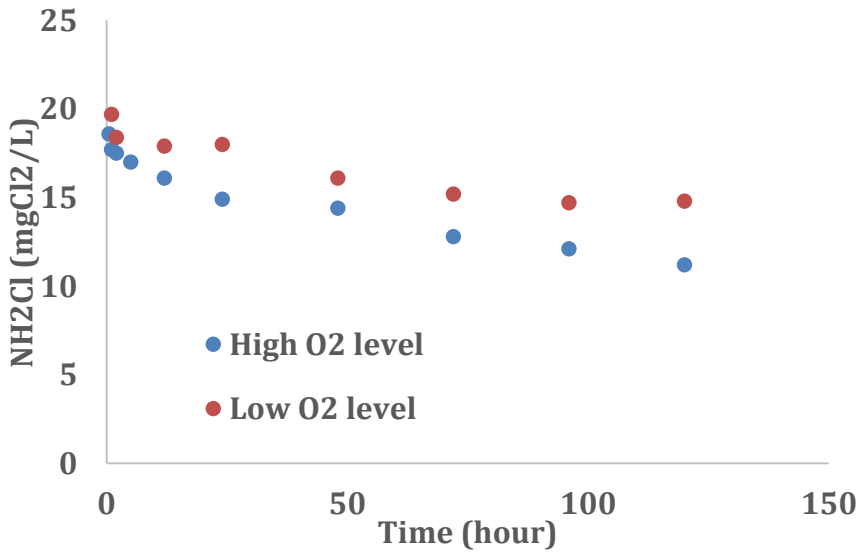

Figure 6.6: Monochloramine (NH_2Cl) decay kinetics at two dissolved O_2 levels

In general, dissolved oxygen behaved similarly to monochloramine in NDMA formation kinetics. Dissolved oxygen could possibly be included in the kinetics model, resulting in a third order reaction model.

6.3.3 Effect of buffer system

The effect of buffer species on NDMA formation was investigated. NDMA formation potential was investigated using commonly used buffer systems such as

borate (Hanigan et al., 2012), phosphate (Selbes et al., 2013) and bicarbonate (Schreiber and Mitch, 2006b). As shown in Figure 6.7, no effect of buffer species on NDMA formation from the four model precursors as well as in wastewater and surface water was observed. In addition, no effect of buffer concentration was observed. In the borate buffer at 100 mM NDMA formation was reduced, however this was the result of a lower pH (7 vs 8) when the borate buffer concentration increased.

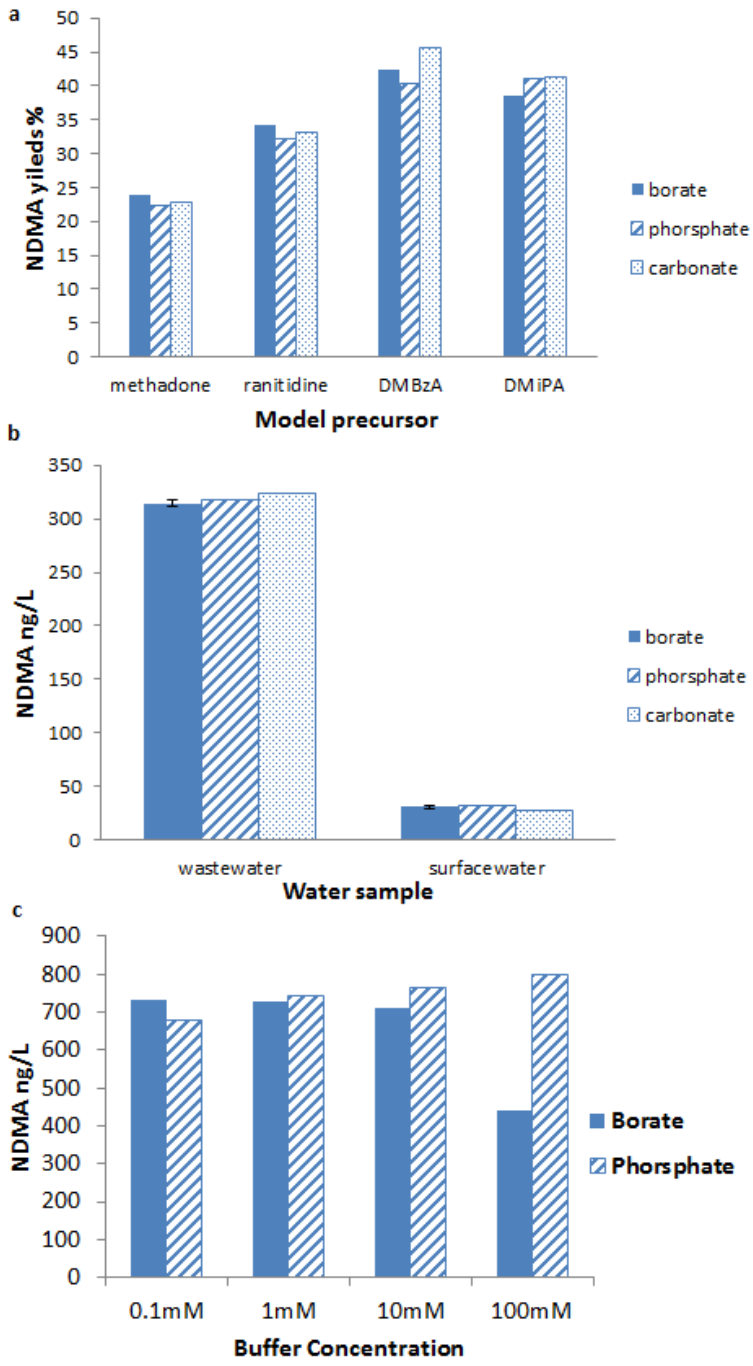

Figure 6.7: (a) NDMA formation from model precursors (pH=8); (b) NDMA formation in buffered (pH=8) wastewater and surface water; (c) NDMA formation in buffered wastewater with buffer concentration from 0.1 mM to 100 mM.

6.4 Conclusions

In the first part of this work, experiments were designed to explore the NDMA formations from dichloramine. However, the approaches of enhancement and suppression of dichloramine were not successful. Dichloramine formation could only be enhanced to 10% of monochloramine by increasing Cl_2:N mass ratio to 6:1 at pH = 8. Aging of monochloramine could produce ~50% dichloramine after 24 hours in stock solution (2000 mgCl_2/L) but the chloramine concentration was reduced to less than 250 mgCl_2/L in stock solution and pH decreased to ~2. Dichloramine could also be enhanced at pH lower than 7 (Figure 6.2), but the problem is that the low pH does not apply to the real waters such as surface water or wastewater effluents. The suppression of dichloramine formation also turned out unsuccessful. In our experiments we did not observe that the excess ammonium (NH_4^+) could inhibit the formation of dichloramine in either chloramine stock solution and in water sample. Large excess of ammonium (mass ratio NH_3: NH_2Cl = 100:4) in the stock solution will however affect the pH of the chloramine stock solution. Ammonia was found to be able to inhibit the dichloramine formation in water samples but the pH increase to 9 after ammonia addition, but the dichloramine formation happened after 24 hours. Therefore, in our preliminary tests neither ammonium nor ammonia was able to suppress the dichloramine formation under controlled pH conditions.

Another challenge in exploring NDMA formation from dichloramine is dichloramine measurements. The current two methods as described in section 6.1, due to their high detection limits, are not able to quantify the dichloramine concentration or monitor the change of dichloramine concentrations over time in water samples where monochloramine concentrations are <5 mgCl_2/L and at pH >7. The measurement of dichloramine could be interfered by species in water samples. In the Hach method, the

ammonium could affect the chloramine measurement. Organic matter would significantly influence the measurement of monochloramine and dichloramine in the UV method. To model the NDMA formation from dichloramine it would be necessary to develop a more sensitive method that can measure dichloramine at concentrations lower than 0.1 mgCl_2/L and free from interferences.

In the last part of this chapter, we found that NDMA formation was not influenced by buffer species or buffer concentrations. Dissolved oxygen showed a substantial impact on NDMA formation in the wastewater effluents. NDMA formation is higher in the presence of more dissolved oxygen. Future experiments are needed to reveal the role of dissolved oxygen in the NDMA formation yields and kinetics.

CHAPTER 7

SUMMARY AND OUTLOOK

This chapter will summarize the main findings of this thesis and provide suggestions for further study.

7.1 Summary

Chapter 2- N-Nitrosodimethylamine (NDMA) Measurements in Air

- Analytical methods based on SPME and SPE coupled with GC-MS were developed for NDMA measurement in air.
- PDMS/DVB and CAR/PDMS fibers were tested for the SPME method. PDMS/DVB showed a short equilibrium time of 30 mins while the CAR/PDMS fiber could not reach equilibrium even after 9 hours. SPME sampling is possible but leads to high detection limits (~ 1 ng/m^3 and 8 ng/m^3 for CAR/PDMS and PDMS/DVB, respectively) which might allow for high exposure monitoring but is too high for ambient monitoring.
- The SPE sampling method using commercially available coconut charcoal cartridges allows for low detections limit of 0.003ng/m^3 for a 2 m^3 air sample. The collection efficiency of SPE cartridges is more than 90% with negligible breakthrough or physical losses. It is free of positive or negative artifact formation under typical ambient sampling conditions.
- The SPE method was applied to ambient sampling in various environments and NDMA was found in all field samples at concentrations between 0.1 and 13.0 ng/m^3, higher than EPA's suggested screening level of NDMA in ambient air of 0.07 ng/m^3.

Chapter 3- Optical Properties of Water Soluble Organic Carbon (WSOC) in Atmospheric Aerosols and Fog/Cloud Waters

- WSOC has a stronger impact on NDMA photolysis than inorganic species such as nitrate or nitrite. The screening effect from organic matter can increase the lifetime of NDMA by 2 to 3 fold under typical fog and cloud conditions.
- WSOC from atmospheric aerosols has a higher mass absorption efficiency (MAE) than organic matter in fog and cloud water, resulting from a different composition, especially in regards of volatile species, that are not very absorbing but abundant in fogs and clouds..
- The mass absorption efficiency of WSOC varied by locations and particulate matter source. WSOC associated with vehicle emissions showed higher absorption than WSOC from biomass burning or other biogenic sources.
- In some instances the MAE of WSOC seems to be related to changes of ambient relative humidity, possibly indicating reactions in wet aerosols.

Chapter 4- *N*-Nitrosamine Formation Kinetics in Wastewater Effluents and Surface Waters

- NDMA formation increased to its maximum over hundreds of hours. NDMA maximum formations were observed in the range of 100 -1000 ng/L and 15-50 ng/L for wastewater and surface waters, respectively.
- NDMA formation is dependent on monochloramine concentrations.
- A simple model based on a second order reaction between monochloramine and NDMA precursors was developed to fit NDMA formation. NDMA formation was well predicted by the model with correlation coefficients higher than 0.9.

- The model fitted rate constants were in range of 0.01-0.09 $M^{-1}s^{-1}$ for different water samples, indicating formation of similar intermediates and a similar rate limiting step of NDMA formation for different amine precursors.
- With the measurement of NDMA formation and monochloramine exposure, the proposed model could be applied to predict NDMA concentrations in water treatment and distribution systems.

Chapter 5- Modeling NDMA Formation Kinetics during Chloramination of Model Compounds and Surface Waters Impacted by Wastewater Discharges

- NDMA formation data from the literature, including natural organic matter (NOM) and model precursors, were successfully fitted with the second order model over a variety of reaction conditions.
- NDMA formation rate constants were able to describe how water conditions such as pH and DOC impact NDMA formation kinetics.
- The model simulations revealed the relative importance of mono- or di-chloramine reactions in NDMA formation.
- Precursors with different NDMA formation yields were found to have similar rate constants to form NDMA in the same reaction conditions, suggesting a similar rate-limit step among different precursors.

Chapter 6- Investigations on Improving the NDMA Formation Model

- Dichloramine formation could be enhanced to 10% of monochloramine by increasing Cl_2:N mass ratio to 6:1.
- Dichloramine formation could not suppressed by NH^{4+}. Ammonia could inhibit the dichloramine formation for a limited time (less than 24h), but ammonia will change pH of the reaction system.

- Dissolved oxygen showed a substantial impact on NDMA formation and could possibly be included in the kinetics model.
- No effect of buffer species or concentrations was observed for NDMA formation.

7.2 Suggestions of Future Research

For NDMA measurement in air, the SPME method has not been used in ambient sampling due to its high detection limit. However, the SPME with GC-MS could still be applied to measure NDMA in locations such as indoor area, especially with tobacco smoking activities, so further testing to evaluate such applications could be interesting.

Not only NDMA but also other nitrosamines are present in air. Therefore, further evaluation of SPE and SPME sampling performance in monitoring other nitrosamines is needed. In addition, gas-particle partitioning of nitrosamines needs to be investigated as emerging studies showed that there are nitrosamines in particulate matter.

WSOC from particulate matter has shown to impact NDMA photolysis and it is found to have different absorptivity from organic matter in fog and cloud. It will be interesting to explore what other species could be impacted by such 'screening' effect of organic matter and the extent of this effect. Additionally, it remains unknown how the organic matter influence the indirect photolysis by scavenging or generating radicals which will react with the species we are interested, such as nitrosamines.

Although in this work the developed second order reaction model fitted NDMA formation data well in our experiments and in literature data, additional NDMA kinetics work is needed, especially for those precursors that have been recently identified, such as methadone or coagulation polymers. The kinetics model needs to be further

developed as we have identified possible impacts of dichloramine and dissolved oxygen, which might limit the conditions under which the model remains valid.

The measurement of dichloramine is challenging due to the high detection limit using current methods. To explore the NDMA formation from dichloramine at trace level in water treatment or distribution systems a more sensitive method needs to be developed.

Finally, the hypothesis of the formation of a common intermediate in nitrosamine formation from different precursors needs to be investigated.

REFERENCES

Afonso Perera, A. M., in: Nollet, L. M. L. (Ed.), 2006. Chromatographic Analysis of the Environment, CRC Press–Taylor & Francis, Boca Raton, FL, pp. 419–452 (Chapter 12).

Agilent, 2012. https://www.agilent.com/cs/library/applications/5991-1554EN.pdf (accessed March 26th, 2014)

Akyüz, M. and Ata, Ş., 2013. Seasonal variations of particle-associated nitrosamines by gas chromatography–mass spectrometry in the atmospheric environment of Zonguldak, Turkey. Environmental Science and Pollution Research, 20(10), pp.7398-7412.

Allen, J.M., Allen, S.K. and Baertschi, S.W., 2000. 2-Nitrobenzaldehyde: a convenient UV-A and UV-B chemical actinometer for drug photostability testing. Journal of Pharmaceutical and Biomedical Analysis, 24(2), pp.167-178.

Andrade, R., Reyes, F.G. and Rath, S., 2005. A method for the determination of volatile N-nitrosamines in food by HS-SPME-GC-TEA. Food Chemistry, 91(1), pp.173-179.

Andreae, M.O. and Gelencsér, A., 2006. Black carbon or brown carbon? The nature of light-absorbing carbonaceous aerosols. Atmospheric Chemistry and Physics, 6(10), pp.3131-3148.

Andrzejewski, P., Kasprzyk-Hordern, B. and Nawrocki, J., 2008. N-nitrosodimethylamine (NDMA) formation during ozonation of dimethylamine-containing waters. Water Research, 42(4), pp.863-870.

Aragón, M., Marcé, R.M. and Borrull, F., 2013. Determination of N-nitrosamines and nicotine in air particulate matter samples by pressurised liquid extraction and gas chromatography-ion trap tandem mass spectrometry. Talanta, 115, pp.896-901.

ATSDR. 1999. "ToxFAQs – N-Nitrosodimethylamine."

Ayanaba, A. and Alexander, M., 1974. Transformations of methylamines and formation of a hazardous product, dimethylnitrosamine, in samples of treated sewage and lake water. Journal of Environmental Quality, 3(1), pp.83-89.

Baisautova, Z., 2008. Environmental Fate Assessment of the Rocket Fuel Compound, 1, 1-dimethylhydrazine and Its By-product N-nitrosodimethylamine. ProQuest.

Bartsch, H. and Spiegelhalder, B., 1996. Environmental exposure to N-nitroso compounds (NNOC) and precursors: an overview. European Journal of Cancer Prevention, 5, pp.11-17.

Benn, T., Herckes, P., Westerhoff, P., 2012. Fullerenes in Environmental Samples: C60 in atmospheric particulate matter, in Analysis and Risk of Nanomaterials in Environmental and Food Samples, Edited by Damia Barcelo and Marinella Farré, Elsevier Science, Comprehensive Analytical Chemistry Series, #59

Bolto, B., 2005. Reaction of chlorine with organic polyelectrolytes in water treatment: a review. Journal of Water Supply: Research and Technology-Aqua, 54(8), pp.531-544.

Bond, T.C., 2001. Spectral dependence of visible light absorption by carbonaceous particles emitted from coal combustion. Geophysical Research Letters, 28(21), pp.4075-4078.

Bones, D.L., Henricksen, D.K., Mang, S.A., Gonsior, M., Bateman, A.P., Nguyen, T.B., Cooper, W.J. and Nizkorodov, S.A., 2010. Appearance of strong absorbers and fluorophores in limonene‐O3 secondary organic aerosol due to NH4+‐mediated chemical aging over long time scales. Journal of Geophysical Research: Atmospheres, 115(D5).

Boyd, J.M., Hrudey, S.E., Li, X.F. and Richardson, S.D., 2011. Solid-phase extraction and high-performance liquid chromatography mass spectrometry analysis of nitrosamines in treated drinking water and wastewater. TrAC Trends in Analytical Chemistry, 30(9), pp.1410-1421.

Brito, J., Rizzo, L.V., Herckes, P., Vasconcellos, P.D.C., Caumo, S.E.D.S., Fornaro, A., Ynoue, R.Y., Artaxo, P. and Andrade, M.D.F., 2013. Physical–chemical characterisation of the particulate matter inside two road tunnels in the São Paulo Metropolitan Area. Atmospheric Chemistry and Physics, 13(24), pp.12199-12213.

Brown, S.G., Frankel, A. and Hafner, H.R., 2007. Source apportionment of VOCs in the Los Angeles area using positive matrix factorization. Atmospheric Environment, 41(2), pp.227-237.

Brubaker, K.L., Stetter, J.R., Demirgian, J.C., Boparai, A. and Schneider, J.F., 1985. Products of the neutralization of hydrazine fuels with hypochlorite (No. CONF-8511110-4). Argonne National Lab., IL (USA).

Brunnemann, K.D., Yu, L. and Hoffmann, D., 1977. Assessment of carcinogenic volatile N-nitrosamines in tobacco and in mainstream and sidestream smoke from cigarettes. Cancer Research, 37(9), pp.3218-3222.

Brunnemann, K.D., Stahnke, G. and Hoffmann, D., 1978. Chemical studies on tobacco smoke. LXI. Volatile pyridines: Quantitative analysis in mainstream and sidestream smoke of cigarettes and cigars. Analytical Letters, 11(7), pp.545-560.

CDPH, NDMA and other nitrosamines - Drinking water issues, 2013. Http://www.waterboards.ca.gov/drinking_water/certlic/drinkingwater/NDMA.shtml (accessed September 26th, 2014)

Carrico, C.M., Petters, M.D., Kreidenweis, S.M., Sullivan, A.P., McMeeking, G.R., Levin, E.J.T., Engling, G., Malm, W.C. and Collett Jr, J.L., 2010. Water uptake and chemical composition of fresh aerosols generated in open burning of biomass. Atmospheric Chemistry and Physics, 10(11), pp.5165-5178.

Charrois, J.W., Arend, M.W., Froese, K.L. and Hrudey, S.E., 2004. Detecting N-nitrosamines in drinking water at nanogram per liter levels using ammonia positive chemical ionization. Environmental Science & Technology, 38(18), pp.4835-4841.

Charrois, J.W. and Hrudey, S.E., 2007. Breakpoint chlorination and free-chlorine contact time: Implications for drinking water N-nitrosodimethylamine concentrations. Water Research, 41(3), pp.674-682.

Chen, B. and Westerhoff, P., 2010. Predicting disinfection by-product formation potential in water. Water Research, 44(13), pp.3755-3762.

Chen, B., Lee, W., Westerhoff, P.K., Krasner, S.W. and Herckes, P., 2010. Solar photolysis kinetics of disinfection byproducts. Water Research, 44(11), pp.3401-3409.

Chen, Z. and Valentine, R.L., 2006. Modeling the formation of N-nitrosodimethylamine (NDMA) from the reaction of natural organic matter (NOM) with monochloramine. Environmental Science & Technology, 40(23), pp.7290-7297.

Cheng, Y., He, K.B., Zheng, M., Duan, F.K., Du, Z.Y., Ma, Y.L., Tan, J.H., Yang, F.M., Liu, J.M., Zhang, X.L. and Weber, R.J., 2011. Mass absorption efficiency of elemental carbon and water-soluble organic carbon in Beijing, China. Atmospheric Chemistry and Physics, 11(22), pp.11497-11510.

Choi, J. and Valentine, R.L., 2002. Formation of N-nitrosodimethylamine (NDMA) from reaction of monochloramine: a new disinfection by-product. Water Research, 36(4), pp.817-824.

Choi, J. and Valentine, R.L., 2003. N-nitrosodimethylamine formation by free-chlorine-enhanced nitrosation of dimethylamine. Environmental Science & Technology, 37(21), pp.4871-4876.

da Silva, E.F. and Booth, A.M., 2013. Emissions from postcombustion CO2 capture plants. Environmental Science & Technology, 47(2), pp.659-660.

da Silva, E.F., Hoff, K.A. and Booth, A., 2013a. Emissions from CO2 capture plants; an overview. Energy Procedia, 37, pp.784-790.

da Silva, E.F., et al., 2013b. Emission studies from a CO2 capture pilot plant. Energy Procedia 37, 778–783.

DHS, 2002. California Department of Health Services;NDMA in California Drinking Water; March 15, http://www. dhs.ca.gov/ps/ddwem/chemicals/NDMA/history.htm.

Du, Z., He, K., Cheng, Y., Duan, F., Ma, Y., Liu, J., Zhang, X., Zheng, M. and Weber, R., 2014. A yearlong study of water-soluble organic carbon in Beijing II: Light absorption properties. Atmospheric Environment, 89, pp.235-241.

Duirk, S.E., Gombert, B., Croué, J.P. and Valentine, R.L., 2005. Modeling monochloramine loss in the presence of natural organic matter. Water Research, 39(14), pp.3418-3431.

Ehrenhauser, F.S., Khadapkar, K., Wang, Y., Hutchings, J.W., Delhomme, O., Kommalapati, R.R., Herckes, P., Wornat, M.J. and Valsaraj, K.T., 2012. Processing of atmospheric polycyclic aromatic hydrocarbons by fog in an urban environment. Journal of Environmental Monitoring, 14(10), pp.2566-2579.

Ervens, B.T.B.W.R., Turpin, B.J. and Weber, R.J., 2011. Secondary organic aerosol formation in cloud droplets and aqueous particles (aqSOA): a review of laboratory, field and model studies. Atmospheric Chemistry and Physics, 11(21), pp.11069-11102.

Fajen, J.M., Carson, G.A., Rounbehler, D.P., Fan, T.Y., Vita, R., Goff, U.E., Wolf, M.H., Edwards, G.S., Fine, D.H., Reinhold, V. and Biemann, K., 1979. N-nitrosamines in the rubber and tire industry. Science, 205(4412), pp.1262-1264.

Farren, N.J., Ramírez, N., Lee, J.D., Finessi, E., Lewis, A.C. and Hamilton, J.F., 2015. Estimated Exposure Risks from Carcinogenic Nitrosamines in Urban Airborne Particulate Matter. Environmental Science & Technology, 49(16), pp.9648-9656.

Feng, J., Hu, M., Chan, C.K., Lau, P.S., Fang, M., He, L. and Tang, X., 2006. A comparative study of the organic matter in PM 2.5 from three Chinese megacities in three different climatic zones. Atmospheric Environment, 40(21), pp.3983-3994.

Fine, D.H., Rounbehler, D.P. and Belcher, N.M., 1976a. N-Nitroso compounds: Detection in ambient air. Science, 192(4246), pp.1328-1330.

Fine, D.H., Rounbehler, D.P., Pellizzari, E.D., Bunch, J.E., Berkley, R.W., McCrae, J., Bursey, J.T., Sawicki, E., Krost, K. and DeMarrais, G.A., 1976b. N-nitrosodimethylamine in air. Bulletin of environmental contamination and toxicology, 15(6), pp.739-746.

Fine, D.H., Reinhold, V. and Biemann, K., 1979. N-nitrosamines in the rubber and tire industry. Science, 205(4412), pp.1262-1264.

Finlayson-Pitts, B.J. and Pitts Jr, J.N., 1999. Chemistry of the upper and lower atmosphere: theory, experiments, and applications. Academic press.

Ge, X., Wexler, A.S. and Clegg, S.L., 2011. Atmospheric amines–Part I. A review. Atmospheric Environment, 45(3), pp.524-546.

Gerecke, A.C. and Sedlak, D.L., 2003. Precursors of N-nitrosodimethylamine in natural waters. Environmental Science & Technology, 37(7), pp.1331-1336.

Gordon R. J., 1978. Survey for Airborne Nitrosamines Prepared by University of California, School of Medicine, for the California Air Resources Board. Contract No. A6-096-30.

Hallquist, M., Wenger, J.C., Baltensperger, U., Rudich, Y., Simpson, D., Claeys, M., Dommen, J., Donahue, N.M., George, C., Goldstein, A.H. and Hamilton, J.F., 2009. The formation, properties and impact of secondary organic aerosol: current and emerging issues. Atmospheric Chemistry and Physics, 9(14), pp.5155-5236.

Hanigan, D., Zhang, J., Herckes, P., Krasner, S.W., Chen, C. and Westerhoff, P., 2012. Adsorption of N-nitrosodimethylamine precursors by powdered and granular activated carbon. Environmental Science & Technology, 46(22), pp.12630-12639.

Hanigan, D., Thurman, E.M., Ferrer, I., Zhao, Y., Andrews, S., Zhang, J., Herckes, P. and Westerhoff, P., 2015. Methadone Contributes to N-Nitrosodimethylamine Formation in Surface Waters and Wastewaters during Chloramination. Environmental Science & Technology Letters, 2(6), pp.151-157.

Hanst, P.L., Spence, J.W. and Miller, M., 1977. Atmospheric chemistry of N-nitroso dimethylamine. Environmental Science & Technology, 11(4), pp.403-405.

Haruta, S., Jiao, W., Chen, W., Chang, A.C. and Gan, J., 2011. Evaluating Henry's law constant of N-nitrosodimethylamine (NDMA). Water Science & Technology, 64(8).

Hecobian, A., Zhang, X., Zheng, M., Frank, N., Edgerton, E.S. and Weber, R.J., 2010. Water-Soluble Organic Aerosol material and the light-absorption characteristics of aqueous extracts measured over the Southeastern United States. Atmospheric Chemistry and Physics, 10(13), pp.5965-5977.

Hennigan, C.J., Bergin, M.H., Russell, A.G., Nenes, A. and Weber, R.J., 2009. Gas/particle partitioning of water-soluble organic aerosol in Atlanta. Atmospheric Chemistry and Physics, 9(11), pp.3613-3628.

Herckes, P., Leenheer, J.A. and Collett, J.L., 2007. Comprehensive characterization of atmospheric organic matter in Fresno, California fog water. Environmental Science & Technology, 41(2), pp.393-399.

Herckes, P., Valsaraj, K.T. and Collett, J.L., 2013. A review of observations of organic matter in fogs and clouds: Origin, processing and fate. Atmospheric Research, 132, pp.434-449.

Hoffer, A., Gelencsér, A., Guyon, P., Kiss, G., Schmid, O., Frank, G.P., Artaxo, P. and Andreae, M.O., 2006. Optical properties of humic-like substances (HULIS) in biomass-burning aerosols. Atmospheric Chemistry and Physics, 6(11), pp.3563-3570.

Hung, H.W., Lin, T.F., Chiu, C.H., Chang, Y.C. and Hsieh, T.Y., 2010. Trace analysis of N-nitrosamines in water using solid-phase microextraction coupled with gas chromatograph–tandem mass spectrometry. Water, Air, & Soil Pollution, 213(1-4), pp.459-469.

Hutchings, J.W., Robinson, M.S., McIlwraith, H., Kingston, J.T. and Herckes, P., 2009. The chemistry of intercepted clouds in Northern Arizona during the North American monsoon season. Water, Air, and Soil Pollution, 199(1-4), pp.191-202.

Hutchings, J.W., Ervens, B., Straub, D. and Herckes, P., 2010. N-nitrosodimethylamine occurrence, formation and cycling in clouds and fogs. Environmental Science & Technology, 44(21), pp.8128-8133.

IARC, 1987. Some N-nitroso compounds. IARC Monographs on the Evaluation of the Carcinogenic Risk of Chemicals to Humans, vol. 17. Lyon, France

Ianni, J. C., Kintecus. Windows Version 2.80, 2002, www.kintecus.com. (accessed September 10th, 2014)

Jaffrezo, J.L., Aymoz, G., Delaval, C. and Cozic, J., 2005. Seasonal variations of the water soluble organic carbon mass fraction of aerosol in two valleys of the French Alps. Atmospheric Chemistry and Physics, 5(10), pp.2809-2821.

Karl, M., Dye, C., Wisthaler, A., Schmidbauer, N., Mikoviny, T., Lanza, M., D'Anna, B., Meme, A., Vázquez-Moreno, M., Muñoz, A., Garciá, M.R., Bórras, E., 2013. Photo-oxidation of two amines for use in CO2 capture: Experimental studies in the European Photo Reactor EUPHORE. Kjeller, NILU (NILU OR, 44/2013)

Kemper, J.M., Walse, S.S. and Mitch, W.A., 2010. Quaternary amines as nitrosamine precursors: a role for consumer products?. Environmental Science & Technology, 44(4), pp.1224-1231.

Kim, H., Kim, J.Y., Jin, H.C., Lee, J.Y. and Lee, S.P., 2016. Seasonal variations in the light-absorbing properties of water-soluble and insoluble organic aerosols in Seoul, Korea. Atmospheric Environment.

Kirchstetter, T.W., Novakov, T. and Hobbs, P.V., 2004. Evidence that the spectral dependence of light absorption by aerosols is affected by organic carbon. Journal of Geophysical Research: Atmospheres, 109(D21).

Kirillova, E.N., Andersson, A., Han, J., Lee, M. and Gustafsson, Ö., 2014. Sources and light absorption of water-soluble organic carbon aerosols in the outflow from northern China. Atmospheric Chemistry and Physics, 14(3), pp.1413-1422.

Kohut, K.D. and Andrews, S.A., 2003. Polyelectrolyte age and N-nitrosodimethylamine formation in drinking water treatment. Water Quality Research Journal of Canada, 38(4), pp.719-735.

Krasner, S.W., Westerhoff, P., Chen, B., Rittmann, B.E. and Amy, G., 2009. Occurrence of disinfection byproducts in United States wastewater treatment plant effluents. Environmental Science & Technology, 43(21), pp.8320-8325.

Krasner, S.W., Westerhoff, P., Mitch, W.A. and Skadsen, J., 2012. Case studies on nitrosamine formation and control at full-scale drinking water treatment plants. In Proceedings of the 2012 American Water Works Association Water Quality Technology Conference, Denver, Colo.

Krasner, S.W., Mitch, W.A., McCurry, D.L., Hanigan, D. and Westerhoff, P., 2013. Formation, precursors, control, and occurrence of nitrosamines in drinking water: a review. Water Research, 47(13), pp.4433-4450.

Langford, V.S., Gray, J.D., Maclagan, R.G., Milligan, D.B. and McEwan, M.J., 2015. Real-time measurements of nitrosamines in air. International Journal of Mass Spectrometry, 377, pp.490-495.

Le Roux, J., Gallard, H. and Croué, J.P., 2011. Chloramination of nitrogenous contaminants (pharmaceuticals and pesticides): NDMA and halogenated DBPs formation. Water Research, 45(10), pp.3164-3174.

Le Roux, J., Gallard, H., Croué, J.P., Papot, S. and Deborde, M., 2012. NDMA formation by chloramination of ranitidine: kinetics and mechanism. Environmental Science & Technology, 46(20), pp.11095-11103.

Lee, A.K., Hayden, K.L., Herckes, P., Leaitch, W.R., Liggio, J., Macdonald, A.M. and Abbatt, J.P.D., 2012. Characterization of aerosol and cloud water at a mountain site during WACS 2010: secondary organic aerosol formation through oxidative cloud processing. Atmospheric Chemistry and Physics, 12(15), pp.7103-7116.

Lee, C., Schmidt, C., Yoon, J. and Von Gunten, U., 2007. Oxidation of N-nitrosodimethylamine (NDMA) precursors with ozone and chlorine dioxide: kinetics and effect on NDMA formation potential. Environmental Science & Technology, 41(6), pp.2056-2063.

Lestremau, F., Desauziers, V. and Fanlo, J.L., 2001. Formation of artefacts during air analysis of volatile amines by solid-phase micro extraction. Analyst, 126(11), pp.1969-1973.

Li, C, 2011. Trends and Effects of Chloramine in Drinking Water. Water Conditioning & Purification, 53(10), 52-56.

Liew, D., Linge, K.L., Joll, C., Heitz, A., Trolio, R., Breckler, L., Henderson, R. and Charrois, J.W.A., 2011. Formation of nitrogenous disinfection by-products (N-DBPs) in raw and treated drinking water. In 2011 Oz Water Conference.

Liu, Y.D., Selbes, M., Zeng, C., Zhong, R. and Karanfil, T., 2014. Formation Mechanism of NDMA from ranitidine, trimethylamine, and other tertiary amines during chloramination: A computational study. Environmental Science & Technology, 48(15), pp.8653-8663.

Lunn, G. and Sansone, E.B., 1994. Oxidation of 1, 1-dimethylhydrazine (UDMH) in aqueous solution with air and hydrogen peroxide. Chemosphere, 29(7), pp.1577-1590.

Lunn, G., Sansone, E.D., Andrews, A.W. and Zeiger, E., 1991. Aerial oxidation of hydrazines to nitrosamines. Environmental and Molecular Mutagenesis, 17(1), pp.59-62.

Mahanama, K.R. and Daisey, J.M., 1996. Volatile N-nitrosamines in environmental tobacco smoke: sampling, analysis, emission factors, and indoor air exposures. Environmental Science & Technology, 30(5), pp.1477-1484.

Mancilla, Y., Mendoza, A., Fraser, M.P. and Herckes, P., 2015. Chemical characterization of fine organic aerosol for source apportionment at Monterrey, Mexico. Atmospheric Chemistry and Physics Discussions, 15(13), pp.17967-18010.

Masuda, M., Mower, H.F., Pignatelli, B., Celan, I., Friesen, M.D., Nishino, H. and Ohshima, H., 2000. Formation of N-nitrosamines and N-nitramines by the reaction of secondary amines with peroxynitrite and other reactive nitrogen species: comparison with nitrotyrosine formation. Chemical Research in Toxicology, 13(4), pp.301-308.

Mirvish, S.S., Issenberg, P. and Sornson, H.C., 1976. Air—Water and Ether—Water Distribution of N—Nitroso Compounds: Implications for Laboratory Safety, Analytic Methodology, and Carcinogenicity for the Rat Esophagus, Nose, and Liver. Journal of the National Cancer Institute, 56(6), pp.1125-1129.

Mirvish, S.S., 1995. Role of N-nitroso compounds (NOC) and N-nitrosation in etiology of gastric, esophageal, nasopharyngeal and bladder cancer and contribution to cancer of known exposures to NOC. Cancer Letters, 93(1), pp.17-48

Mitch, W., Krasner, S. W., Westerhoff, P., Dotson, A. 2009. Occurrence and Formation of Nitrogenous Disinfection By-Products (Final Report, Project #3014); AwwaRF/USEPA: Denver, CO, 2009; p 145.

Mitch, W.A. and Sedlak, D.L., 2002a. Formation of N-nitrosodimethylamine (NDMA) from dimethylamine during chlorination. Environmental Science & Technology, 36(4), pp.588-595.

Mitch, W.A. and Sedlak, D.L., 2002b. Factors controlling nitrosamine formation during wastewater chlorination. Water Science and Technology: Water Supply, 2(3), pp.191-198.

Mitch, W.A., Sharp, J.O., Trussell, R.R., Valentine, R.L., Alvarez-Cohen, L. and Sedlak, D.L., 2003. N-nitrosodimethylamine (NDMA) as a drinking water contaminant: a review. Environmental Engineering Science, 20(5), pp.389-404.

Mitch, W.A. and Sedlak, D.L., 2004. Characterization and fate of N-nitrosodimethylamine precursors in municipal wastewater treatment plants. Environmental Science & Technology, 38(5), pp.1445-1454.

Mitch, W.A. and Schreiber, I.M., 2008. Degradation of tertiary alkylamines during chlorination/chloramination: implications for formation of aldehydes, nitriles, halonitroalkanes, and nitrosamines. Environmental Science & Technology, 42(13), pp.4811-4817.

Miyazaki, Y., Kondo, Y., Takegawa, N., Komazaki, Y., Fukuda, M., Kawamura, K., Mochida, M., Okuzawa, K. and Weber, R.J., 2006. Time-resolved measurements of water-soluble organic carbon in Tokyo. Journal of Geophysical Research: Atmospheres, 111(D23).

Müller, J.F., Stavrakou, T., Wallens, S., Smedt, I.D., Roozendael, M.V., Potosnak, M.J., Rinne, J., Munger, B., Goldstein, A. and Guenther, A.B., 2008. Global isoprene emissions estimated using MEGAN, ECMWF analyses and a detailed canopy environment model. Atmospheric Chemistry and Physics, 8(5), pp.1329-1341.

Munch, J.W. and Bassett, M.V., 2004. Method 521 determination of nitrosamines in drinking water by solid phase extraction and capillary column gas chromatography with large volume injection and chemical ionization tandem mass spectrometry (MS/MS). National Exposure Research Laboratory Office of Research and Development, US Environmental Protection Agency, Cincinnati.

Najm, I. and Trussell, R.R., 2001. NDMA formation IN WATER AND WASTEMATER. Journal (American Water Works Association), 93(2), pp.92-99.

Nielsen, C.J., Herrmann, H. and Weller, C., 2012. Atmospheric chemistry and environmental impact of the use of amines in carbon capture and storage (CCS). Chemical Society Reviews, 41(19), pp.6684-6704.

NIOSH Method 2522, No. 2, August 15, 1994

OEHHA, 2006. Public Health Goal for Chemicals in Drinking Water: N-Nitrosodimethylamine.

OSHA Method #27, US Department of Labor, Organic Methods Evaluation Branch, OSHA Analytical Laboratory, Salt Lake City, UT, https://www.osha.gov/dts/sltc/methods/organic/org027/org027.html (accessed October 20June 6th, 2015)

Ozekin, K., Valentine, R.L. and Vikesland, P.J., 1996. Modeling the decomposition of disinfecting residuals of chloramine. Water Disinfection and Natural Organic Matter, 649, pp.115-125.

Padhye, L.P., Hertzberg, B., Yushin, G. and Huang, C.H., 2011. N-nitrosamines formation from secondary amines by nitrogen fixation on the surface of activated carbon. Environmental Science & Technology, 45(19), pp.8368-8376.

Park, S.H., Wei, S., Mizaikoff, B., Taylor, A.E., Favero, C. and Huang, C.H., 2009. Degradation of amine-based water treatment polymers during chloramination as N-nitrosodimethylamine (NDMA) precursors. Environmental Science & Technology, 43(5), pp.1360-1366.

Park, S.S. and Cho, S.Y., 2011. Tracking sources and behaviors of water-soluble organic carbon in fine particulate matter measured at an urban site in Korea. Atmospheric Environment, 45(1), pp.60-72.

Pérez, D.M., Alatorre, G.G., Álvarez, E.B., Silva, E.E. and Alvarado, J.F.J., 2008. Solid-phase microextraction of N-nitrosodimethylamine in beer. Food Chemistry, 107(3), pp.1348-1352.

Plumlee, M.H. and Reinhard, M., 2007. Photochemical attenuation of N-nitrosodimethylamine (NDMA) and other nitrosamines in surface water. Environmental Science & Technology, 41(17), pp.6170-6176.

Popp, P. and Paschke, A., 1997. Solid phase microextraction of volatile organic compounds using carboxen-polydimethylsiloxane fibers. Chromatographia, 46(7-8), pp.419-424.

Reynolds, A.J., Verheyen, T.V., Adeloju, S.B., Meuleman, E. and Feron, P., 2012. Towards commercial scale postcombustion capture of CO2 with monoethanolamine solvent: key considerations for solvent management and environmental impacts. Environmental Science & Technology, 46(7), pp.3643-3654.

Ridd, J.H., 1961. Nitrosation, diazotisation, and deamination. Quarterly Reviews, Chemical Society, 15(4), pp.418-441.

Rochelle, G.T., 2009. Amine scrubbing for CO2 capture. Science, 325(5948), pp.1652-1654.

Rounbehler, D.P., Reisch, J.W., Coombs, J.R. and Fine, D.H., 1980. Nitrosamine air sampling sorbents compared for quantitative collection and artifact formation. Analytical Chemistry, 52(2), pp.273-276.

Rühl, C., Adams, J.D. and Hoffmann, D., 1980. Chemical Studies on Tobacco Smoke LXVI. Comparative Assessment of Volatile and Tobacco-Specific N-Nitrosamines in the Smoke of Selected Cigarettes from the USA, West Germany and France. Journal of Analytical Toxicology, 4(5), pp.255-259.

Russell, C. G.; Blute, N. K.; Via, S.; Wu, X.; Chowdhury, Z.; More, R., 2012. Nationwide assessment of nitrosamine occurrence and trends. Journal (American Water Works Association), 104 (3), 57-58.

Sacher, F., Schmidt, C., Lee, C., & von Gunten, U., 2008. Strategies for minimizing nitrosamine formation during disinfection. Water Research Foundation: Denver, Colorado.

Schmidt, C.K. and Brauch, H.J., 2008. N, N-dimethylsulfamide as precursor for N-nitrosodimethylamine (NDMA) formation upon ozonation and its fate during drinking water treatment. Environmental Science & Technology, 42(17), pp.6340-6346.

Schreiber, I.M. and Mitch, W.A., 2006a. Occurrence and fate of nitrosamines and nitrosamine precursors in wastewater-impacted surface waters using boron as a conservative tracer. Environmental Science & Technology, 40(10), pp.3203-3210.

Schreiber, I.M. and Mitch, W.A., 2006b. Nitrosamine formation pathway revisited: the importance of chloramine speciation and dissolved oxygen. Environmental Science & Technology, 40(19), pp.6007-6014.

Schreiber, I.M. and Mitch, W.A., 2007. Enhanced nitrogenous disinfection byproduct formation near the breakpoint: implications for nitrification control. Environmental Science & Technology, 41(20), pp.7039-7046.

Selbes, M., 2014. The effects of amine structure, chloramine species and oxidation strategies on the formation of N-nitrosodimethylamine.

Selbes, M., Kim, D., Ates, N. and Karanfil, T., 2013. The roles of tertiary amine structure, background organic matter and chloramine species on NDMA formation. Water Research, 47(2), pp.945-953.

Shah, A.D. and Mitch, W.A., 2011. Halonitroalkanes, halonitriles, haloamides, and N-nitrosamines: a critical review of nitrogenous disinfection byproduct formation pathways. Environmental Science & Technology, 46(1), pp.119-131.

Shen, R. and Andrews, S.A., 2011a. Demonstration of 20 pharmaceuticals and personal care products (PPCPs) as nitrosamine precursors during chloramine disinfection. Water Research, 45(2), pp.944-952.

Shen, R. and Andrews, S.A., 2011b. NDMA formation kinetics from three pharmaceuticals in four water matrices. Water Research, 45(17), pp.5687-5694.

Shen, R. and Andrews, S.A., 2013a. Formation of NDMA from ranitidine and sumatriptan: The role of pH. Water Research, 47(2), pp.802-810.

Shen, R. and Andrews, S.A., 2013b. NDMA formation from amine-based pharmaceuticals–impact from prechlorination and water matrix. Water Research, 47(7), pp.2446-2457.

Sørensen, L., Zahlsen, K., Hyldbakk, A., da Silva, E.F. and Booth, A.M., 2015. Photodegradation in natural waters of nitrosamines and nitramines derived from CO 2 capture plant operation. International Journal of Greenhouse Gas Control, 32, pp.106-114.

Spiegelhalder, B. and Preussmann, R., 1981. Nitrosamines and rubber. IARC scientific publications, (41), pp.231-243.

Spiegelhalder, B. and Preussmann, R., 1983. Occupational nitrosamine exposure. 1. Rubber and tyre industry. Carcinogenesis, 4(9), pp.1147-1152.

Spiegelhalder, B. and Preussmann, R., 1986. Nitrosamine measurements in ambient air of an industrial area in Austria. IARC scientific publications, (84), pp.411-414.

Stefan, M.I. and Bolton, J.R., 2002. UV direct photolysis of N-nitrosodimethylamine (NDMA): Kinetic and product study. Helvetica Chimica Acta, 85(5), pp.1416-1426.

Stehlik, G., Richter, O. and Altmann, H., 1982. Concentration of dimethylnitrosamine in the air of smoke-filled rooms. Ecotoxicology and Environmental Safety, 6(6), pp.495-500.

Straub, D.J., Hutchings, J.W. and Herckes, P., 2012. Measurements of fog composition at a rural site. Atmospheric Environment, 47, pp.195-205.

Straif, K., Weiland, S.K., Bungers, M., Holthenrich, D., Taeger, D., Yi, S. and Keil, U., 2000. Exposure to high concentrations of nitrosamines and cancer mortality among a cohort of rubber workers. Occupational and Environmental Medicine, 57(3), pp.180-187.

Strazisar, B.R., Anderson, R.R. and White, C.M., 2003. Degradation pathways for monoethanolamine in a CO2 capture facility. Energy & Fuels, 17(4), pp.1034-1039.

Sullivan, A.P., Peltier, R.E., Brock, C.A., De Gouw, J.A., Holloway, J.S., Warneke, C., Wollny, A.G. and Weber, R.J., 2006. Airborne measurements of carbonaceous aerosol soluble in water over northeastern United States: Method development and an investigation into water-soluble organic carbon sources. Journal of Geophysical Research: Atmospheres, 111(D23).

Tønnesen, D., Dye, C. and Bøhler, T., 2011. Baseline study on air and precipitation quality for CO2 Technology Centre Mongstad. Norwegian Institute for Air Research, NILU OR, 73.

Tricker, A.R. and Preussmann, R., 1991. Carcinogenic N-nitrosamines in the diet: occurrence, formation, mechanisms and carcinogenic potential. Mutation Research/Genetic Toxicology, 259(3), pp.277-289.

Tuazon, E.C., Carter, W.P., Atkinson, R., Winer, A.M. and Pitts, J.N., 1984. Atmospheric reactions of N-nitrosodimethylamine and dimethylnitramine. Environmental Science & Technology, 18(1), pp.49-54.

USEPA, 2005. Unregulated Contaminant Monitoring Rule 2

USEPA. Contaminant Candidate List 3 (CCL3). 2009. http://water.epa.ov/scitech/drinkingwater/dws/ccl/ccl3.cfm (accessed September 26th, 2014)

USEPA. Risk-Based Screening Table. 2015.
http://semspub.epa.gov/work/03/2218450.pdf (accessed September 26th, 2015)

Valentine, R. L.; Choi, J.; Chen, Z.; Barrett, S. E.; Hwang, C. J.; Guo, Y.; Wehner, M.; Fitzsimmons, S.; Andrews, S. A.; Werker, A. G.; Brubacher, C.; Kohut, K. D., 2005. Factors affecting the formation of NDMA in water and occurrence. AWWA Research Foundation, Denver, CO.

Reynolds, A.J., Verheyen, T.V., Adeloju, S.B., Meuleman, E. and Feron, P., 2012. Towards commercial scale postcombustion capture of CO2 with monoethanolamine solvent: key considerations for solvent management and environmental impacts. Environmental Science & Technology, 46(7), pp.3643-3654.

Ventanas, S. and Ruiz, J., 2006. On-site analysis of volatile nitrosamines in food model systems by solid-phase microextraction coupled to a direct extraction device. Talanta, 70(5), pp.1017-1023.

Vikesland, P.J., Ozekin, K. and Valentine, R.L., 2001. Monochloramine decay in model and distribution system waters. Water Research, 35(7), pp.1766-1776.

Von Gunten, U., Salhi, E., Schmidt, C.K. and Arnold, W.A., 2010. Kinetics and mechanisms of N-nitrosodimethylamine formation upon ozonation of N, N-dimethylsulfamide-containing waters: bromide catalysis. Environmental Science & Technology, 44(15), pp.5762-5768.

Walker, E.A., Castegnaro, M., Griciute, L. and Lyle, R.E., 1978.Environmental aspects of N-nitroso compounds (No. 19).

Weber, R.J., Sullivan, A.P., Peltier, R.E., Russell, A., Yan, B., Zheng, M., De Gouw, J., Warneke, C., Brock, C., Holloway, J.S. and Atlas, E.L., 2007. A study of secondary organic aerosol formation in the anthropogenic-influenced southeastern United States. Journal of Geophysical Research: Atmospheres, 112(D13).

WHO, 2002a. http://www.who.int/ipcs/publications/cicad/en/cicad38.pdf (accessed March 26th, 2015)

WHO, 2002b.
http://www.who.int/water_sanitation_health/dwq/chemicals/ndma2ndadd.pdf
(accessed March 26th, 2015)

Yan, B., Zheng, M., Hu, Y., Ding, X., Sullivan, A.P., Weber, R.J., Baek, J., Edgerton, E.S. and Russell, A.G., 2009. Roadside, urban, and rural comparison of primary and secondary organic molecular markers in ambient PM2. 5. Environmental Science & Technology, 43(12), pp.4287-4293.

Yang, L., Chen, Z., Shen, J., Xu, Z., Liang, H., Tian, J., Ben, Y., Zhai, X., Shi, W. and Li, G., 2009. Reinvestigation of the nitrosamine-formation mechanism during ozonation. Environmental Science & Technology, 43(14), pp.5481-5487.

Zhang, J., Hanigan, D., Westerhoff, P. and Herckes, P., 2016. N-Nitrosamine formation kinetics in wastewater effluents and surface waters. Environmental Science: Water Research & Technology.

Zhang, X., Hecobian, A., Zheng, M., Frank, N.H. and Weber, R.J., 2010. Biomass burning impact on PM 2.5 over the southeastern US during 2007: integrating chemically speciated FRM filter measurements, MODIS fire counts and PMF analysis. Atmospheric Chemistry and Physics, 10(14), pp.6839-6853.

APPENDIX A

CHAPTER 3 SAMPLE INFORMATION

Table A1: Sample information of aerosol and fog/cloud water

Aerosol	Location		particle size	Reference
050612 LSA pm>2.5	Tempe AZ	Life Sciences A Wing	PM>2.5	
050912 LSA pm>2.5				
LSA 120416 pm>2.5				
LSA 120420 pm>2.5				
LSA QF FINE 022709			PM2.5	
LSA QF FINE 020309				
ASU 032205 10		Campus Weather Station		
ASU 030205 01				
ASU 03262008		Life Sciences A Wing		
ASU 03312008				
120512 LSA pm2.5				
120509LSA pm2.5				
120506 LSA pm2.5				
asu05/06/05				
asu05/18/02 01				
asu06/28/05				
asu07/01/05				
ls09/24/09				
ls10/05/09				
LS 092309 qf pm2.5				
LS 101209 qf pm2.5				
LS 11.10.09 qf 2.5				
LS 11.03.09 qf 2.5				
FL-HZ 030808 PM10	Higley AZ		PM10	
FL-HZ 020708 PM10				
FL-HZ 040508 PM10				
FL-HZ 020708 PM2.5			PM2.5	
FL-HZ 040508PM2.5				
FL-HZ 030808 PM2.5				
FL-GT051907 PM2.5	Galveston TX			
FL-BBTX 090206 PM2.5	Big Bend TX			
FL-SPTX 051807 PM2.5	South Padre Island TX			
FL-PCTX 051907 PM2.5	Port O'Connor TX			
G ALASKAN DUFF	FLAME experiment	Biomass burning	PM2.5	Carrico et al.,2010
CEAMPTHUS				

L LODGEPOLE PINE	in Fire lab in Missoula			
E ASIAN RICE STRAW				
E ASIAN M PR WOODS				
01082011DavisQFF pm2.5	Davis, CA	UC Davis campus	PM2.5	Ehrenhauser et al., 2012
01092011DavisQFF pm2.5				
01202011 DAVIS QFF PM2.5				
01072011 DAVIS QFF PM2.5				
WMAT 112807 mav ig 2007Q1G1A	AZ (white mountain Apache tribe)	prescribed burn	PM2.5	Robinson et al., 2011
WMAT 112907 LOFTER PILE 2007QSM1B				
FC PM2.5 062502 GE T8B1	Fort Collins, CO	CSU Christman Field	PM2.5	
FC TSP 062502GE T7B1			TSP	
TYL 05042010 PM>2.5	Tempe, AZ	parking garage	PM>2.5	Benn et al., 2012
TYL 05062010 PM>2.5 46h				
TYL05102010pm2.5 72h			PM2.5	
TYL05712010 pm2.5				
rn0725	Whistler, BC	Raven's Nest	PM2.5	Lee et al., 2012
rn0718		Raven's Nest		
pieJQ	São Paulo, Brazil	Tunnel LDVs	PM2.5	Brito et al., 2013
pieTR		Tunnel HDVs		
Monterrey Aerosol				
2011/5/28 day	Monterrey, Mexico	Monterrey Metropolitan Area	PM2.5	Mancilla et al., 2015
2011/5/28 night				
2011/5/30 day				
2011/5/30 night				
2011/6/1 day				
2011/6/1 night				
2011/6/3 day				
2011/6/3 night				
2011/6/5 day				
2011/6/5 night				
2011/6/9 day				
2011/6/9 night				
2011/6/11 day				

2011/6/11 night				
Bakersfield Aerosol				
2013/1/19	Bakersfield, CA		PM2.5	
2013/1/20				
2013/1/21				
2013/1/22				
2013/1/23				
2013/1/24				
2013/1/25				
2013/1/29				
2013/1/30				
2013/1/31				
2013/2/1				
2013/2/2				
2013/2/3				
2013/2/4				
2013/2/5				
2013/2/9				
2013/2/10				
2013/2/11				
Fog				
SU 092009	Selinsgrove ,PA		fog	Straub et al., 2012
SU103107				
DAA 011511P3	Davis, CA	UC Davis campus		Ehrenhauser et al., 2012
DAA 011711P1				
XL CASCC F010910P3	Fresno, CA	CSU Fresno cmapus		
XL CASCC F010910P2 FILTERED				
Cloud				
ELDEN 080205 2 OF 2	Mt. Elden, AZ		cloud	Hutchings et al., 2009
ELDEN 091207	Mt. Elden, AZ			
RN0705P1	Whistler, BC	Raven's Nest		Lee et al., 2012
RN0621P1				
RN0712				
RN0722				

APPENDIX B

SUPPORTING INFORMATION FOR CHAPTER 4

Text A1: NDMA formation pathways in chloramination. NAs could be formed from primary amines through a nitrosation pathway, these NAs are not stable and decay rapidly (Ridd, 1961).[1] Secondary amines which form stable secondary NAs have been studied in greater detail (Choi and Valentine, 2002; Mitch and Sedlak, 2002; Schreiber and Mitch, 2006a; Schreiber and Mitch, 2006b; Shah and Mitch, 2012). Tertiary amines were also found to be important precursors. Some tertiary amines (e.g. trimethylamine (TMA)) decay nearly instantaneously and quantitatively in presence of chlorine to release a secondary amine which forms the nitrosamine upon chloramination (Mitch and Schreiber, 2008). Mechanistic studies found that nitrosamine yields from most secondary amines and tertiary amines are similar (i.e., ~0-2%). Some other tertiary amines (e.g. where one of the alkyl substituents contained an aromatic group in the □-position to the dimethylamine (DMA) nitrogen such as a benzyl functional group, or those alkyl substituents containing branched alkyl groups next to the nitrogen of DMA) have much higher yields of NDMA in chloramination (Le Roux et al., 2012; Shen and Andrews., 2011a; Shen and Andrews., 2011b). In particular, ranitidine, a widely used amine-based pharmaceutical, forms NDMA at yields higher than 80%. It suggests that these tertiary amines form nitrosamines through different pathways.

NDMA is thought to be produced in chloraminated drinking waters through three pathways. Two pathways assume unprotonated DMA undergoes nucleophilic substitution with either mono- or di-chloramine, yielding unsymmetrical dimethylhydrazine (UDMH) (NH_2Cl) in or chlorinated UDMH intermediate (Cl-UDMH) ($NHCl_2$) (Choi and Valentine, 2002; Schreiber and Mitch, 2006b). UDMH is then oxidized by monochloramine to produce NDMA or Cl-UDMH is oxidized by oxygen to produce NDMA. Based upon competition kinetics, it has been suggested that monochloramine pathway is negligible compared with dichloramine pathway. The

importance of the two reaction mechanisms remains debated, with dichloramine producing NDMA concentrations orders of magnitude higher than monochloramine when reacted with amine-containing model compounds (Shah and Mitch, 2012). However, research on suspected NDMA precursors found that compounds with electron withdrawing groups react preferentially with monochloramine while compounds with electron donating groups react preferentially with dichloramine.[11] As the molar yield of NDMA from DMA is low (i.e., <5%), it was suspected that a third pathway, not through DMA, existed. Recently it was shown that compounds such as ranitidine follow a different series of reactions involving nucleophilic attack of the amine group in organic amines. Further reaction involving dissolved O_2 allows for the direct formation of NDMA and a resulting sister carbocation (Le Roux et al., 2012). When the requisite β-aryl tertiary amine is present on a parent compound, molar yields of NDMA are always in excess of 20% (Selbes, 2013). Other NDMA-forming compounds typically have molar conversion of <5% and therefore β-aryl tertiary amine containing compounds are thought to be of great importance.

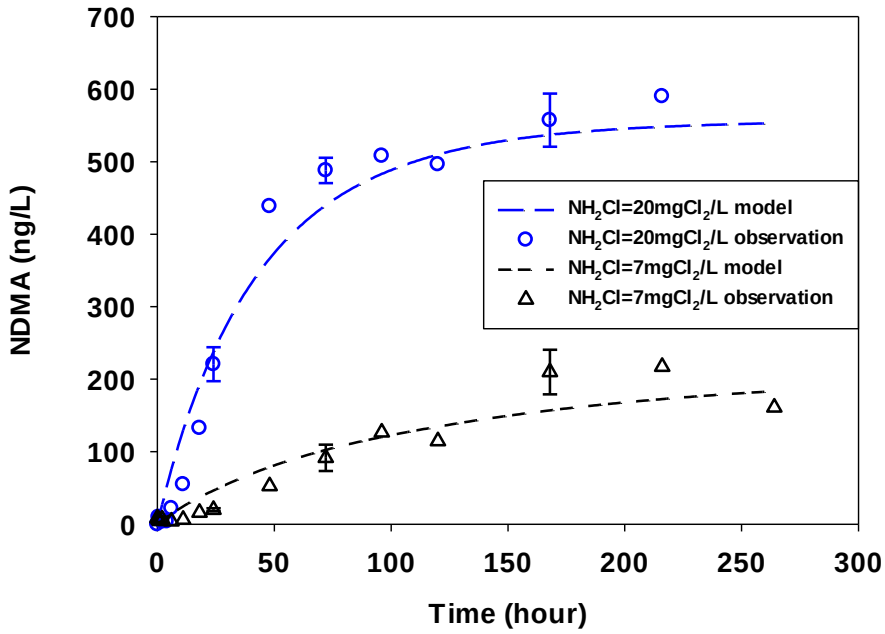

Figure A1. NDMA formation observed (symbols) and fitted by Equations 2&3 (line) in WW2 at two initial monochloramine doses. (pH=8.0, 23 ± 1°C)

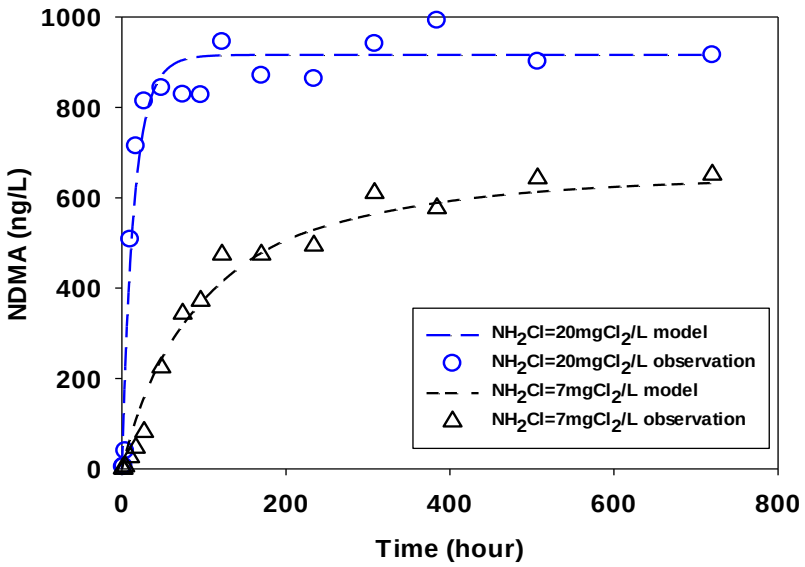

Figure A2. NDMA formation observed (symbols) and fitted by Equations 4-2&4-3 (line) in WW3 at two initial monochloramine doses. (pH=8.0, 23 ± 1°C)

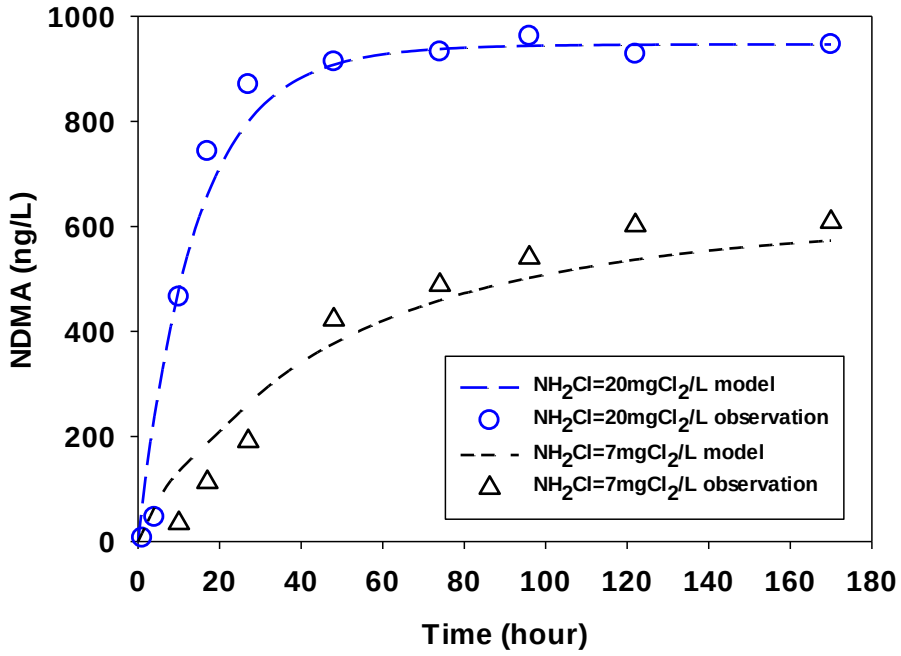

Figure A3. NDMA formation observed (symbols) and fitted by Equations 4-2&4-3 (line) in WW4 at two initial monochloramine doses. (pH=8.0, 23 ± 1°C)

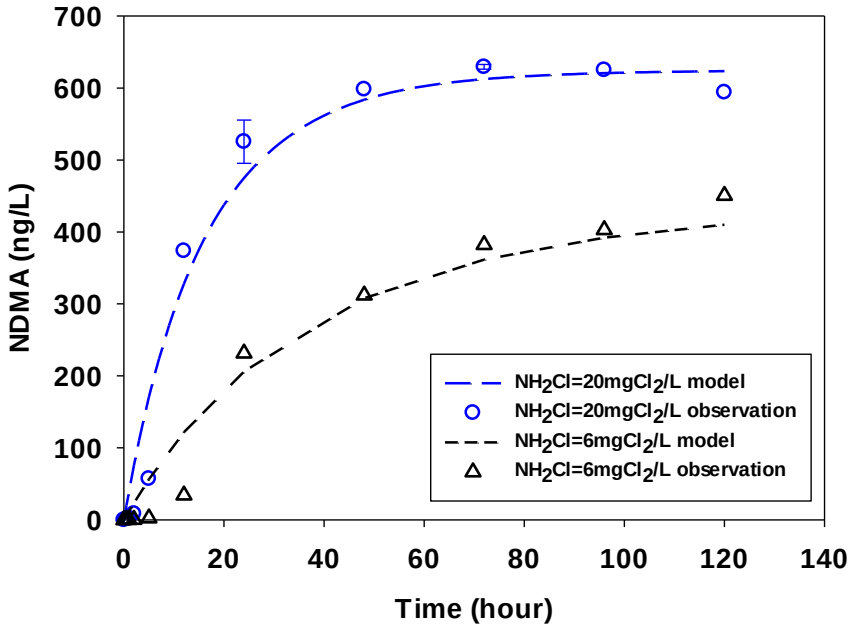

Figure A4. NDMA formation observed (symbols) and fitted by Equations 4-2&4-3 (line) in WW5 at two initial monochloramine doses. (pH=8.0, 23 ± 1°C)

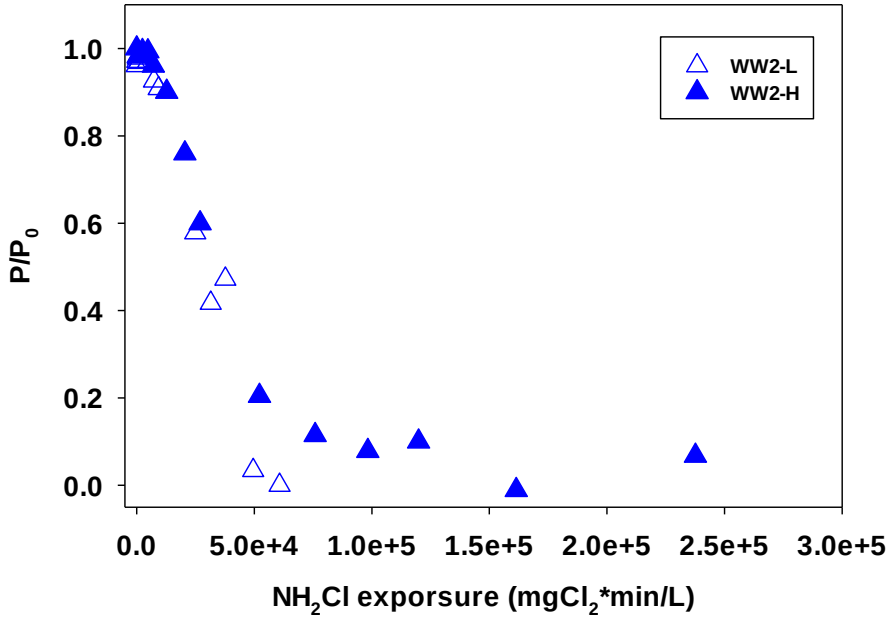

Figure A5: Plots of P/P_0 verses monochloramine exposure for water samples WW2, L=lower, H=higher, represent samples with lower or higher NH_2Cl concentration.

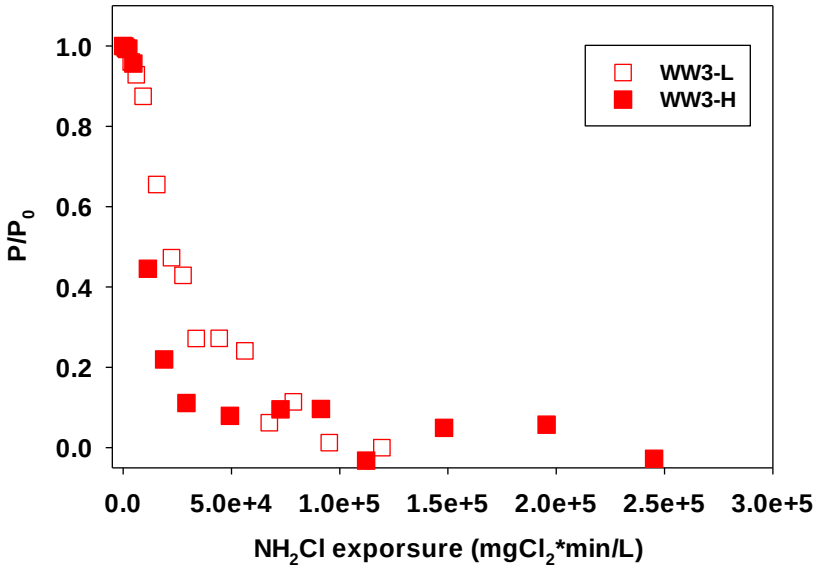

Figure A6: Plots of P/P_0 verses monochloramine exposure for water samples WW3, L=lower, H=higher, represent samples with lower or higher NH_2Cl concentration.

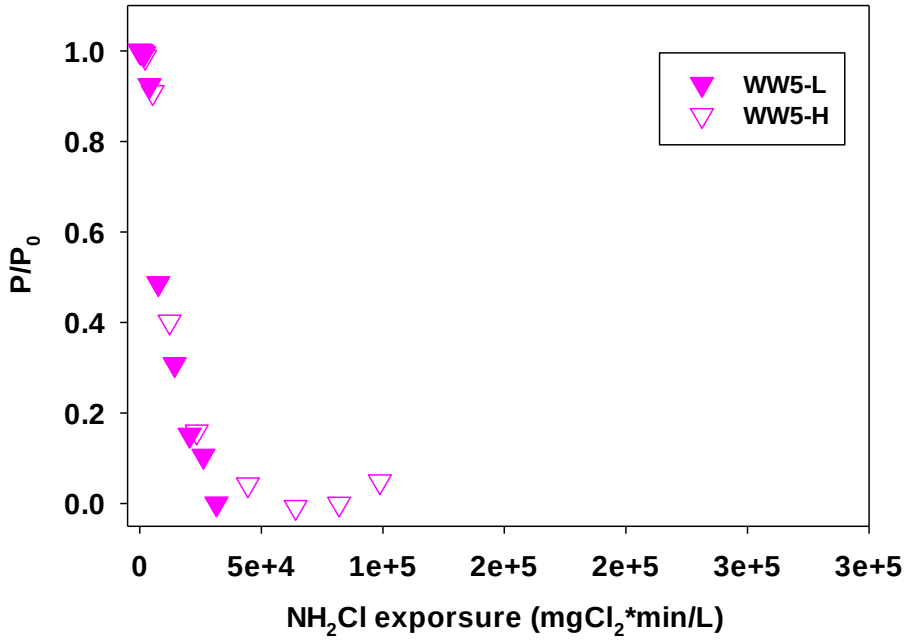

Figure A7: Plots of P/P_0 verses monochloramine exposure for water samples WW5, L=lower, H=higher, represent samples with lower or higher NH_2Cl concentration.

Table A2: Dose-response curve model parameters

Sample ID	Upon Monochloramine Addition				
	Monochloramine dose ($mgCl_2/L$)	pH	$NDMA_{max}$ (nM) [ng/L]	$k(h^{-1})$	R^2
WW1	18	8.2	6 [450]	0.03	0.99
	6		4 [280]	0.02	0.91
WW2	20	8	7 [520]	0.05	0.98
	7		2 [200]	0.01	0.96
WW3	20	8	12[920]	0.17	0.97
	7		9[620]	0.02	0.96
WW4	20	8	12[920]	0.13	0.99
	7		8[580]	0.03	0.98
WW5	20	8	8[600]	0.18	0.99
	6		5.5[380]	0.04	0.98
SW1	36	8	0.7[53]	0.01	0.98
	12		0.4[35]	0.01	0.93
GW1	20	8	0.2[16]	0.04	0.93
	7		0.2[11]	0.07	0.95